Supplementary information

for

Accelerated discovery of organic polymer photocatalysts for hydrogen evolution from water through the integration of experiment and theory

Yang Bai,[a,†] Liam Wilbraham,[b,†] Benjamin J. Slater,[a] Martijn A. Zwijnenburg,[b,*] Reiner Sebastian Sprick,[a,*] and Andrew I. Cooper[a,*]

[a] Department of Chemistry and Materials Innovation Factory, University of Liverpool, Crown Street, Liverpool, L69 7ZD, U.K.

[b] Department of Chemistry, University College London, 20 Gordon Street, London, WC1H 0AJ, U.K.

1. General methods

Reagents and solvents were purchased from commercial suppliers (Manchester Organics, Sigma-Aldrich, Fluorochem, Ark Pharm, Apollo, Combi-Blocks, TCI Europe, Carbosynth) and used with no further purification, unless specified. 2,7-Dibromopyrene-4,5,9,10-tetraone (monomer 45)[1] and 2-(2,7-dibromo-9*H*-fluoren-9-ylidene)-malononitrile (monomer 88)[2] were synthesized using previously reported procedures. All reactions were set up using a Chemspeed Technologies Sweigher platform, operating with a constant N_2 purge. Water for the hydrogen evolution experiments was purified using an ELGA LabWater system with a Purelab Option S filtration and ion exchange column (ρ = 15 MΩ cm) without pH level adjustment. CHN analysis was performed on a Thermo EA1112 Flash CHNS-O Analyzer using standard microanalytical procedures. The solutions were diluted with water before the measurement and the instrument was calibrated with Pd standards in aqueous solution and Y-89 as the internal standard. Transmission FT-IR spectra were recorded on a Bruker Tensor 27 at room temperature with an ATR method. Thermogravimetric analysis was performed on an EXSTAR6000 by heating samples at 10 °C min^{-1} under air in open platinum pans from 25 to 800 °C. The UV-visible absorption spectra of the polymers were recorded on a Shimadzu UV-2550 UV-Vis spectrometer as powders in the solid state. Photoluminescence spectra of the polymer powders were measured with a Shimadzu RF-5301PC fluorescence spectrometer at room temperature. Time-correlated single photon counting (TCSPC) experiments were performed on an Edinburgh Instruments LS980-D2S2-STM spectrometer equipped with picosecond pulsed LED excitation sources and a R928 detector, with a stop count rate below 5%. An EPL-375 diode (λ = 370.5 nm, instrument response 100 ps, fwhm) was used. Suspensions were prepared by ultrasonicating the polymer in water. The instrument response was measured with colloidal silica (LUDOX® HS-40, Sigma-Aldrich) at the excitation wavelength. Decay times were fitted in the FAST software using suggested lifetime estimates. PXRD measurements were performed on a PANalytical X'Pert PRO MPD, with a Cu X-ray source, used in high throughput transmission mode with Kα focusing mirror and PIXCEL 1D detector. Static light scattering measurements were performed on a Malvern Mastersizer 3000 Particle Sizer, polymers were dispersed in water/methanol/triethylamine (1:1:1) mixture by 10 minutes of ultrasonication and the resultant suspensions were injected into a stirred Hydro SV quartz cell, containing more of the water/methanol/triethylamine (1:1:1) mixture, to give a laser obscuration of 5–10%. Particle sizes were fitted according to Mie theory, using the Malvern 'General Purpose' analysis model, for non-spherical particles with fine powder mode turned on. A polymer refractive index of 1.59, polymer absorbance of 0.1 and solvent refractive index of 1.37 were used for fitting. Transmittance of high-throughput samples was measured on a Formulaction S.A.S. Turbiscan AGS system with an 880 nm NIR diode and a detector at 180° (relative to the light source) in a cylindrical glass cell. Samples were prepared by dispersing the materials in a 1:1:1 mixture of 5 mL water/methanol/TEA and then diluted with water

up to 30 mL total volume. All samples were sonicated before each measurement, and transmittance result is the number average from 4 mm to 30 mm height of sample in the cell. High-throughput polymerizations were carried out using a Biotage Robot Eight & Robot Sixty microwave equipped with a 2.45 GHz magnetron and a magnetic stirrer system (800 rpm) or a Discover SP Microwave System with an Explorer 48 Autosampler microwave. Surface areas were measured by nitrogen adsorption and desorption at 77.3 K. Powder samples were degassed offline at 110 °C for 15 hours under dynamic vacuum (10^{-5} bar) before analysis. Isotherms were measured using a Micromeritics 2420 volumetric adsorption analyzer. Surface areas were calculated in the relative pressure (P/P_0) range from 0.01 to 0.10 of the adsorption branch.

High-throughput instrument for the rapid screening of porous materials enabling up to 96 materials to be tested for porosity to a wide range of gases. The system uses thermal imaging to simultaneously measure the temperature change of up to 96 materials as they adsorb or desorb a gas. A 96-well ProxiPlate was loaded with the samples at different locations which was then heated at 80 °C overnight. The plate was left to cool to room temperature and then CO_2 was charged to the system in 70 mbar dose and the thermal change of each of the materials was recorded.

Inductively coupled plasma optical emission spectrometry (ICP-OES) analysis was performed on an ICP-OES Agilent 5110 with equipped with a collision/reaction cell after a microwave digest of the materials in nitric acid (67-69%, trace metal analysis grade) in a microwave. The solutions were diluted with water before the measurement and the instrument was calibrated with Pd standards in aqueous solution and Y-89 as the internal standard.

2. Experimental set-ups

2.1 High-throughput polymer synthesis workflow

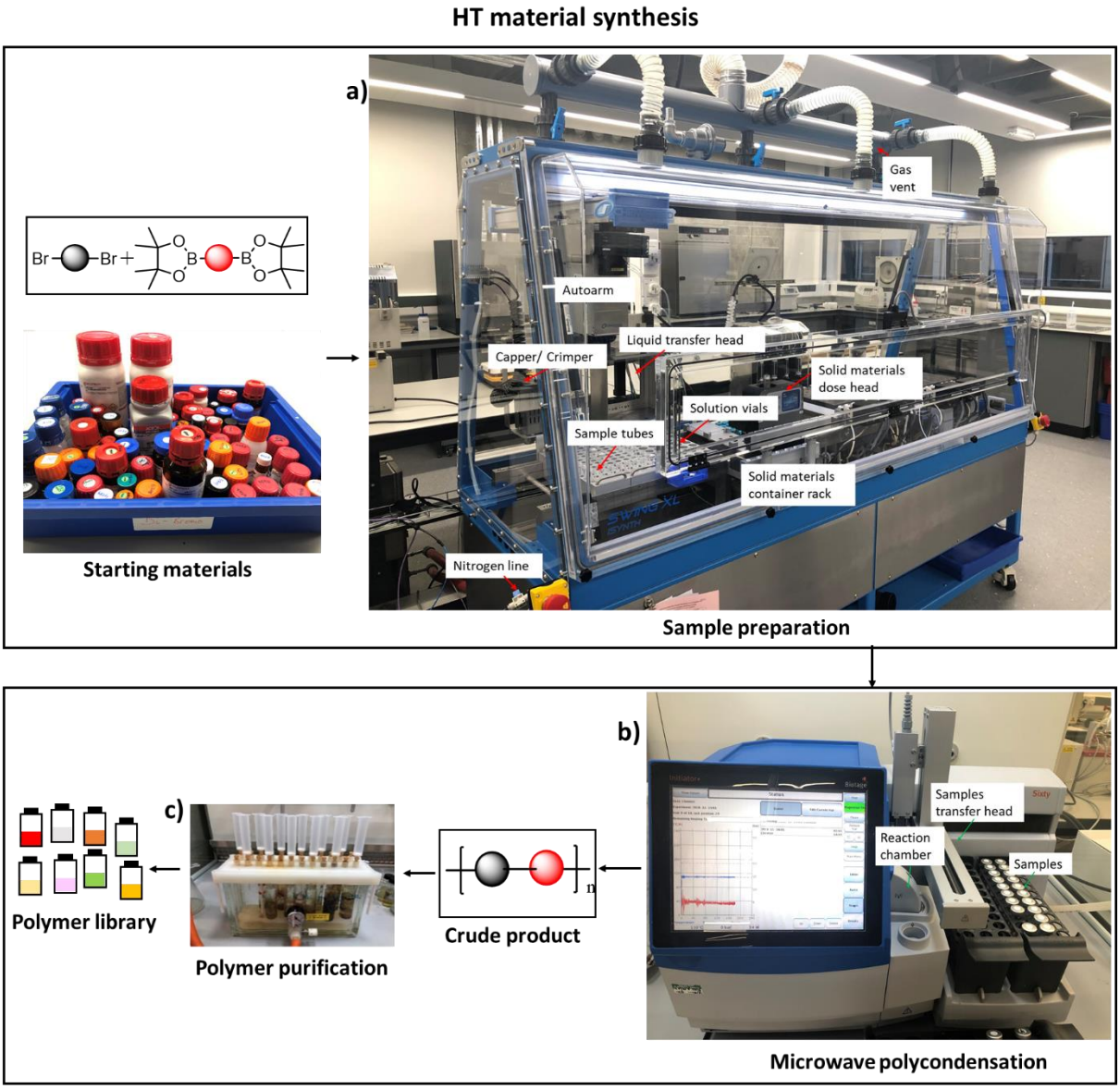

Figure S-1 Workflow for high-throughput synthesis using a) a Isynth by Chemspeed technologies; b) Biotage Microwave: The sample is heated to 100 ºC, kept for 20 seconds and then the temperature is increased to 160 ºC, kept for 1 hour, and then cooled down to room temperature; c) Filtration and wash with water, then methanol.

2.2 High-throughput microwave screening conditions

The conditions for the high-throughput library synthesis were first optimized using 1,4-phenylenediboronic acid and 1,4-dibromobenzene to yield poly(*p*-phenylene) (see Table S-1, below).

For this 1,4-phenylenediboronic acid (59 mg, 0.356 mmol), 1,4-dibromobenzene (83.5 mg, 0.356 mmol), and [$PdCl_2$(dppf)] (0.65 mol%) were added to a glass microwave tube (40 mL). Toluene (3 mL, containing 1.5 vol. % Starks' catalyst) and base solution (2 mL) were then added under inert conditions and the mixture was heated to the temperature and time specified. After cooling to room temperature, water was added to the reaction vessel and filtered. The crude polymer was further washed with distilled water, then methanol and dried *in vacuo*.

Based on these results we used the following conditions for the library synthesis: aqueous tetrabutylammonium acetate as the base at 160 °C for 60 minutes before work-up

Table S-1. Optimization microwave-assisted experiments conditions

Reaction	Base	Temp[a] / °C	Time / min	Powermax[b] option	Yield
1	K_2CO_3/H_2O (2 M)	160	60	Yes	52 mg (81%)
2	K_2CO_3/H_2O (2 M)	160	60	No	48 mg (74%)
3	K_2CO_3/H_2O (2 M)	160	45	Yes	57 mg (88%)
4	K_2CO_3/H_2O (2 M)	160	60	Yes	54 mg (83%)
5	K_2CO_3/H_2O (2 M)	160	30	Yes	29 mg (45%)
6	K_2CO_3/H_2O (2 M)	160	30	No	16 mg (25%)
7	K_2CO_3/H_2O (2 M)	120	60	yes	28 mg (43%)
8	K_2CO_3/H_2O (2 M)	120	60	No	6 mg (9%)
9	K_3PO_4/H_2O (2 M)	160	60	Yes	15 mg (23%)
10	K_3PO_4/H_2O (2 M)	160	60	No	31 mg (48%)
11	K_3PO_4/H_2O (2 M)	160	60	Yes	27 mg (42%)
12	K_3PO_4/H_2O (2 M)	160	60	Yes	17 mg (26%)
13	Tetrabutylammonium acetate /EtOH (1.5M)	160	60	No	54 mg (84%)
14	Tetrabutylammonium acetate /H_2O (1.5 M)	160	60	Yes	58 mg (90%)
15	Tetrabutylammonium acetate /EtOH (1.5 M)	110	60	Yes	58 mg (90%)
16	Tetrabutylammonium acetate /H_2O (1.5M)	160	60	No	33 mg (51%)
17	Tetrabutylammonium hydroxide	160	60	Yes	16 mg (25%)
18	Tetrabutylammonium hydroxide	160	60	Yes	19 mg (29%)
19	Tetrabutylammonium hydroxide	160	60	No	28 mg (43%)
20	Tetrabutylammonium hydroxide	110	60	Yes	9 mg (14%)
21	Tetrabutylammonium hydroxide	110	30	Yes	15 mg (23%)
22	Tetrabutylammonium hydroxide	160	30	No	31 mg (48%)
23	Tetrabutylammonium hydroxide	160	30	Yes	27 mg (42 %)
24	Tetrabutylammonium acetate /EtOH (1.5 M)	160	60	Yes	17 mg (26%)
25	Tetrabutylammonium acetate /EtOH (1.5 M)	160	60	Yes	64 mg (99%)
26	Tetrabutylammonium acetate /H_2O (1.5 M)	160	60	Yes	42 mg (65%)
27	Tetrabutylammonium acetate /H_2O (1.5 M)	160	60	Yes	59 mg (91%)

[a] Temperature ramp: 30 °C min^{-1}; [b] The power of the microwave was limited to mot exceed 100 W.

2.3 High-throughput polymer synthesis workflow

Aqueous tetrabutylammonium acetate (1 M) and toluene containing Starks' catalyst (1.5 vol. %) were degassed in vials with PTFE caps by N_2 bubbling for 30 minutes. The vials were then placed in the Isynth robot, along with microwave reaction tubes (40 mL) and the various monomers, which were stored in solid dispensing units (see Fig. S-1c). The Isynth robot (Fig S-1 a) was closed and purged with nitrogen for 1 hour, and then the solids were dispensed by the system automatically into each microwave reaction tube (diboronic acid / acid ester aryl, 0.21 mmol; aryl dihalide, 0.21 mmol; [$PdCl_2$(dppf)], 0.65 mol%). Afterwards, liquid transfers were performed by the liquid handing unit from the solution vials into each microwave vial (tetrabutylammonium acetate, 1 M aqueous solution, 2 mL; toluene, 3 mL, containing 1.5 vol. % Starks' catalyst). Finally, the capper/crimper tool was used to seal all microwave reaction tubes. The microwave reaction tubes were removed from the system and transferred to a microwave rack (Fig S-1b). The reaction mixtures were then heated in a microwave (Fig S-1b) to 100 °C, kept at this temperature for 20 seconds, then heated to 160 °C and kept for 1 hour at this temperature. The reaction mixture was cooled to room temperature and poured into water. The precipitate was collected by filtration (Fig S-1c) and washed with H_2O and methanol. The products were dried *in vacuo*.

2.4 High throughput photocatalysis workflow

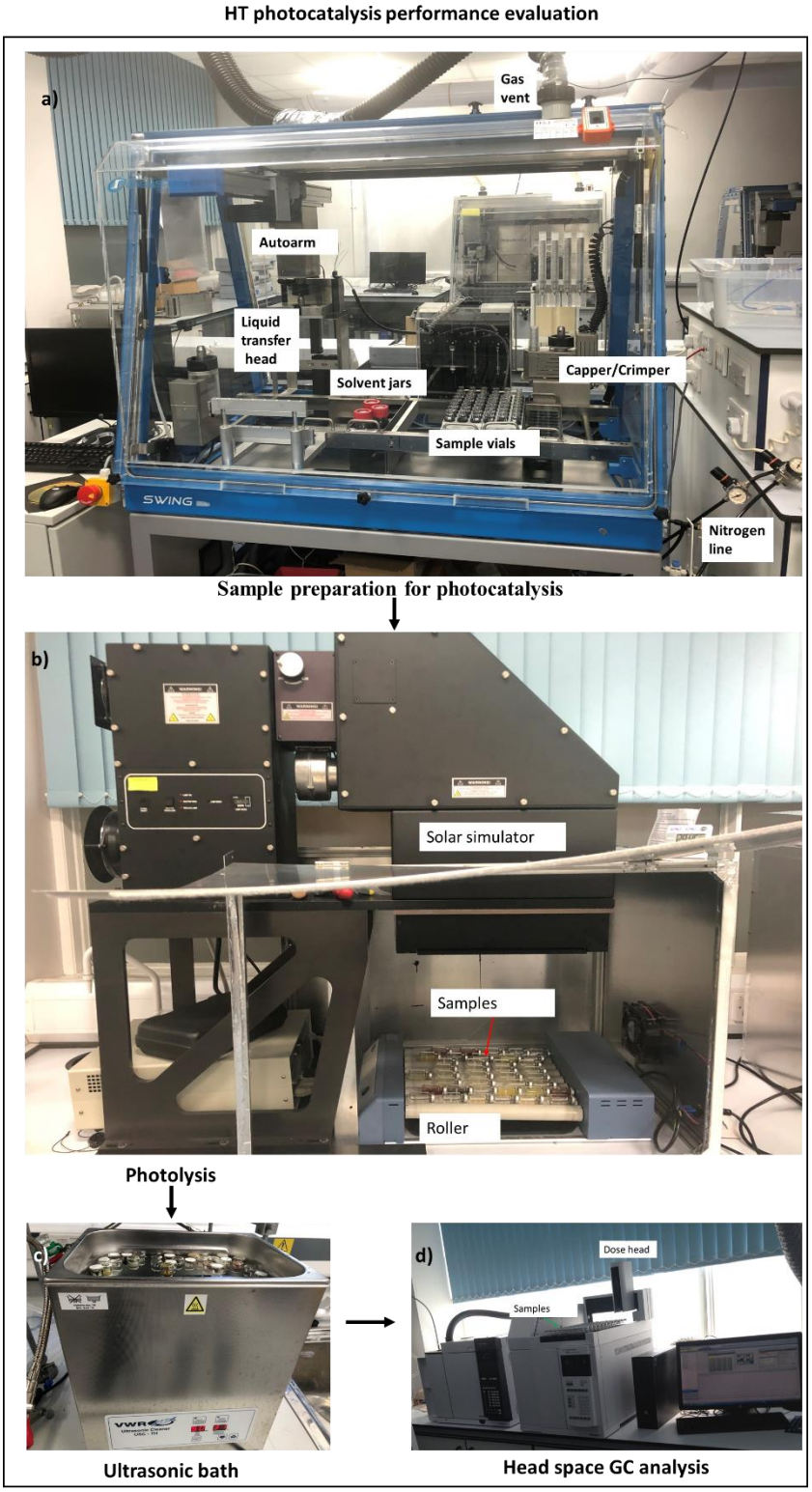

Figure S-2 Workflow for high-throughput screening, a) Sweigher by Chemspeed Technologies; b) Solar simulator (AM1.5G, Class AAA, IEC/JIS/ASTM, 1440 W xenon, 12 × 12 in., MODEL: 94123A) with rocker/roller device; c) Ultrasonic bath (VWR, USC-TH); (d) 7890B GC System and 7697A Headspace Sampler.

Polymers (5 mg) were added into sample vials (V = 12.5 mL) and purged with nitrogen in a Sweigher Chemspeed Technologies robot (Fig S-2a) for 6 hours. The liquid transfer head (handled by the autoarm) was used to transfer scavengers and deionized water (trimethylamine/methanol/water, 1:1:1; Na_2S aq., 0.026 M; 5 mL) *via* the liquid handling system under inert conditions from stock jars inside the system into the sample vials. The capper/crimper tool then capped/crimped the vials automatically under inert conditions. All sample vials were ultrasonicated in an ultrasonic bath for 5 minutes before removing the vials and illuminating them with a solar simulator (AM1.5G, Class AAA, IEC/JIS/ASTM, 1440 W xenon, 12 × 12 in., MODEL:94123A) (Fig S-2b) for the time specified while constantly being redispersed with a rocker/roller device. Gaseous products were analyzed on an Agilent HS-GC (Fig S-2c) injecting a sample from the headspace via a transfer line (temperature 90 °C) onto a molecular sieve 5A column (temperature: 45 °C) with He as the carrier gas at a flow rate of 30 mL min^{-1}. Hydrogen was detected with a flame ionization detector referencing against standard gas with a known concentration of hydrogen. Hydrogen dissolved in the reaction mixture was not measured and the pressure increase generated by the evolved hydrogen was neglected in the calculations. No hydrogen evolution was observed for a mixture of water/methanol/trimethylamine or Na_2S/water under solar simulator illumination in absence of a photocatalyst.

For experiments that involved *in situ* platinum photodeposition, H_2PtCl_6 (8 wt. % in water) was added after the addition of triethylamine, methanol, and water and before capping of the vials.

2.5 Spectral output of light sources

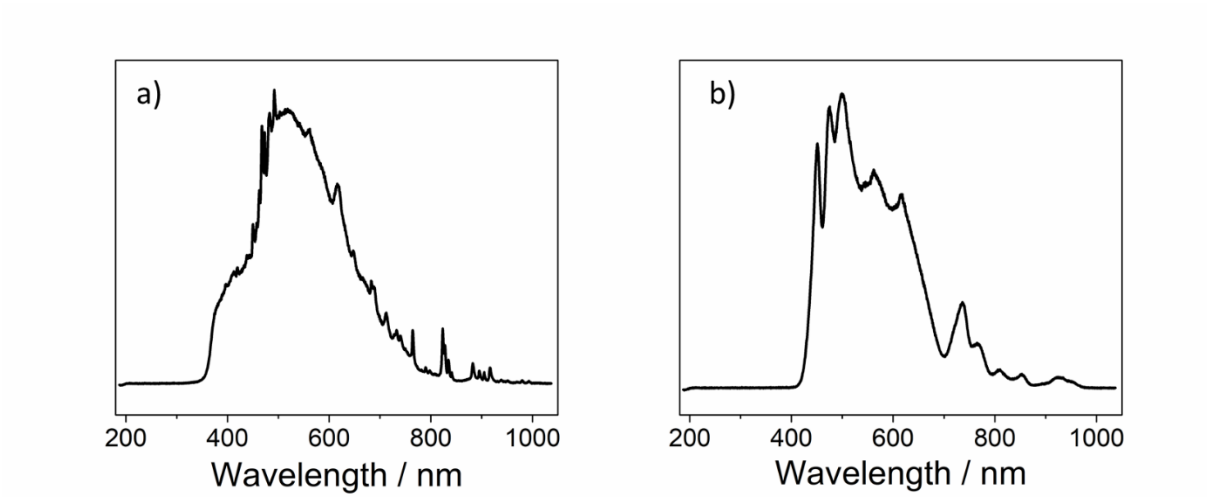

Figure S-3: Spectral output of a) Solar simulator (AM1.5G, Class AAA, IEC/JIS/ASTM, 1440 W Xenon, 12 × 12 in., MODEL: 94123A); b) Solar simulator irradiation (AM1.5G, classification ABA, ASTME927-10).

3. Dibenzo[*b*,*d*]thiophene sulfone co-polymers (P1-XX)

3.1 UV-visible spectra

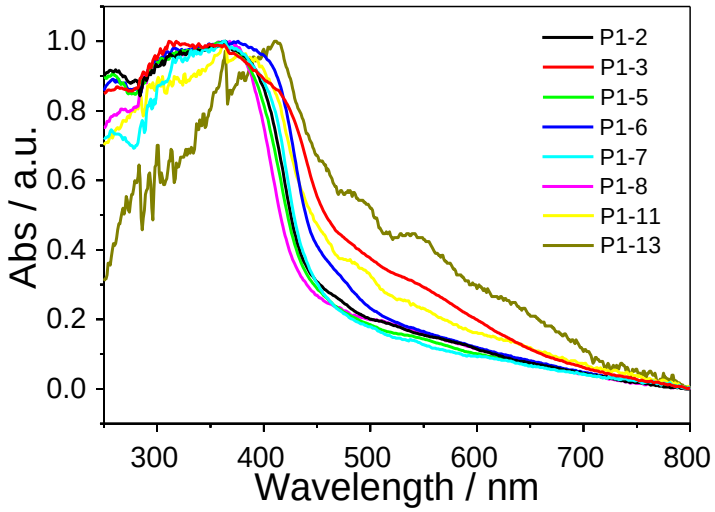

Figure S-4. Solid-state UV-vis spectra of **P1-2** to **P1-13** measured as powders in the solid-state.

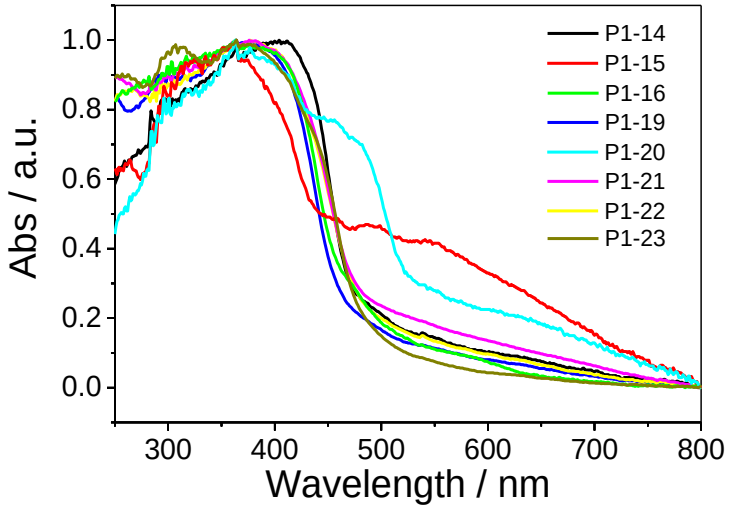

Figure S-5. Solid-state UV-vis spectra of **P1-14** to **P1-23** measured as powders in the solid-state.

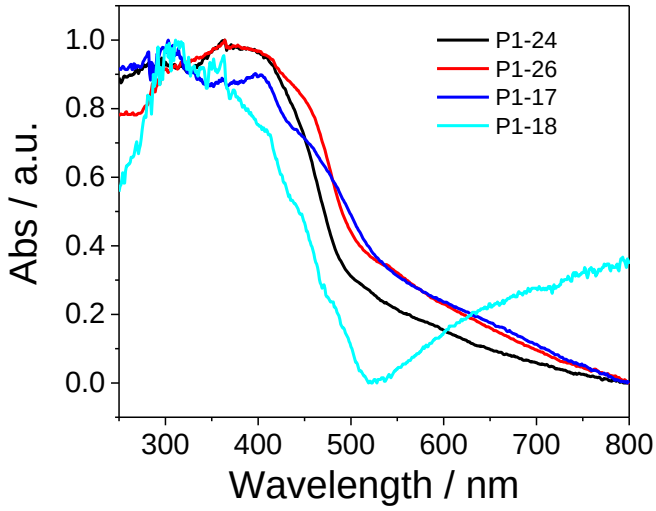

Figure S-6. Solid-state UV-vis spectra of **P1-17** to **P1-26** measured as powders in the solid-state.

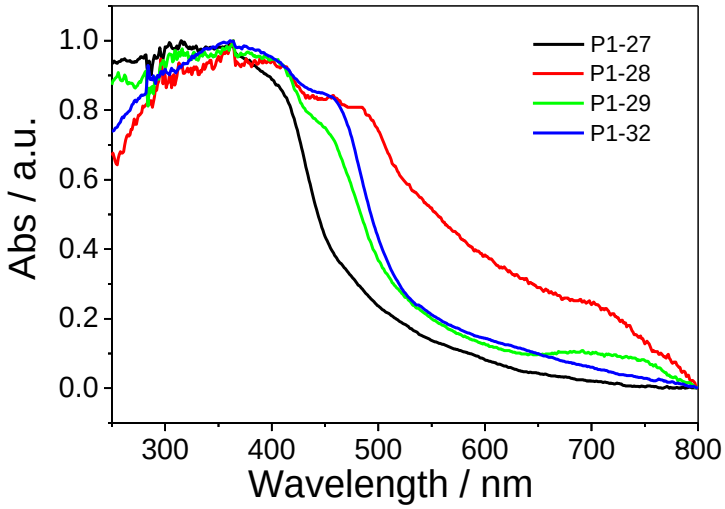

Figure S-7. Solid-state UV-vis spectra of **P1-27** to **P1-32** measured as powders in the solid-state.

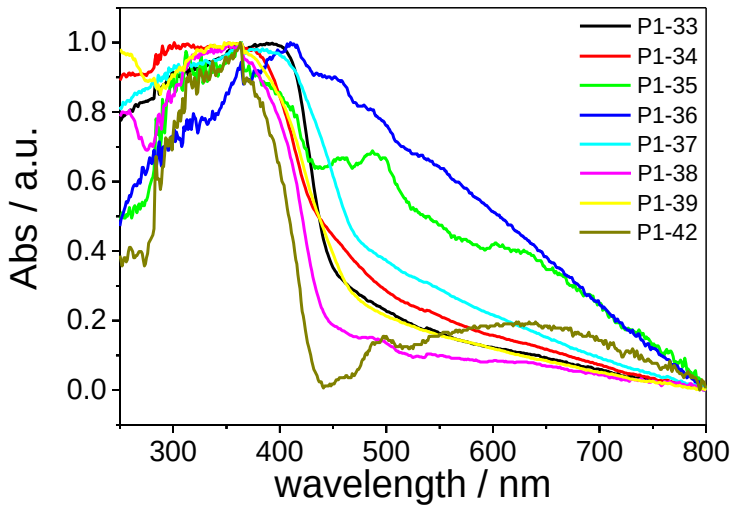

Figure S-8. Solid-state UV-vis spectra of **P1-33** to **P1-42** measured as powders in the solid-state.

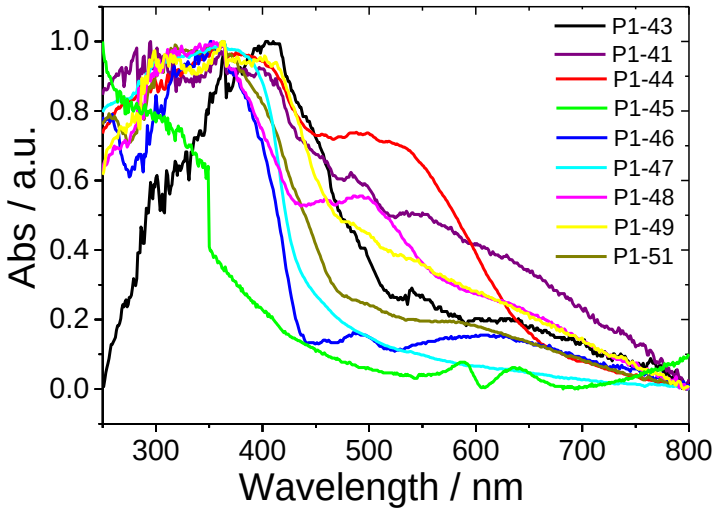

Figure S-9. Solid-state UV-vis spectra of **P1-41** to **P1-51** measured as powders in the solid-state.

.

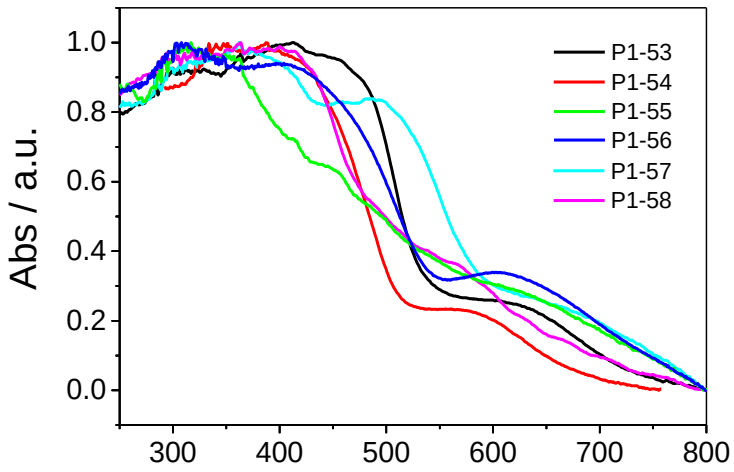

Figure S-10. Solid-state UV-vis spectra of **P1-52** to **P1-57** measured as powders in the solid-state.

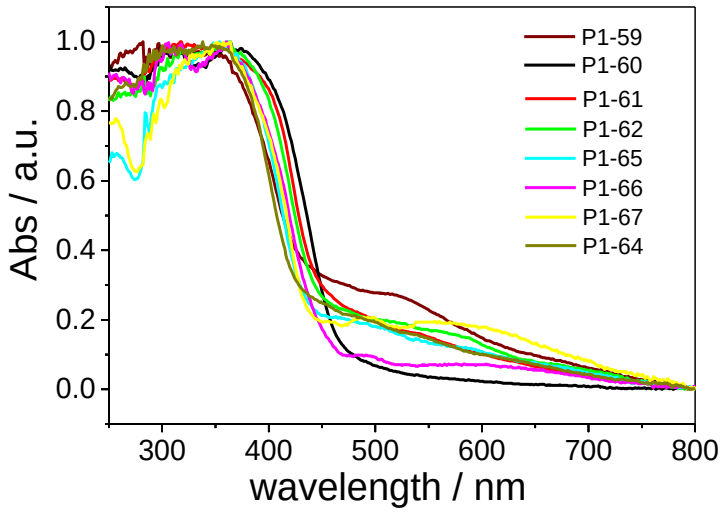

Figure S-11. Solid-state UV-vis spectra of **P1-58** to **P1-63** measured as powders in the solid-state.

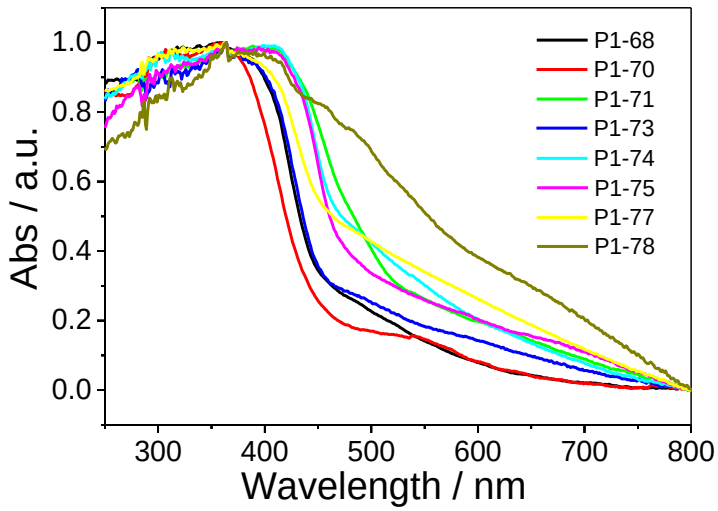

Figure S-12. Solid-state UV-vis spectra of **P1-68** to **P1-78** measured as powders in the solid-state.

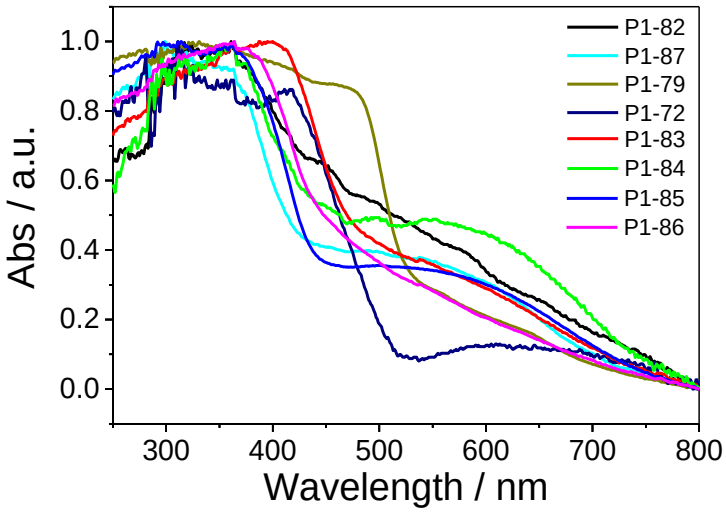

Figure S-13. Solid-state UV-vis spectra of **P1-72** to **P1-86** measured as powders in the solid-state.

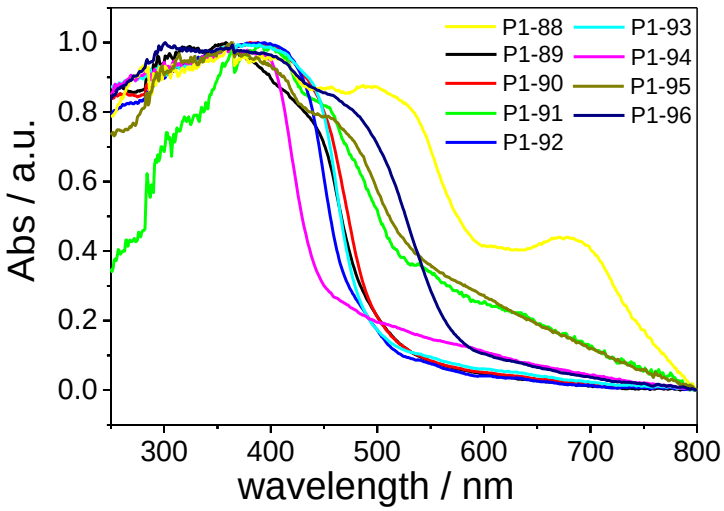

Figure S-14. Solid-state UV-vis spectra of **P1-88** to **P1-96** measured as powders in the solid-state.

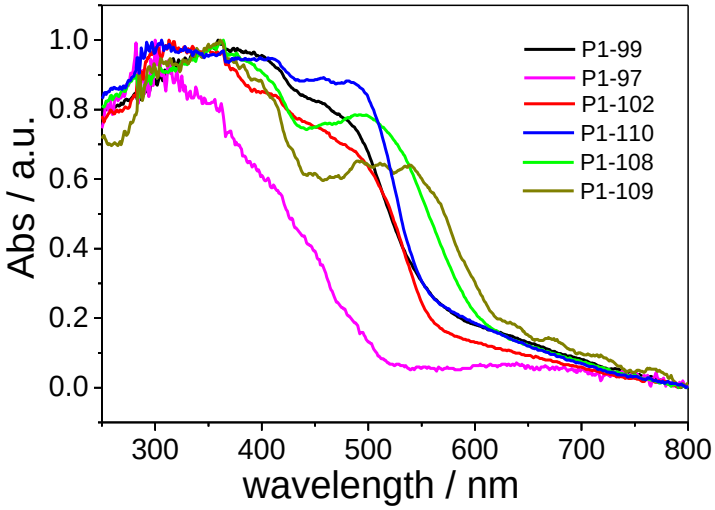

Figure S-15. Solid-state UV-vis spectra of **P1-97** to **P1-110** measured as powders in the solid-state.

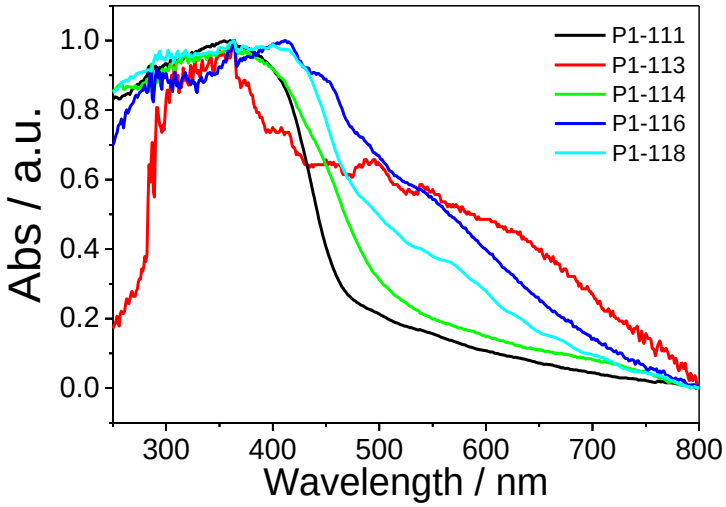

Figure S-16. Solid-state UV-vis spectra of **P1-111** to **P1-118** measured as powders in the solid-state.

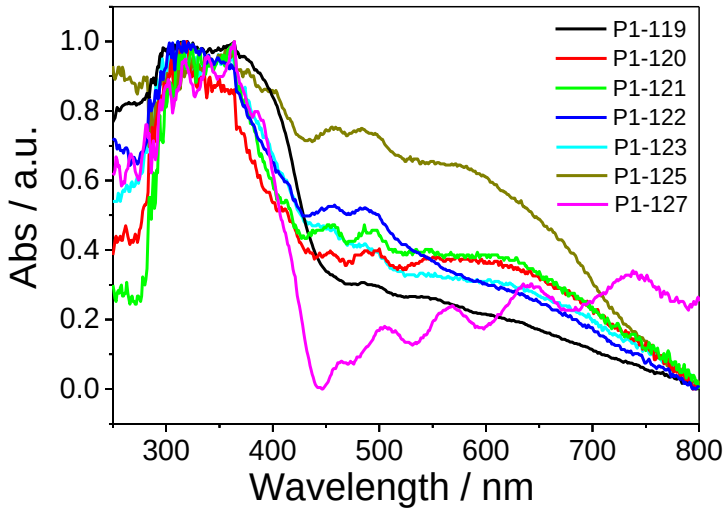

Figure S-17. Solid-state UV-vis spectra of **P1-119** to **P1-127** measured as powders in the solid-state.

3.2 Fourier-transform infrared spectroscopy spectra

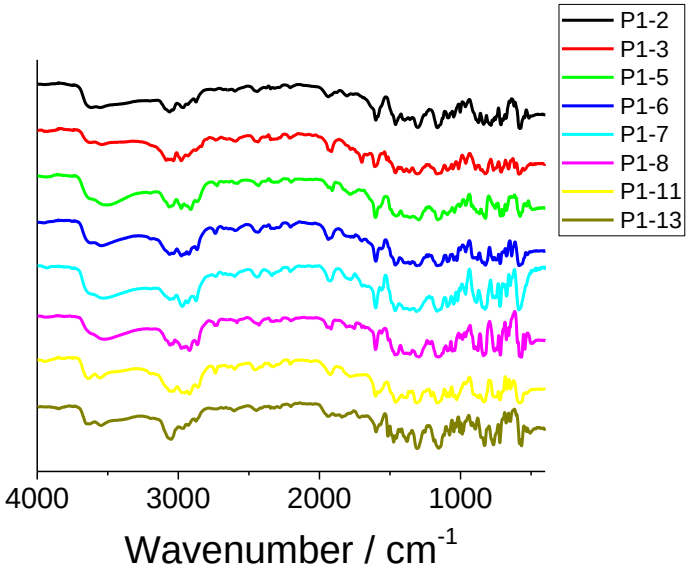

Figure S-18. Transmission FT-IR spectra of P1-2 to P1-13.

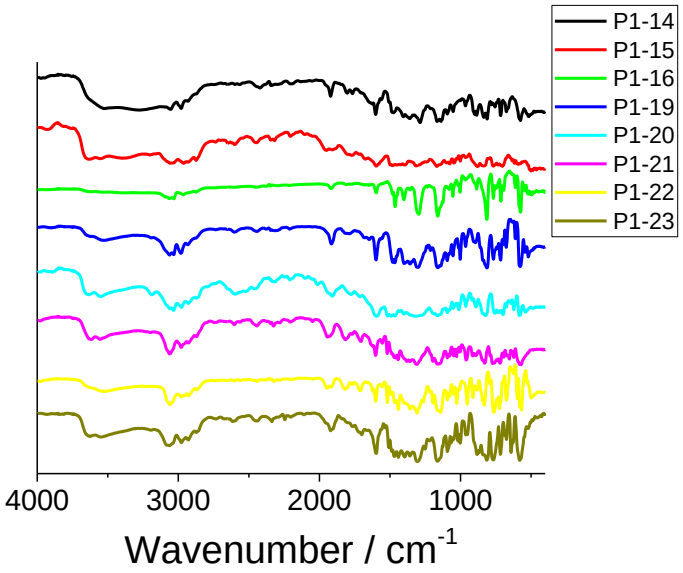

Figure S-19. Transmission FT-IR spectra of P1-14 to P1-23.

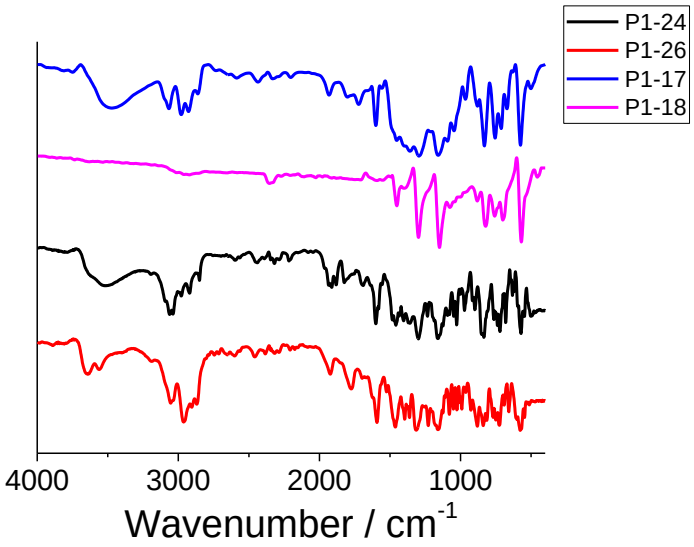

Figure S-20. Transmission FT-IR spectra of P1-17 to P1-26.

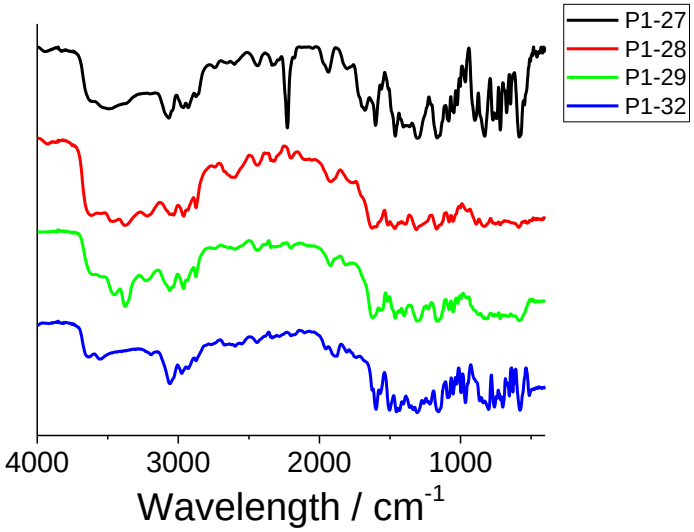

Figure S-21. Transmission FT-IR spectra of P1-27 to P1-32.

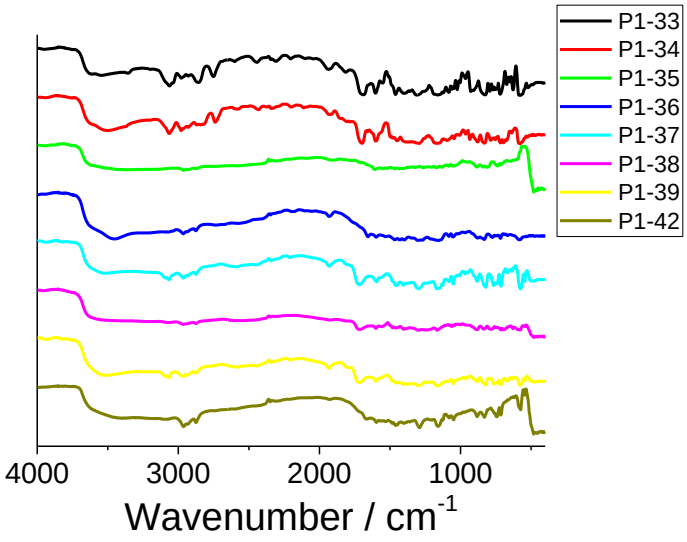

Figure S-22. Transmission FT-IR spectra of P1-33 to P1-42.

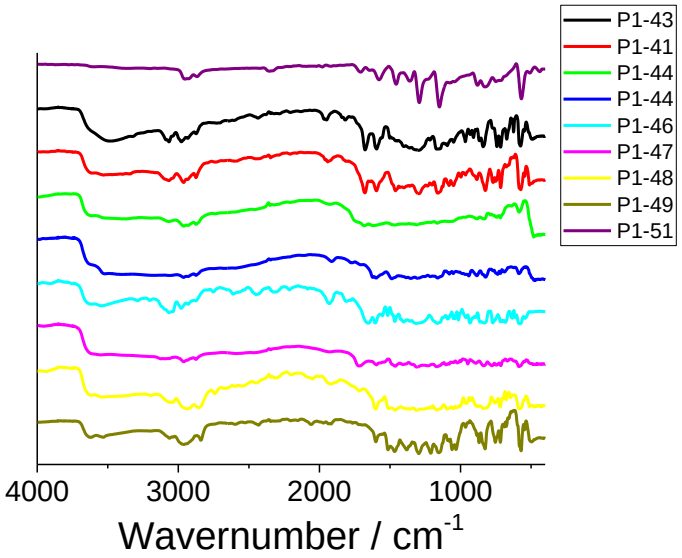

Figure S-23. Transmission FT-IR spectra of P1-43 to P1-51.

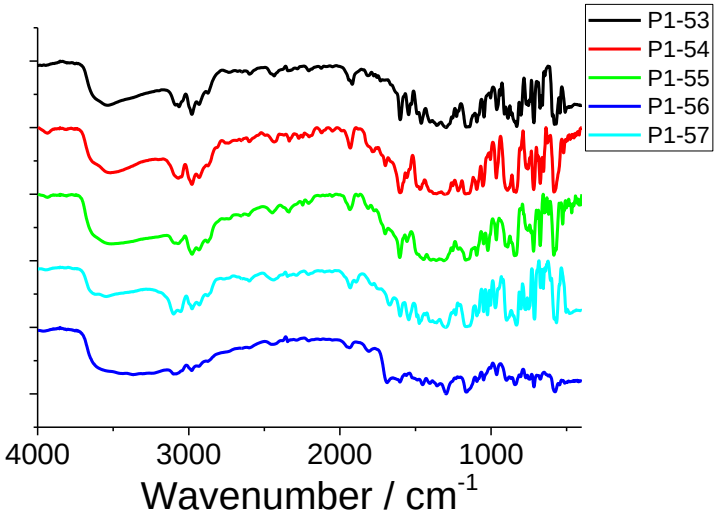

Figure S-24. Transmission FT-IR spectra of P1-52 to P1-56.

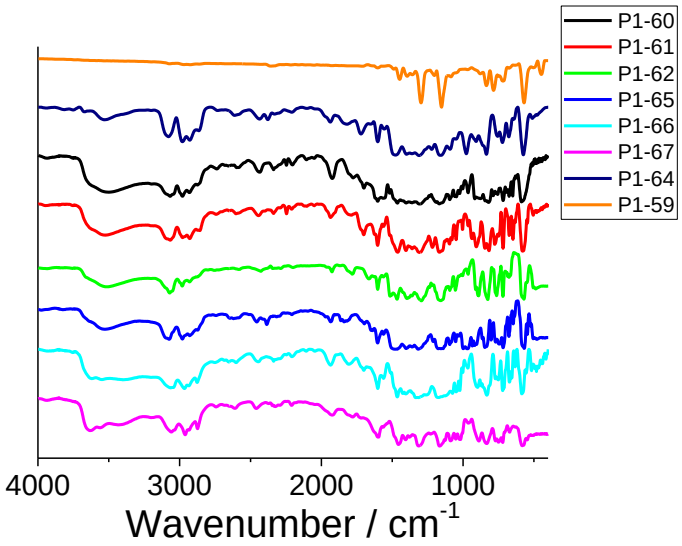

Figure S-25. Transmission FT-IR spectra of P1-59 to P1-67.

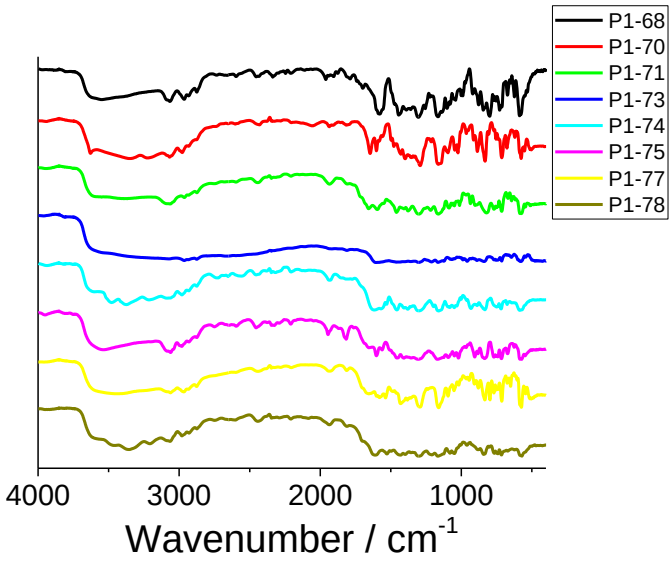

Figure S-26. Transmission FT-IR spectra of P1-68 to P1-78.

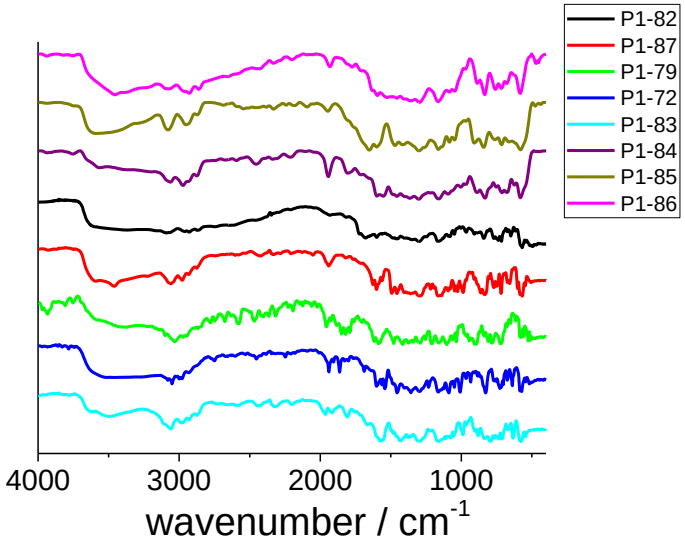

Figure S-27. Transmission FT-IR spectra of P1-72 to P1-87.

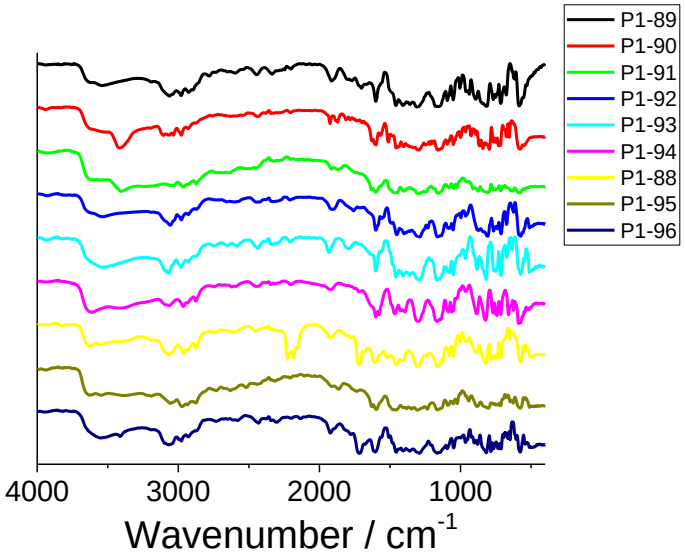

Figure S-28. Transmission FT-IR spectra of P1-88 to P1-96.

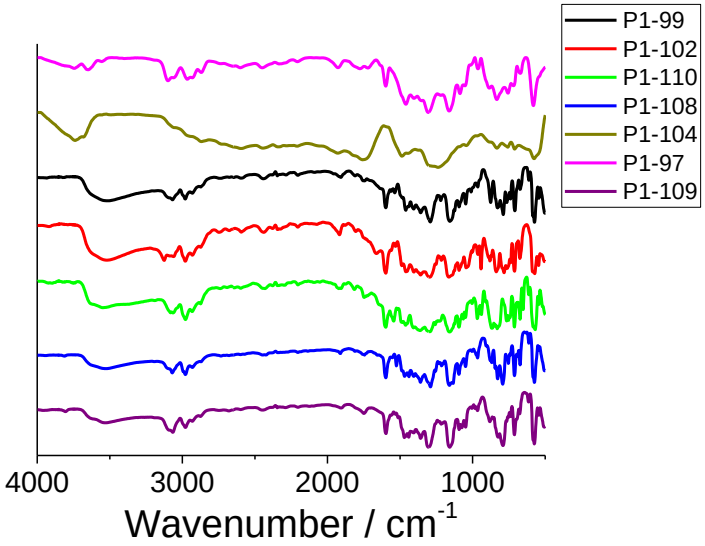

Figure S-29. Transmission FT-IR spectra of P1-97 to P1-110.

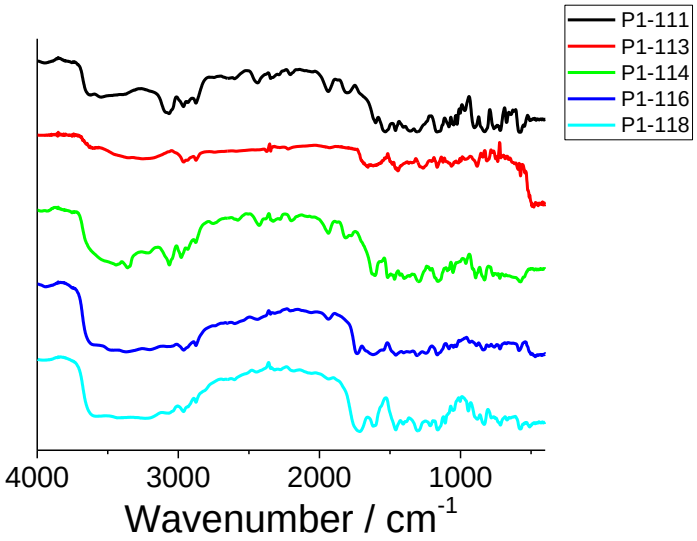

Figure S-30. Transmission FT-IR spectra of P1-111 to P1-118.

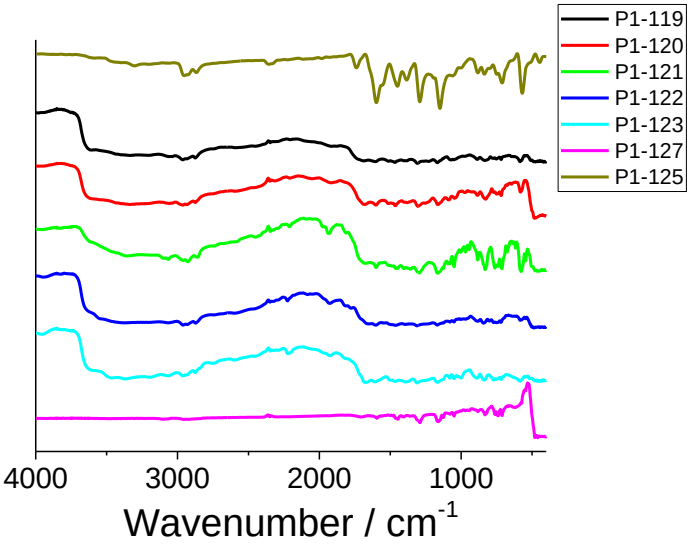

Figure S-31. Transmission FT-IR spectra of P1-119 to P1-127.

3.3 Powder X-ray diffraction patterns

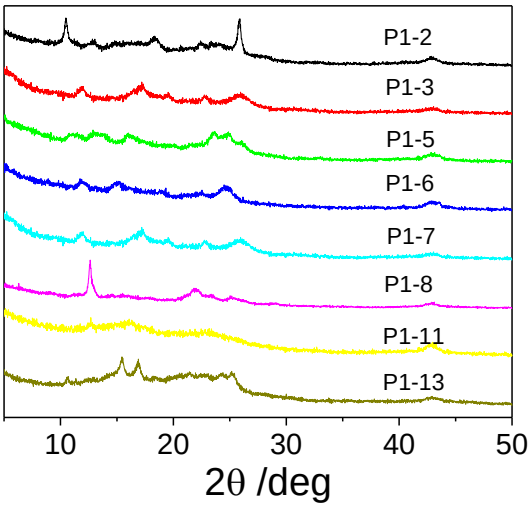

Figure S-32. PXRD patterns for P1-2 to P1-13.

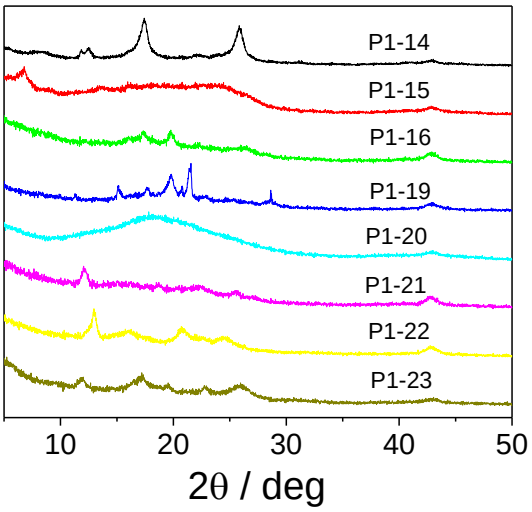

Figure S-33. PXRD patterns for P1-14 to P1-23.

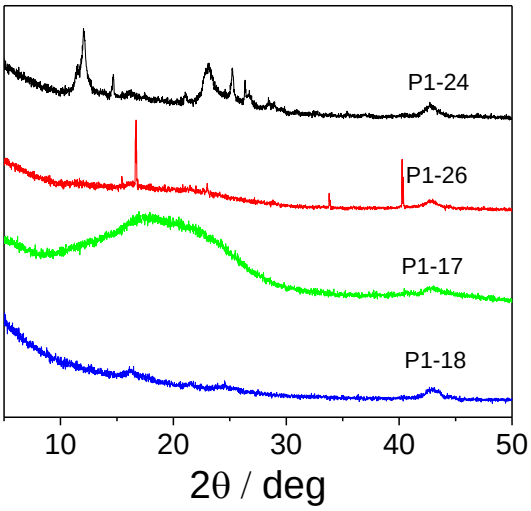

Figure S-34. PXRD patterns for P1-17 to P1-26.

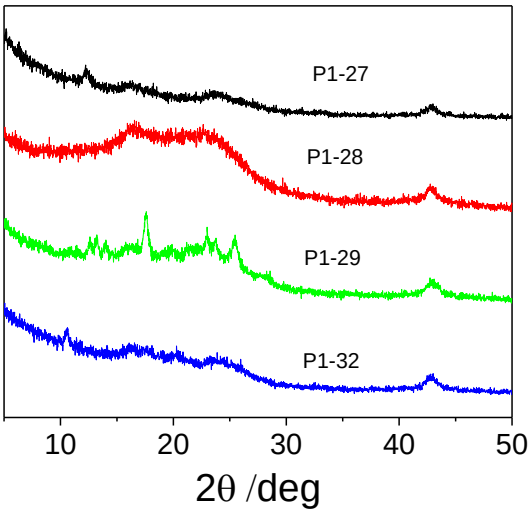

Figure S-35. PXRD patterns for P1-27 to P1-32.

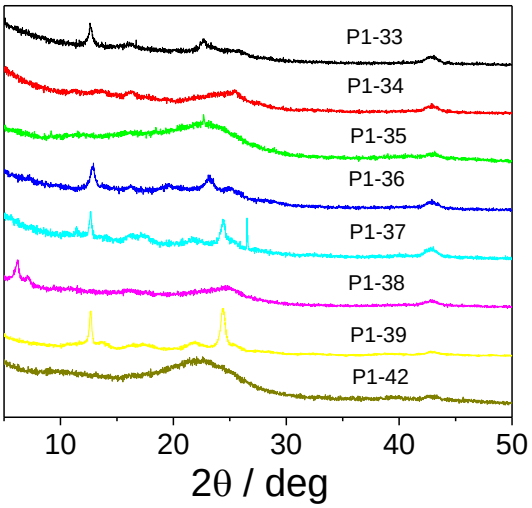

Figure S-36. PXRD patterns for P1-33 to P1-42.

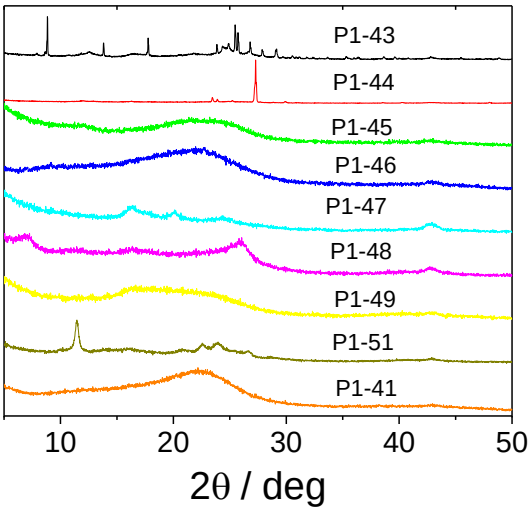

Figure S-37. PXRD patterns for P1-41 to P1-51.

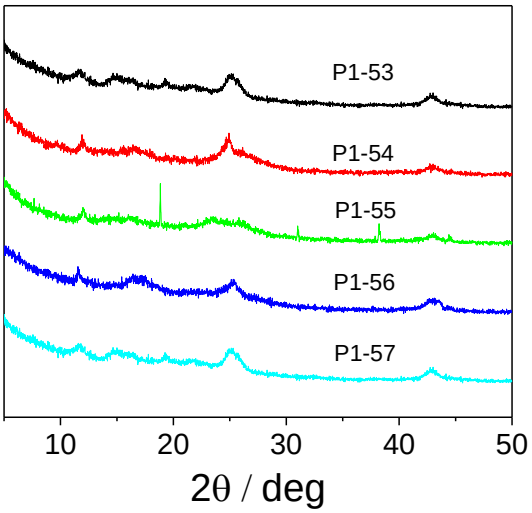

Figure S-38. PXRD patterns for P1-53 to P1-57.

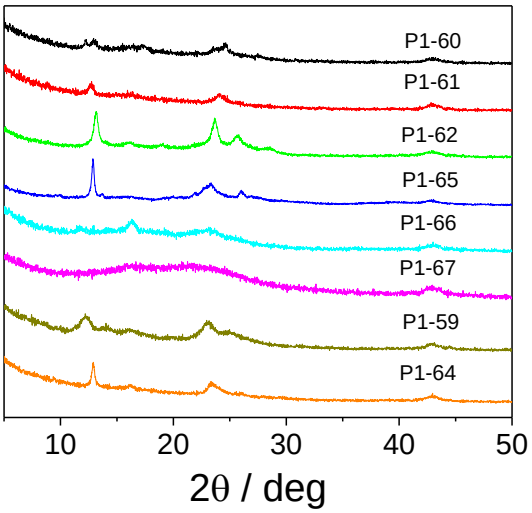

Figure S-39. PXRD patterns for P1-59 to P1-67.

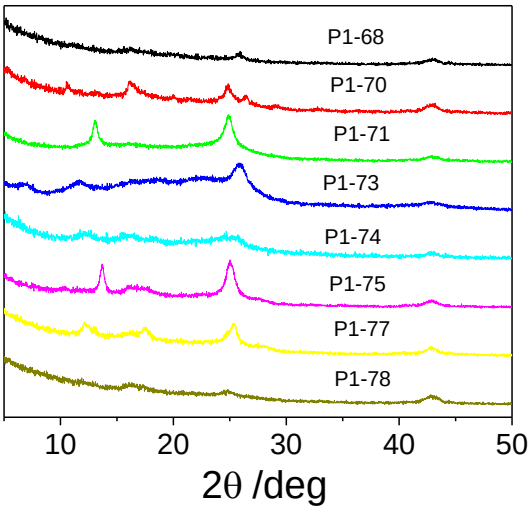

Figure S-40. PXRD patterns for P1-68 to P1-78.

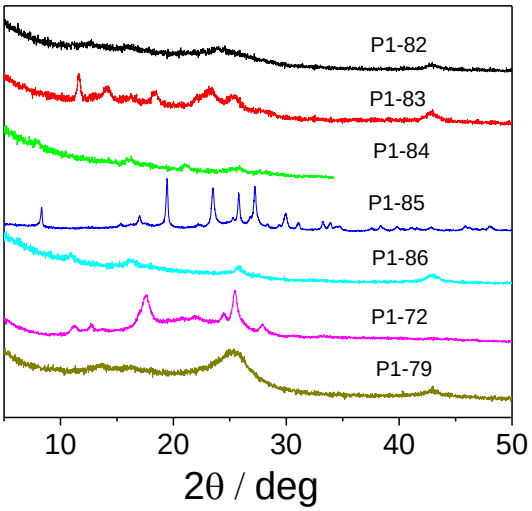

Figure S-41. PXRD patterns for P1-72 to P1-86.

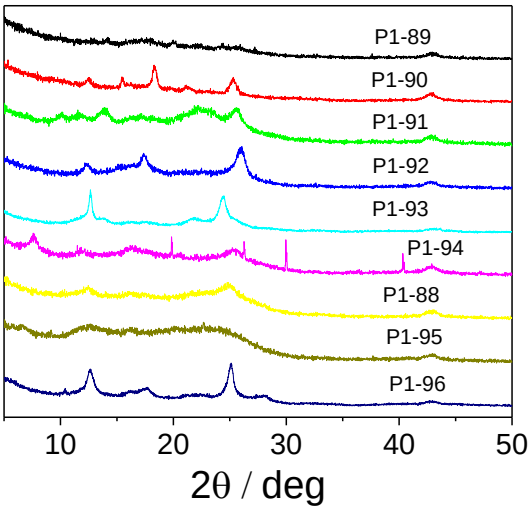

Figure S-42. PXRD patterns for P1-88 to P1-96.

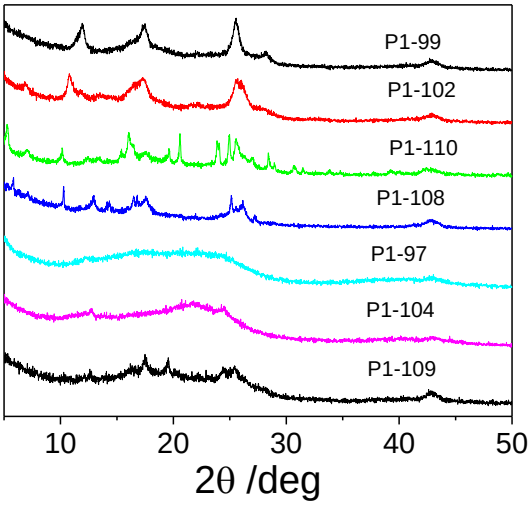

Figure S-43. PXRD patterns for P1-97 to P1-110.

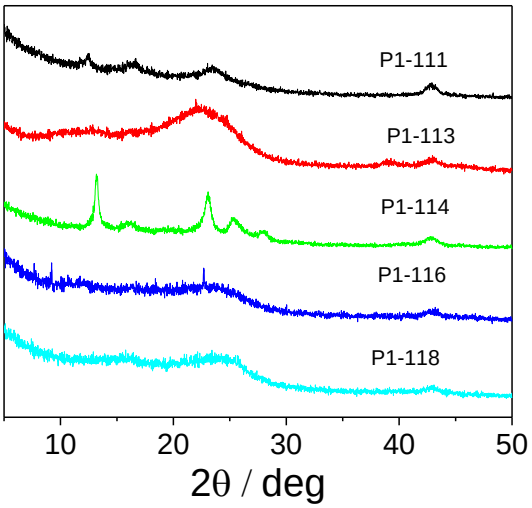

Figure S-44. PXRD patterns for P1-110 to P1-118.

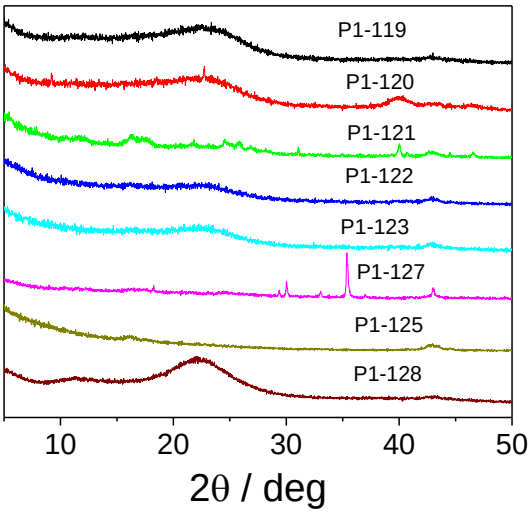

Figure S-45. PXRD patterns for P1-120 to P1-128.

3.4 High-throughput gas uptake experiments

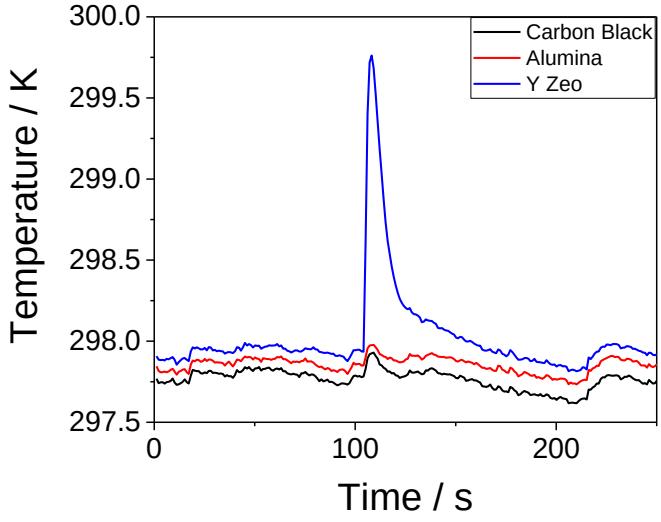

Figure S-46. Temperature change of carbon black, alumina, and Y zeolite after exposure to a dose of CO_2 after being under reduced pressure. The temperature change can be related to surface area measured via CO_2 sorption (carbon black: SA_{BET} = 21 m^2 g^{-1}); alumina: SA_{BET} = 0.5 m^2 g^{-1}; Y zeolite: SA_{BET} = 670 m^2 g^{-1}).

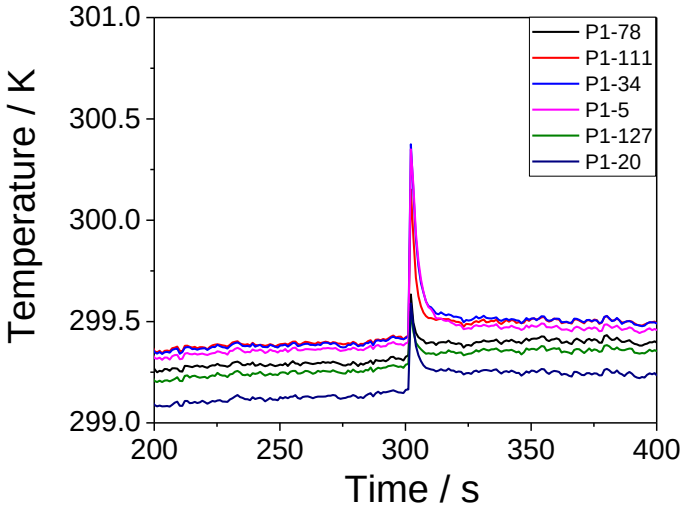

Figure S-47. Temperature change of sulfone co-polymers after exposure to a dose of CO_2 after being under reduced pressure.

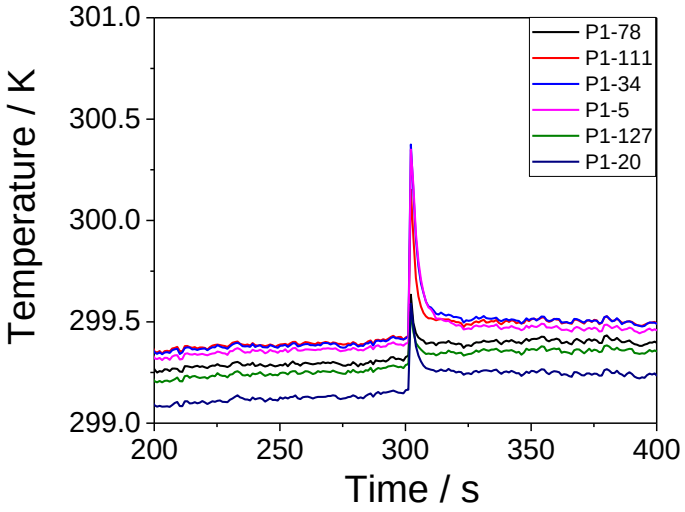

Figure S-48. Temperature change of sulfone co-polymers after exposure to a dose of CO_2 after being under reduced pressure.

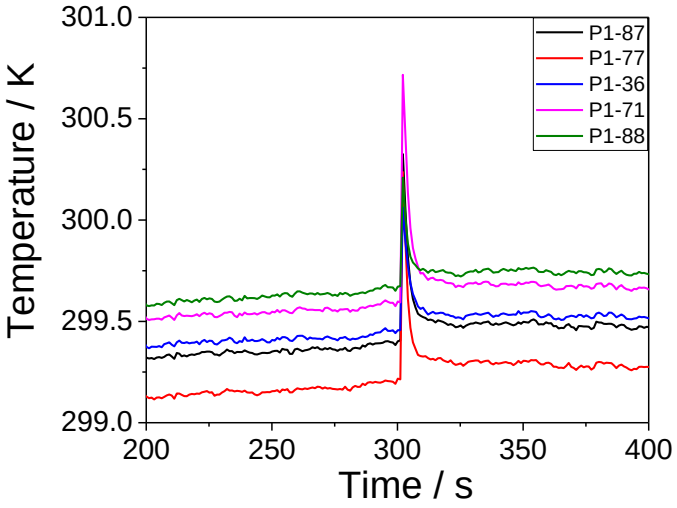

Figure S-49. Temperature change of sulfone co-polymers after exposure to a dose of CO_2 after being under reduced pressure.

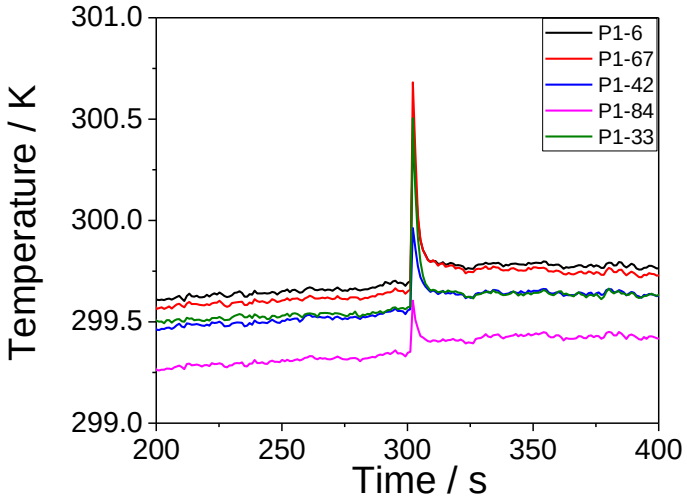

Figure S-50. Temperature change of sulfone co-polymers after exposure to a dose of CO_2 after being under reduced pressure.

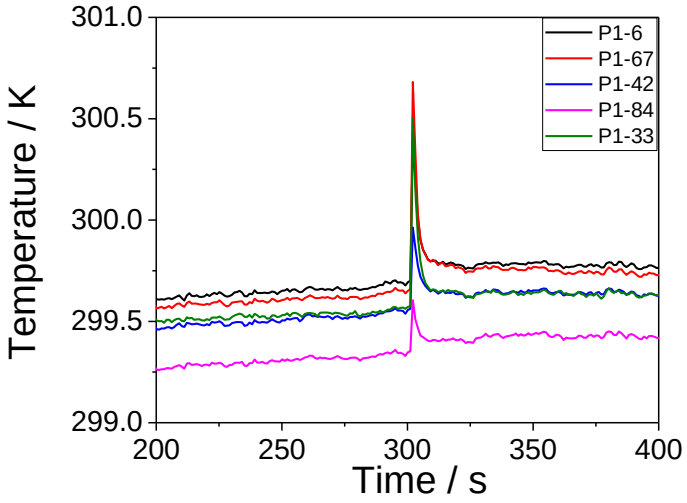

Figure S-51. Temperature change of sulfone co-polymers after exposure to a dose of CO_2 after being under reduced pressure.

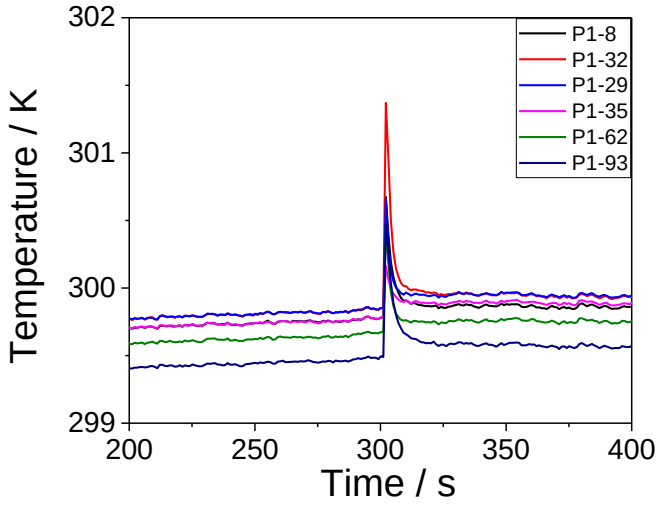

Figure S-52. Temperature change of sulfone co-polymers after exposure to a dose of CO_2 after being under reduced pressure.

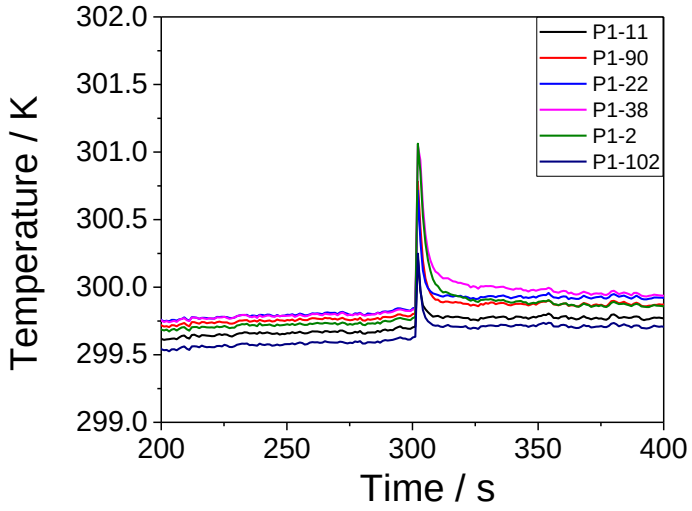

Figure S-53. Temperature change of sulfone co-polymers after exposure to a dose of CO_2 after being under reduced pressure.

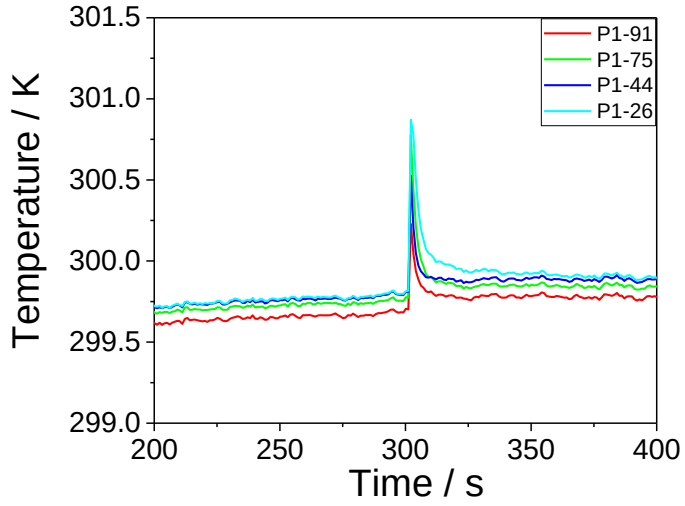

Figure S-54. Temperature change of sulfone co-polymers after exposure to a dose of CO_2 after being under reduced pressure.

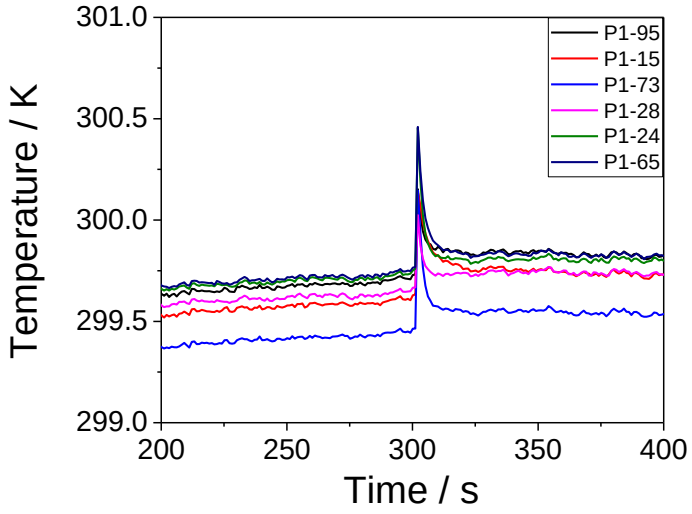

Figure S-55. Temperature change of sulfone co-polymers after exposure to a dose of CO_2 after being under reduced pressure.

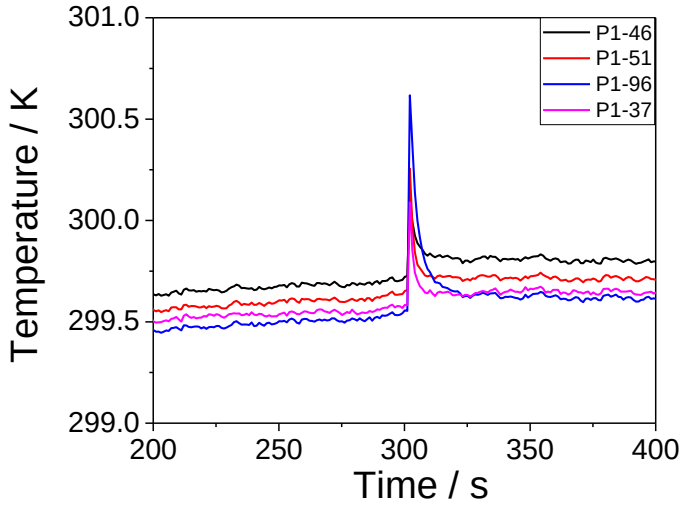

Figure S-56. Temperature change of sulfone co-polymers after exposure to a dose of CO_2 after being under reduced pressure.

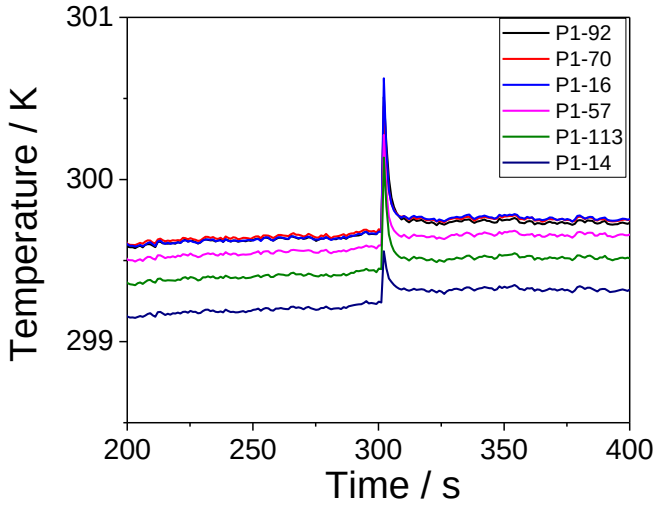

Figure S-57. Temperature change of sulfone co-polymers after exposure to a dose of CO_2 after being under reduced pressure.

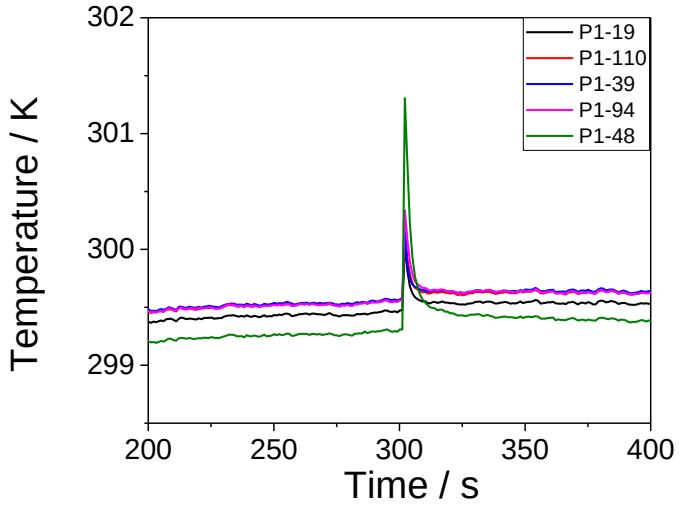

Figure S-58. Temperature change of sulfone co-polymers after exposure to a dose of CO_2 after being under reduced pressure.

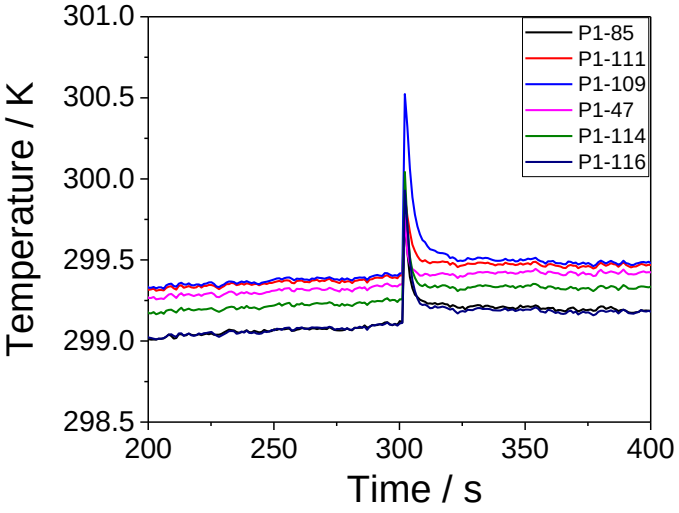

Figure S-59. Temperature change of sulfone co-polymers after exposure to a dose of CO_2 after being under reduced pressure.

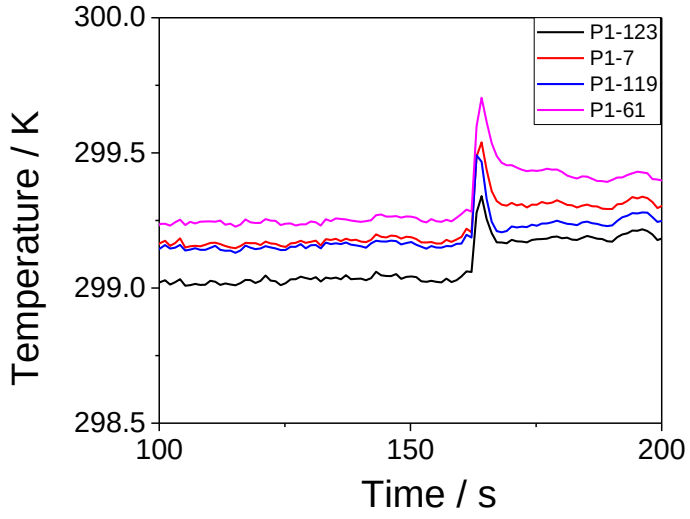

Figure S-60. Temperature change of sulfone co-polymers after exposure to a dose of CO_2 after being under reduced pressure.

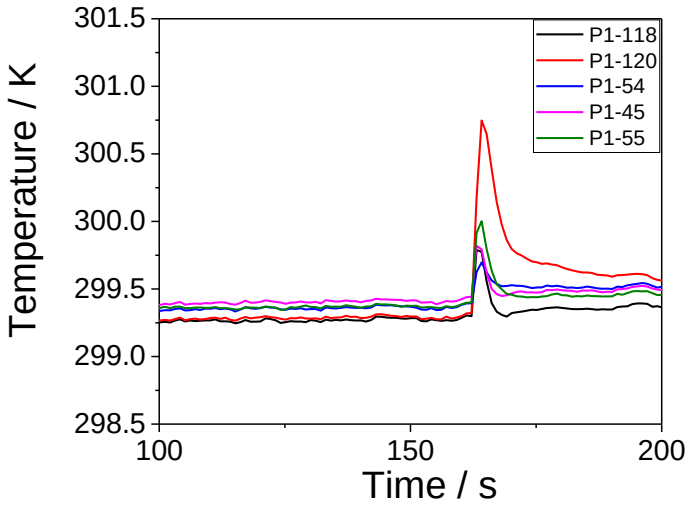

Figure S-61. Temperature change of sulfone co-polymers after exposure to a dose of CO_2 after being under reduced pressure.

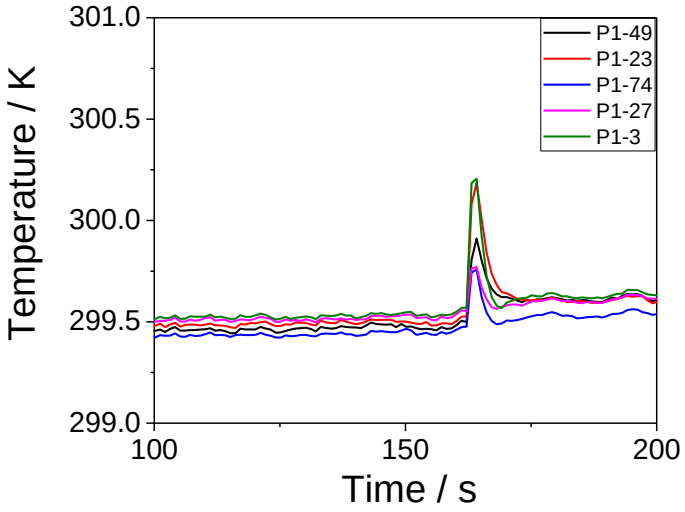

Figure S-62. Temperature change of sulfone co-polymers after exposure to a dose of CO_2 after being under reduced pressure.

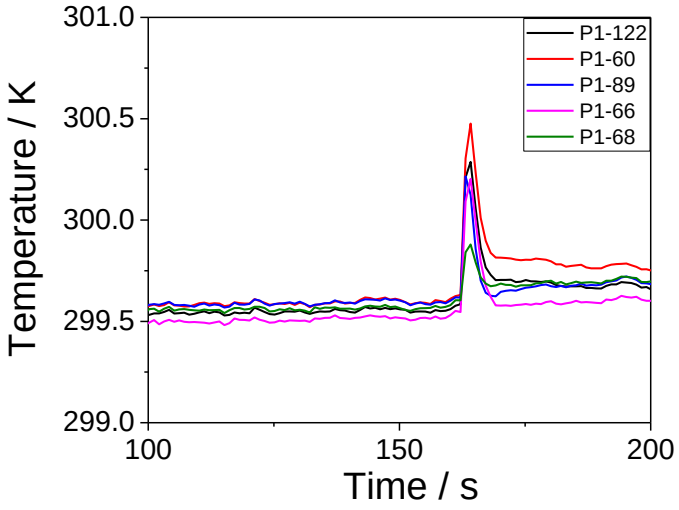

Figure S-63. Temperature change of sulfone co-polymers after exposure to a dose of CO_2 after being under reduced pressure.

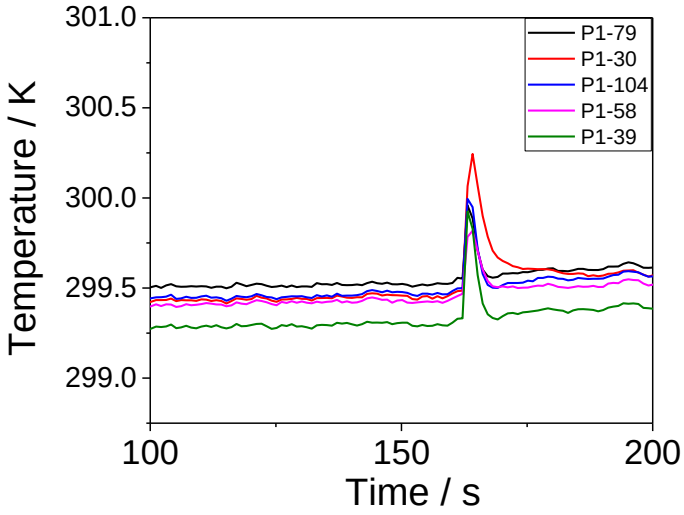

Figure S-64. Temperature change of sulfone co-polymers after exposure to a dose of CO_2 after being under reduced pressure.

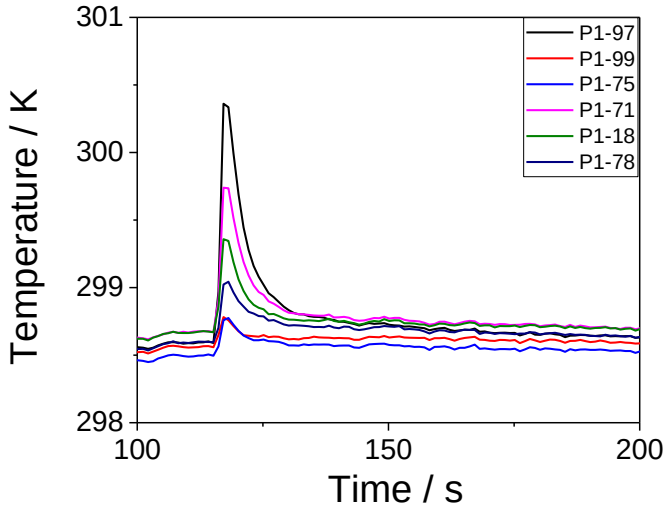

Figure S-65. Temperature change of sulfone co-polymers after exposure to a dose of CO_2 after being under reduced pressure.

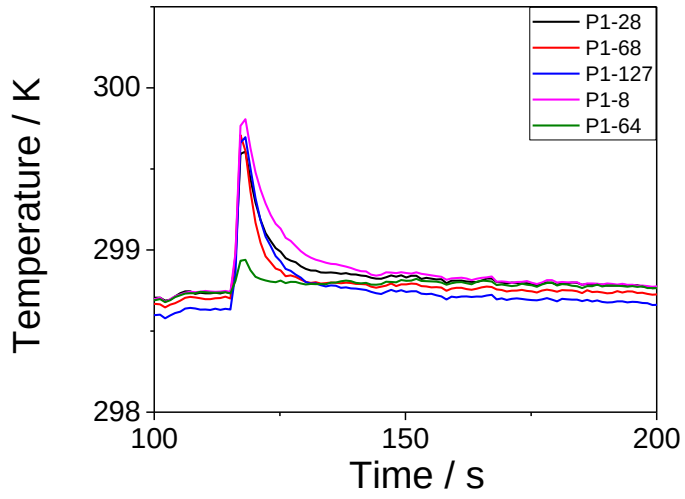

Figure S-66. Temperature change of sulfone co-polymers after exposure to a dose of CO_2 after being under reduced pressure.

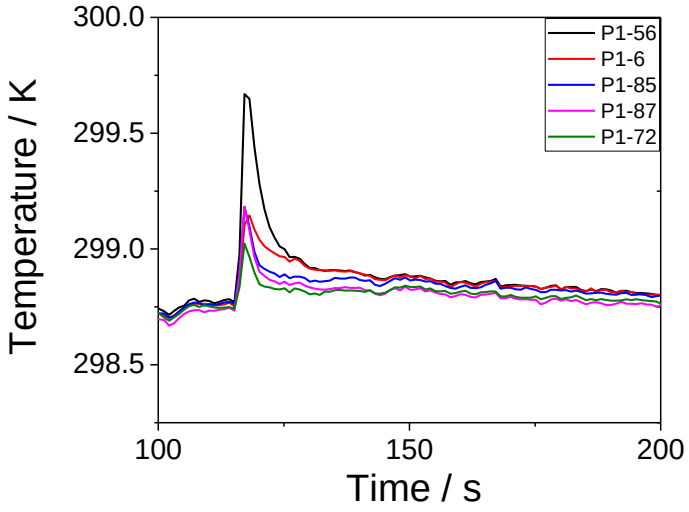

Figure S-67. Temperature change of sulfone co-polymers after exposure to a dose of CO_2 after being under reduced pressure.

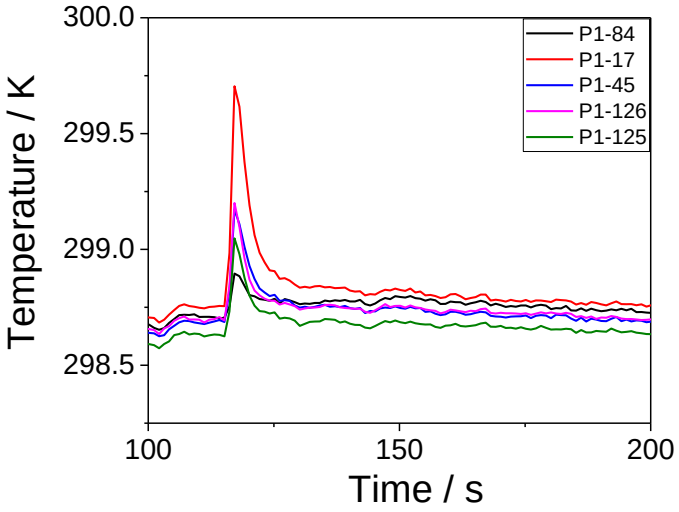

Figure S-68. Temperature change of sulfone co-polymers after exposure to a dose of CO_2 after being under reduced pressure.

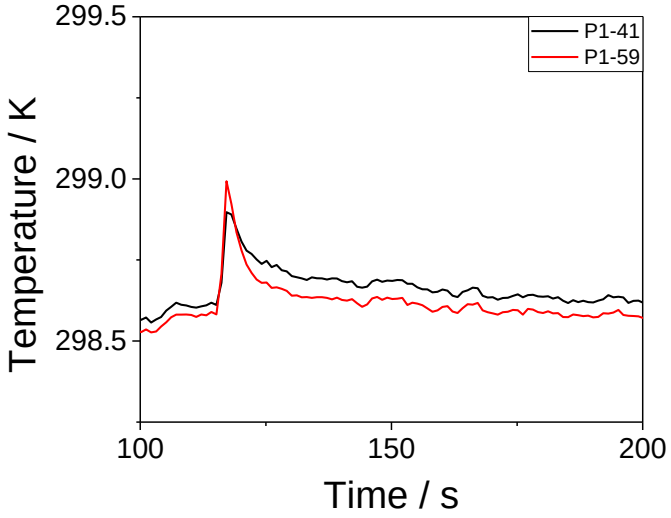

Figure S-69. Temperature change of sulfone co-polymers after exposure to a dose of CO_2 after being under reduced pressure.

3.5 Hydrogen performance with and without added Pt co-catalyst

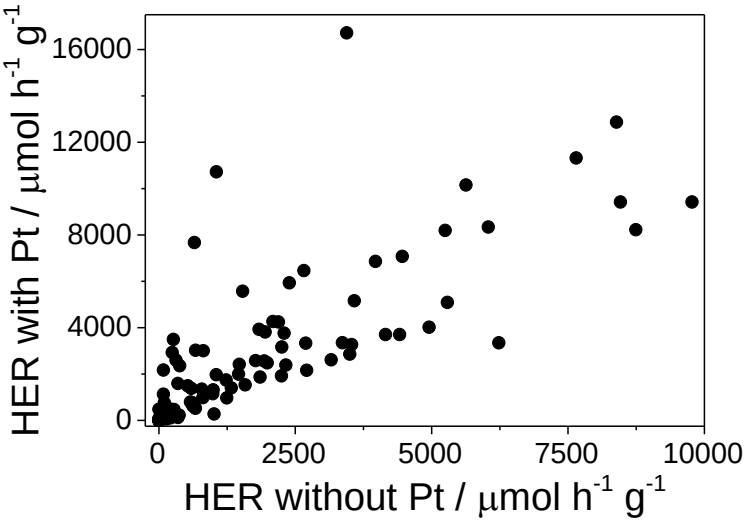

Figure S-70. Photocatalytic hydrogen evolution rate (HER) of polymer photocatalysts without additional Pt from TEA/MeOH/H_2O mixtures plotted against the photocatalytic HER of the same catalysts with added Pt (from H_2PtCl_6, 8 wt. % solution) from TEA/MeOH/H_2O mixtures. 5 mg polymer was suspended in 5 mL water/methanol/triethylamine solution, irradiated by a solar simulator (AM1.5G, Class AAA, IEC/JIS/ASTM, 1440 W xenon, 12 × 12 in., MODEL: 94123A, illumination time: 1 hour).

3.6 Transmittance of samples *vs.* HER

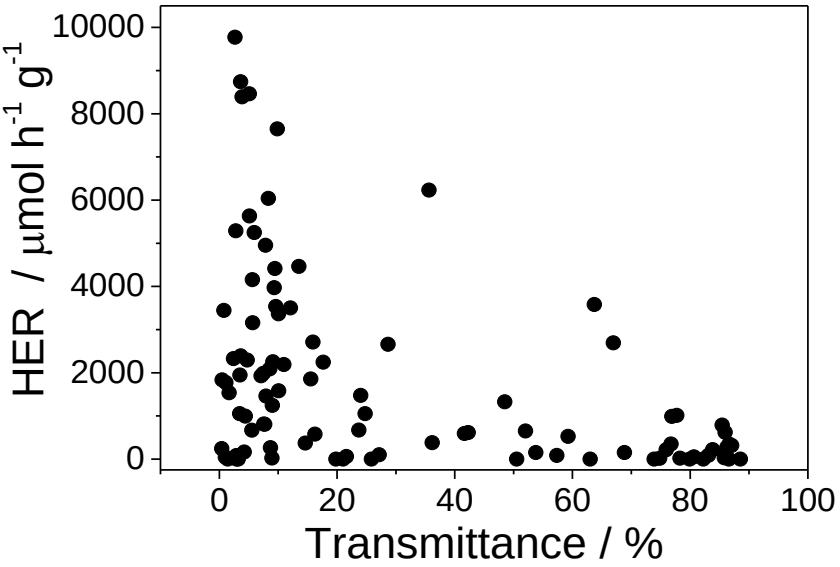

Figure S-71. Photocatalytic hydrogen evolution rate (HER) of polymer photocatalysts from TEA/MeOH/H_2O mixtures plotted against the sample's transmittance in this suspension. Polymer (5 mg) was suspended in 5 mL water/methanol/triethylamine solution, irradiated by a solar simulator (AM1.5G, Class AAA, IEC/JIS/ASTM, 1440 W xenon, 12 × 12 in., MODEL: 94123A, illumination time, 1 hour).

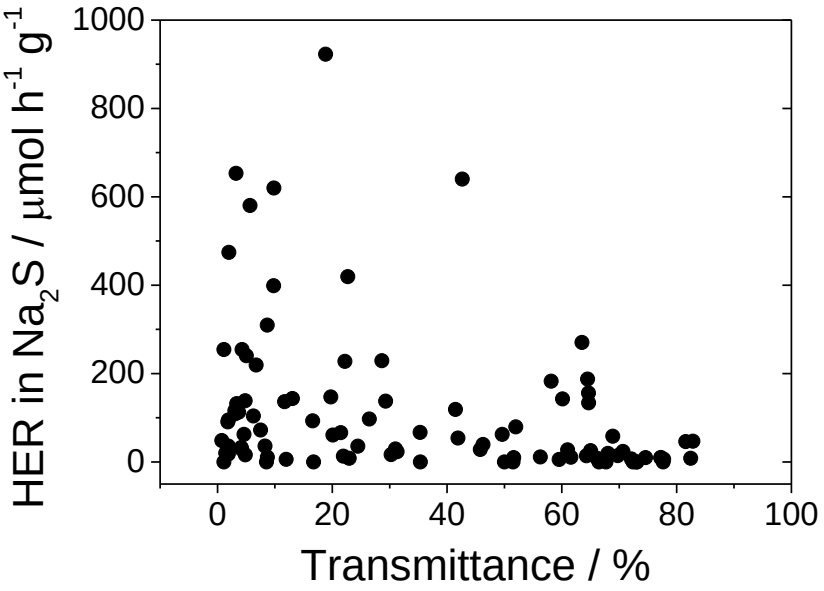

Figure S-72. Photocatalytic hydrogen evolution rate (HER) of polymer photocatalysts from aqueous Na_2S plotted against the sample's transmittance in this suspension. Polymer (5 mg) was suspended in 5 mL of 0.026 M Na_2S aqueous solution, irradiated by a solar simulator (AM1.5G, Class AAA, IEC/JIS/ASTM, 1440 W xenon, 12 × 12 in., MODEL: 94123A, illumination time: 3 hours).

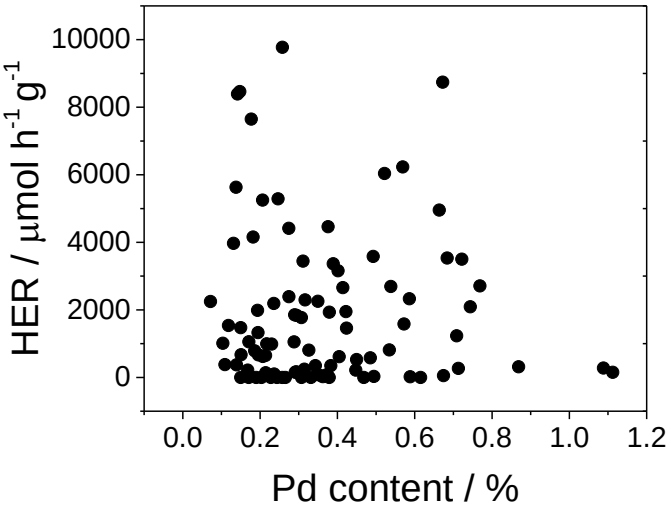

Figure S-73. Photocatalytic hydrogen evolution rate (HER) of polymer photocatalysts from aqueous TEA/MeOH/water plotted against the sample's palladium content.

3.7 Normalized HER *vs.* HT Polymers Characterization

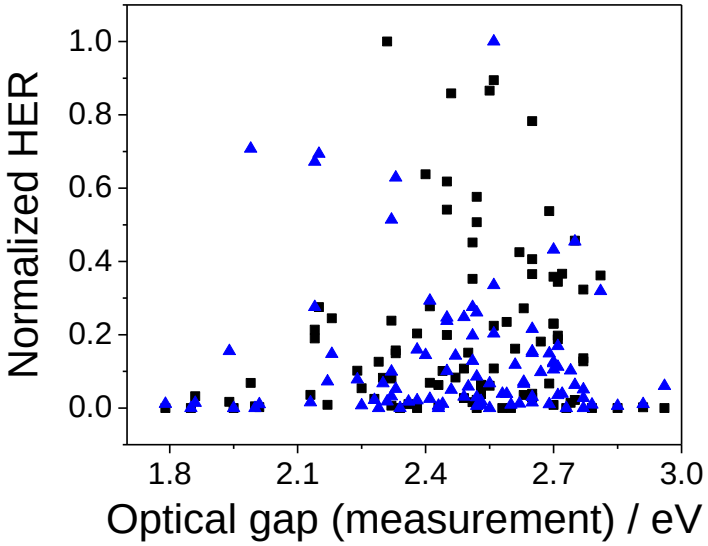

Figure S-74. Min-max normalized photocatalytic hydrogen evolution rates (HER) of photocatalysts under different conditions correlated with the polymers optical gap. The data of the three scavenger systems was subjected to a min-max normalization [0, 1] separately, whereby 1 was assigned to the highest HER, samples that have no HER are given a value of 0 and all other samples within the set are scaled accordingly. Conditions: TEA/MeOH/H_2O (black square), Na_2S (blue triangle). Polymer (5 mg) was suspended in 5 mL water/methanol/triethylamine solution or 0.026 M Na_2S aqueous solution, irradiated by a solar simulator [AM1.5G, Class AAA, IEC/JIS/ASTM, 1440 W xenon, 12 × 12 in., MODEL: 94123A. Illumination time (TEA/MeOH/H_2O): 1 hour; illumination time (Na_2S): 3 hours].

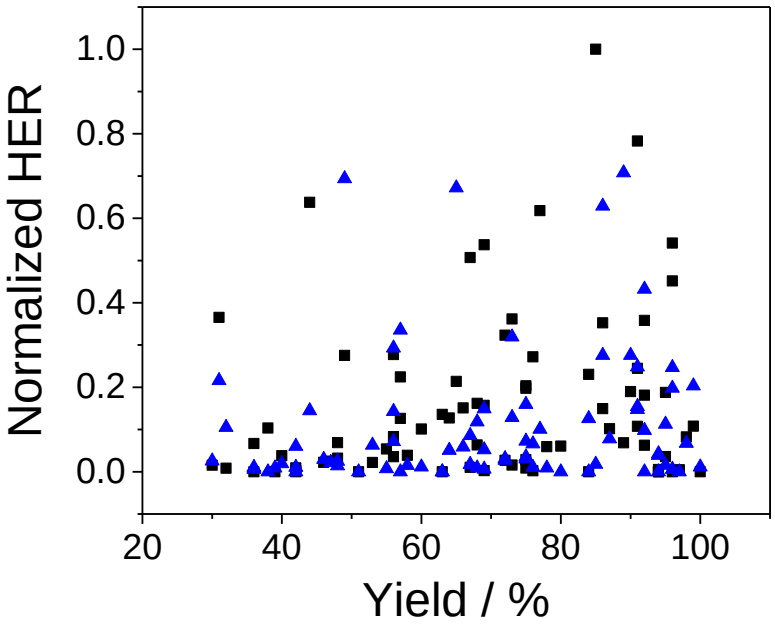

Figure S-75. Min-max normalized photocatalytic hydrogen evolution rates (HER) of photocatalysts under different conditions correlated with the polymers synthesis yield. The data of the three scavenger systems was subjected to a min-max normalization [0, 1] separately, whereby 1 was assigned to the highest HER, samples that have no HER are given a value of 0 and all other samples within the set are scaled accordingly. Conditions: TEA/MeOH/H_2O (black square), Na_2S (blue triangle). Polymer (5 mg) was suspended in 5 mL water/methanol/triethylamine solution or 0.026 M Na_2S aqueous solution, irradiated by a solar simulator [AM1.5G, Class AAA, IEC/JIS/ASTM, 1440 W xenon, 12 × 12 in., MODEL: 94123A. Illumination time (TEA/MeOH/H_2O): 1 hour; illumination time (Na_2S): 3 hours].

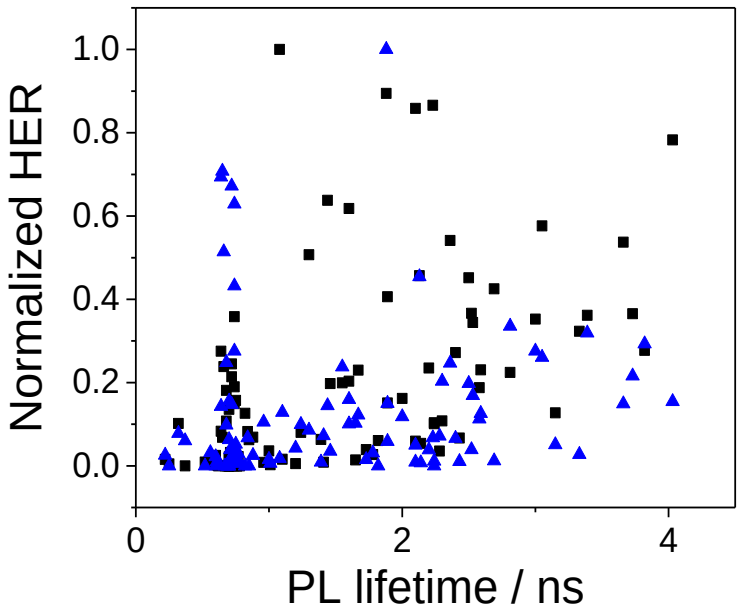

Figure S-76. Min-max normalized photocatalytic hydrogen evolution rates (HER) of photocatalysts under different conditions correlated with the polymers PL lifetime. The data of the three scavenger systems was subjected to a min-max normalization [0, 1] separately, whereby 1 was assigned to the highest HER, samples that have no HER are given a value of 0 and all other samples within the set are scaled accordingly. Conditions: TEA/MeOH/H_2O (black square), Na_2S (blue triangle). Polymer (5 mg) was suspended in 5 mL water/methanol/triethylamine solution or 0.026 M Na_2S aqueous solution, irradiated by a solar simulator [AM1.5G, Class AAA, IEC/JIS/ASTM, 1440 W xenon, 12 × 12 in., MODEL: 94123A. Illumination time (TEA/MeOH/H_2O): 1 hour; illumination time (Na_2S): 3 hours].

3.8 Computational parameters *vs.* HER

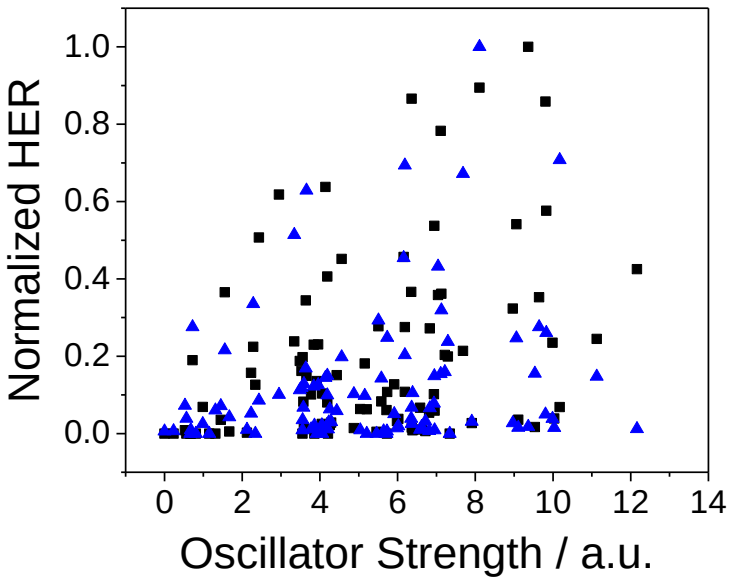

Figure S-77. Min-max normalized photocatalytic hydrogen evolution rates (HER) of photocatalysts under different conditions correlated with the polymers oscillator strength. The data of the three scavenger systems was subjected to a min-max normalization [0, 1] separately, whereby 1 was assigned to the highest HER, samples that have no HER are given a value of 0 and all other samples within the set are scaled accordingly. Conditions: TEA/MeOH/H_2O (black square), Na_2S (blue triangle). Polymer (5 mg) was suspended in 5 mL water/methanol/triethylamine solution or 0.026 M Na_2S aqueous solution, irradiated by a solar simulator [AM1.5G, Class AAA, IEC/JIS/ASTM, 1440 W xenon, 12 × 12 in., MODEL: 94123A. Illumination time (TEA/MeOH/H_2O): 1 hour; illumination time (Na_2S): 3 hours].

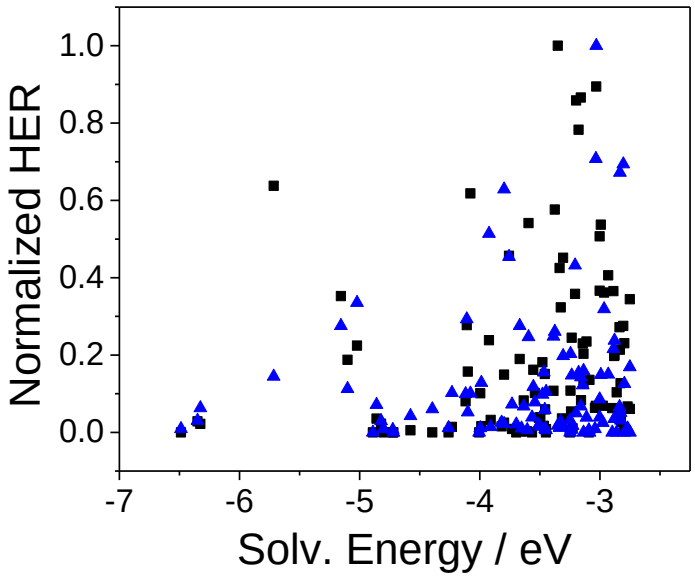

Figure S-78. Min-max normalized photocatalytic hydrogen evolution rates (HER) of photocatalysts under different conditions correlated with the polymers solvent free energy. The data of the three scavenger systems was subjected to a min-max normalization [0, 1] separately, whereby 1 was assigned to the highest HER, samples that have no HER are given a value of 0 and all other samples within the set are scaled accordingly. Conditions: TEA/MeOH/H_2O (black square), Na_2S (blue triangle). Polymer (5 mg) was suspended in 5 mL water/methanol/triethylamine solution or 0.026 M Na_2S aqueous solution, irradiated by a solar simulator [AM1.5G, Class AAA, IEC/JIS/ASTM, 1440 W xenon, 12 × 12 in., MODEL: 94123A. Illumination time (TEA/MeOH/H_2O): 1 hour; illumination time (Na_2S): 3 hours].

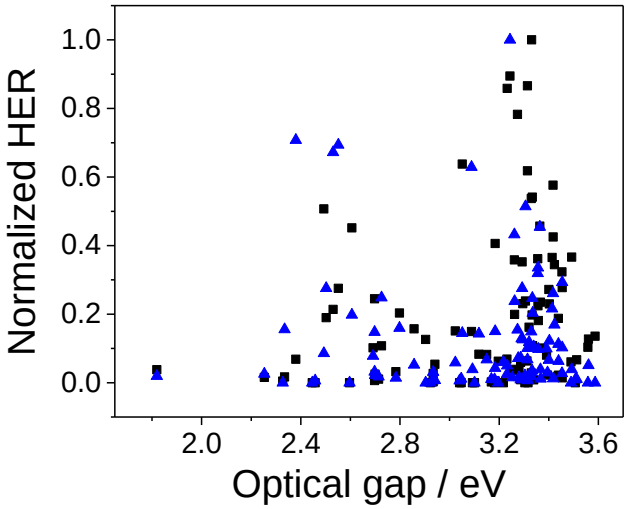

Figure S-79. Min-max normalized photocatalytic hydrogen evolution rates (HER) of photocatalysts under different conditions correlated with the polymers optical gap from calculation. The data of the two scavenger systems was subjected to a min-max normalization [0, 1] separately, whereby 1 was assigned to the highest HER, samples that have no HER are given a value of 0 and all other samples within the set are scaled accordingly. Conditions: TEA/MeOH/H_2O (black square), Na_2S (blue triangle). Polymer (5 mg) was suspended in 5 mL water/methanol/triethylamine solution or 0.026 M Na_2S aqueous solution, irradiated by a solar simulator [AM1.5G, Class AAA, IEC/JIS/ASTM, 1440 W xenon, 12 × 12 in., MODEL: 94123A. Illumination time (TEA/MeOH/H_2O): 1 hour; illumination time (Na_2S): 3 hours].

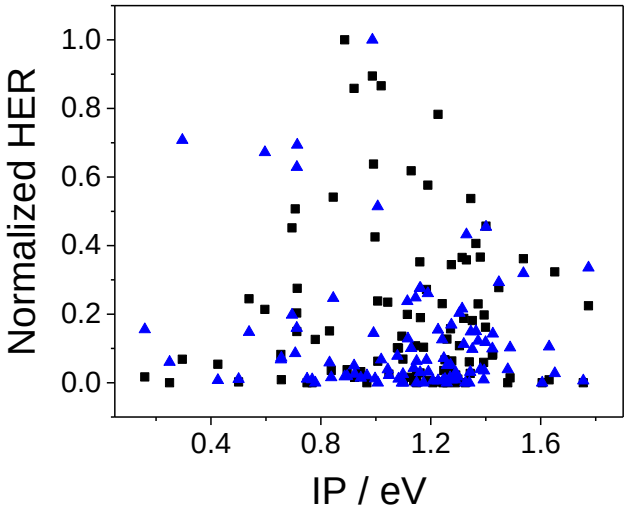

Figure S-80. Min-max normalized photocatalytic hydrogen evolution rates (HER) of photocatalysts under different conditions correlated with the polymers ionisation potential (IP). The data of the two scavenger systems was subjected to a min-max normalization [0, 1] separately, whereby 1 was assigned to the highest HER, samples that have no HER are given a value of 0 and all other samples within the set are scaled accordingly. Conditions: TEA/MeOH/H_2O (black square), Na_2S (blue triangle). Polymer (5 mg) was suspended in 5 mL water/methanol/triethylamine solution or 0.026 M Na_2S aqueous solution, irradiated by a solar simulator [AM1.5G, Class AAA, IEC/JIS/ASTM, 1440 W xenon, 12 × 12 in., MODEL: 94123A. Illumination time (TEA/MeOH/H_2O): 1 hour; illumination time (Na_2S): 3 hours].

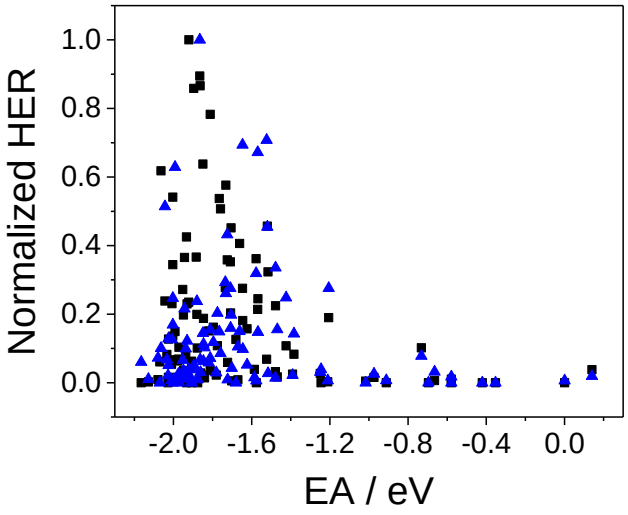

Figure S-81. Min-max normalized photocatalytic hydrogen evolution rates (HER) of photocatalysts under different conditions correlated with the polymers electron affinity (EA). The data of the two scavenger systems was subjected to a min-max normalization [0, 1] separately, whereby 1 was assigned to the highest HER, samples that have no HER are given a value of 0 and all other samples within the set are scaled accordingly. Conditions: TEA/MeOH/H_2O (black square), Na_2S (blue triangle). Polymers (5 mg) was suspended in 5 mL water/methanol/triethylamine solution or 0.026 M Na_2S aqueous solution, irradiated by a solar simulator [AM1.5G, Class AAA, IEC/JIS/ASTM, 1440 W xenon, 12 × 12 in., MODEL: 94123A. Illumination time (TEA/MeOH/H_2O): 1 hour; illumination time (Na_2S): 3 hours].

3.9 Energy potential *vs.* transmittance *vs.* HER

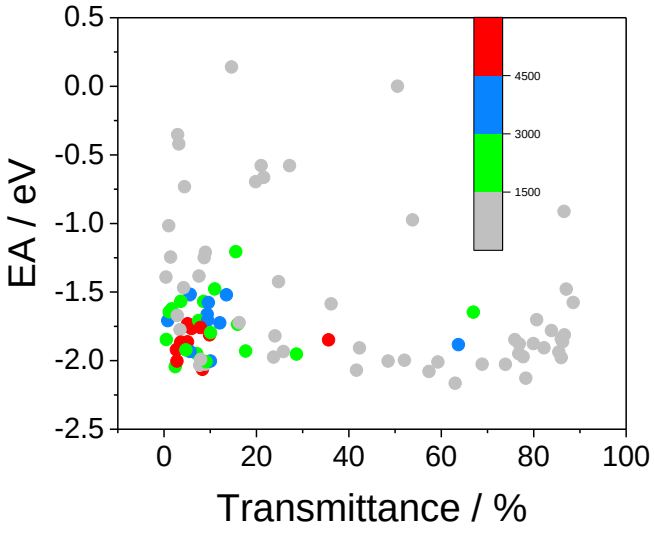

Figure S-82. Photocatalytic hydrogen evolution rate (HER) of photocatalysts from TEA/MeOH/H_2O mixtures plotted against both the polymer's electron affinity (EA) and the sample's transmittance in suspension. Polymer (5 mg) was suspended in 5 mL water/methanol/triethylamine solution irradiated by a solar simulator (AM1.5G, Class AAA, IEC/JIS/ASTM, 1440 W xenon, 12 × 12 in., MODEL: 94123A, illumination time: 1 hour).

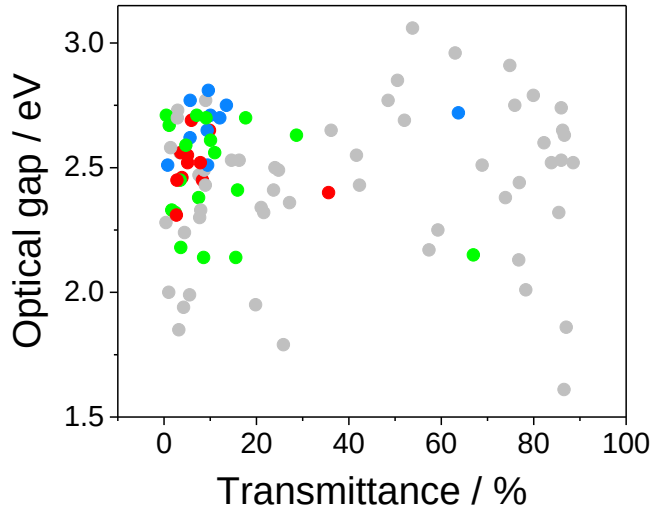

Figure S-83. Photocatalytic hydrogen evolution rate (HER) of photocatalysts from TEA/MeOH/H_2O mixtures plotted against both the polymers optical gap and the sample's transmittance in suspension. Polymer (5 mg) was suspended in 5 mL water/methanol/triethylamine solution irradiated by a solar simulator (AM1.5G, Class AAA, IEC/JIS/ASTM, 1440 W xenon, 12 × 12 in., MODEL: 94123A, illumination time: 1 hour).

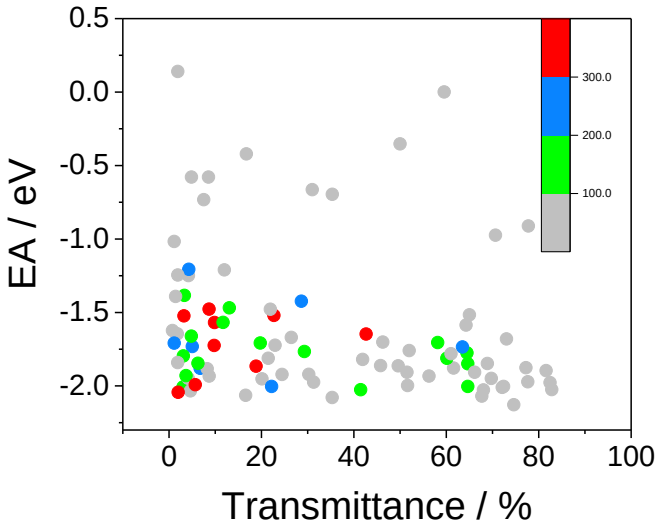

Figure S-84. Photocatalytic hydrogen evolution rate (HER) of photocatalysts from Na_2S aqueous plotted against both the polymers electron affinity (EA) and the sample's transmittance in suspension. Polymer (5 mg) was suspended in 0.026 M Na_2S aqueous solution, irradiated by a solar simulator (AM1.5G, Class AAA, IEC/JIS/ASTM, 1440 W xenon, 12 × 12 in., MODEL: 94123A, illumination time: 3 hours).

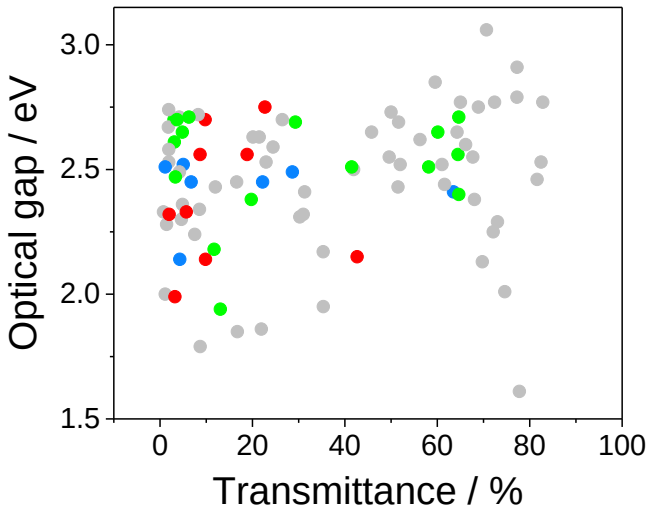

Figure S-85. Photocatalytic hydrogen evolution rate (HER) of photocatalysts from Na_2S aqueous plotted against both the polymers optical gap and the sample's transmittance in suspension. Polymer (5 mg) was suspended in 5 mL 0.026 M Na_2S aqueous solution, irradiated by a solar simulator (AM1.5G, Class AAA, IEC/JIS/ASTM, 1440 W xenon, 12 × 12 in., MODEL: 94123A, illumination time: 3 hours).

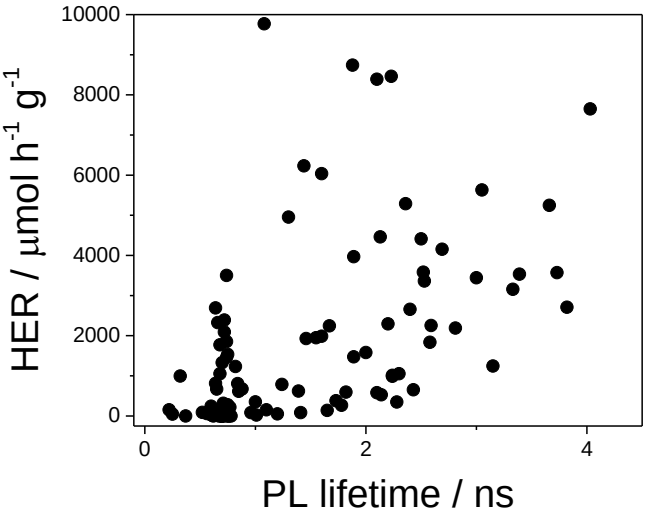

Figure S-86. Photocatalytic hydrogen evolution rates (HER) of photocatalysts from TEA/MeOH/H_2O mixtures plotted against the polymers PL lifetime. Polymer (5 mg) was suspended in 5 mL water/methanol/trimethylamine solution, irradiated by a solar simulator (AM1.5G, Class AAA, IEC/JIS/ASTM, 1440 W xenon, 12 × 12 in., MODEL: 94123A, illumination time: 1 hour).

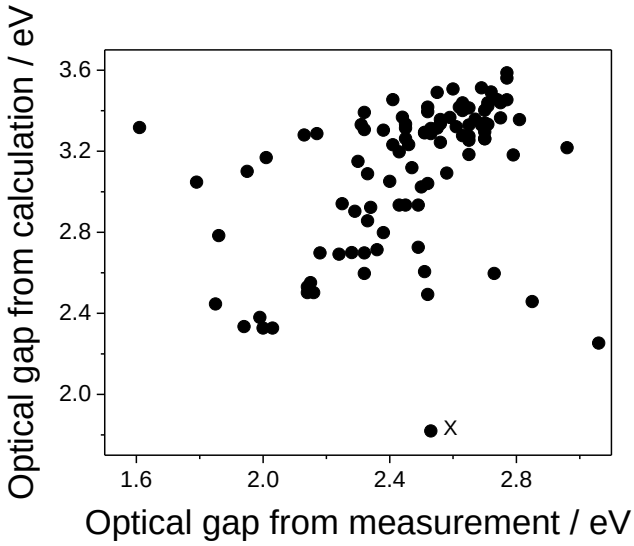

Figure S-87. Optical gap of catalyst from calculations plotted against the optical gap of the catalyst as determined by experimental measurement. See section 3.10 for further discussion.

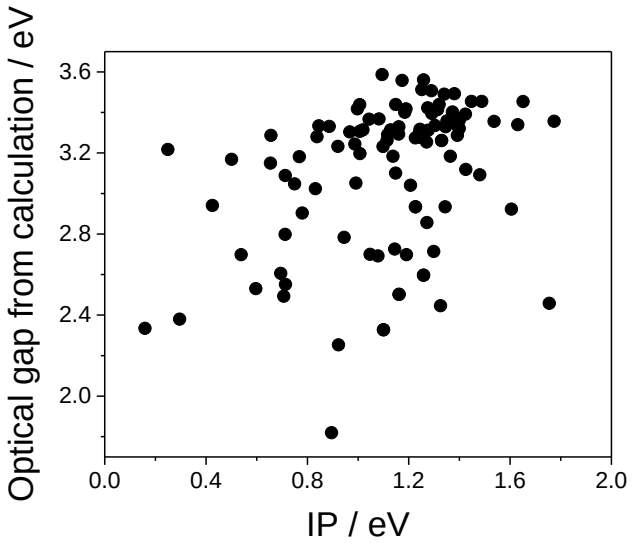

Figure S-88. Optical gap of catalyst from calculation correlated with the polymers ionisation potential (IP).

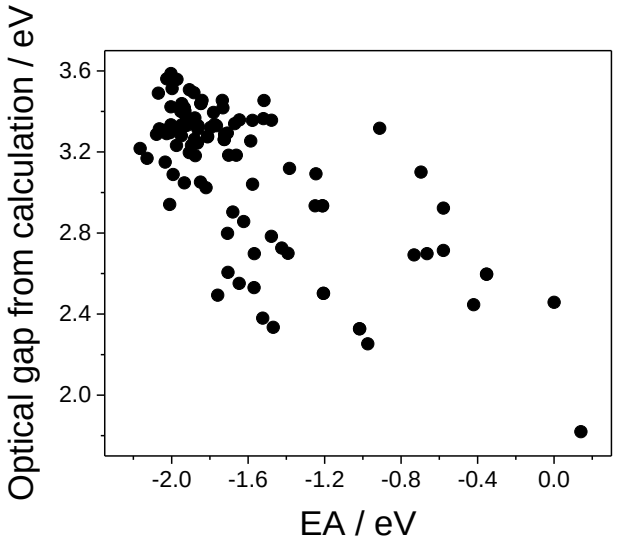

Figure S-89. Optical gap of catalyst from calculation correlated with the polymers electron affinity (EA).

3.10 Experimental vs theoretical optical gap outliers

Differences between the experimental and the theoretical optical gaps for some of the materials can be explained by issues with the fits used in the Tauc plots (as outlined below for 5 examples). However, this is not the case in the case of P1-58 and we found that the molecular weight of this polymer is a more likely explanation for the disagreement (see section 3.10 below).

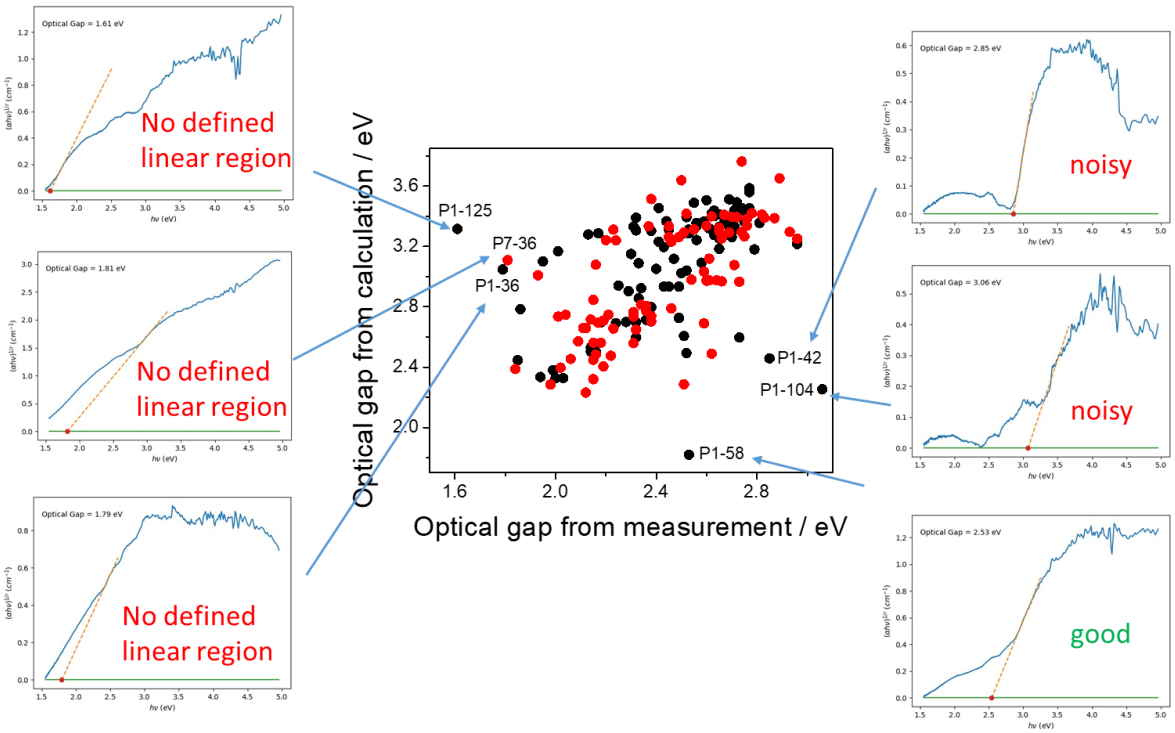

Figure S-90. Optical gap of catalyst from calculation plotted against the optical gap of catalyst from measurement (black dots are dibenzo[*b*,*d*]thiophene sulfone co-polymers, red dots are non-dibenzo[*b*,*d*]thiophene sulfone co-polymers).

3.11 Synthesis of P1-58 (dibenzo[*b*,*d*]thiophene sulfone - 4,8-benzo[1,2-*c*:4,5-*c*']bis([1,2,5]thiadiazole) co-polymer) using $Pd_2(dba)_3$ / (*o*-tol)$_3$P

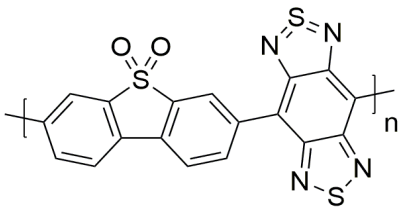

Figure S-91. The structure of P1-58.

Surprisingly, in the case of polymer P1-58 the measured experimental optical gap is much larger than that predicted (see Figure S-68). The material also evolves reasonable amounts of hydrogen in photocatalytic hydrogen evolution experiments, which was not expected for this material based on the predicted EA value. Based on these two observations, we suspected that polymer P1-58 could be a low molecular weight oligomer and hence have a much wider optical-gap and more negative EA value than predicted for the long polymer limit. The monomer 4,8-dibromobenzo[1,2-*c*:4,5-*c*']bis([1,2,5] thiadiazole) showed no hydrogen evolution in TEA/MeOH/H_2O mixtures over the course of a 5 hours run under solar simulator irradiation (AM1.5G, classification ABA, ASTME927-10).[3,4]

We therefore tried using the $Pd_2(dba)_3$/(*o*-tol)$_3$P catalyst system instead of [$PdCl_2$(dppf)] to resynthesize P1-58. This catalytic system has been shown to be highly active in some cases for aryl-aryl polycondensation reactions. We found that the optical gap of the material made using $Pd_2(dba)_3$/(*o*-tol)$_3$P was significantly smaller than that of the material prepared using [$PdCl_2$(dppf)] (2.16 *vs*. 2.53 eV) and much closer to the predicted value of 1.82 eV. When this material was tested, it evolved no hydrogen over the course of a 5 hours run under solar simulator (AM1.5G, Class AAA, IEC/JIS/ASTM, 1440 W Xenon, 12 × 12 in., MODEL: 94123A) compared to the material made using [$PdCl_2$(dppf)], which had a HER of 360 μmol h^{-1} g^{-1}. All of this is in line with our hypothesis that, for this polymer, synthesis using [$PdCl_2$(dppf)] results in the formation of only low molecular weight oligomers (in line with the observed low yields); we suggest that these short oligomers are responsible for the hydrogen evolution activity, which is absent for higher molecular weight polymers.

Synthesis of P1-58 using $Pd_2(dba)_3$ / (*o*-tol)$_3$P: 4,8-Dibromobenzo[1,2-*c*:4,5-*c*']bis([1,2,5]thiadiazole) (176 mg, 0.5 mmol), 3,7-bis(4,4,5,5-tetramethyl-1,3,2-dioxaborolan-2-yl)dibenzo[b,d]thiophene sulfone (234 mg, 0.5 mmol) and K_3PO_4 (1.02 g, 4.8 mmol) were dissolved in toluene/1,4-dioxane/water (2:1:1, 12 mL), followed by the addition of Starks' catalyst (1 drop). After this mixture was degassed with nitrogen for 30 min, $Pd_2(dba)_3$ (5.4 mg, 1.2 mol%) and (*o*-tol)$_3$P (10.8 mg, 0.035 mmol) were added. This resultant mixture was degassed for further 30 minutes then heated at 110 ºC for 24 hours. After cooled to room temperature, the reaction mixture was poured into methanol. The precipitate was collected by filtration and washed with acidic methanol (hydrochloric acid, 37 vol. % in methanol, 1:50,

51 mL), water and acetone, to give polymer as yellow solid. Further purification was carried out by Soxhlet extraction with chloroform and the product was obtained as a light-pink powder (14.4 mg, 7%).

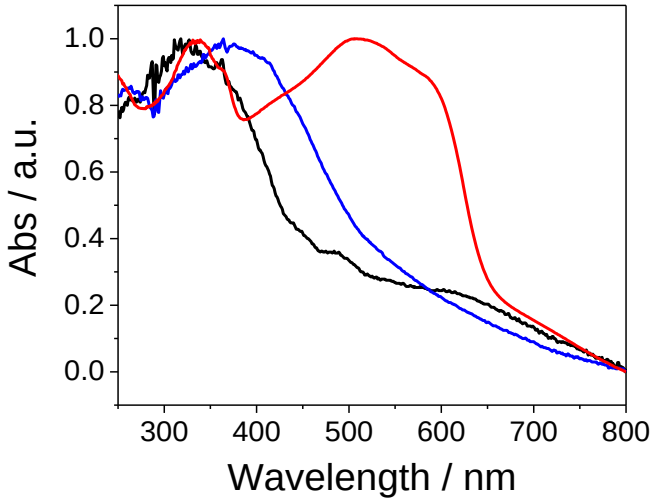

Figure S-92. Solid-state UV-Vis spectra of **P1-58** by different synthesis route, black line is **P1-58** synthesized by catalyst $PdCl_2$(dppf), blue line is **P1-58** synthesized by catalyst [$Pd_2(dba)_3$]/ (*o*-tol)$_3$P, red line is 4,8-Dibromobenzo[1,2-*c*:4,5-*c*']bis([1,2,5]thiadiazole).

Table S-2. The optical gap and HER of P1-59 synthesized by different catalyst

Polymer	**Optical gap / eV[a]**	**HER (TEA/MeOH/H_2O) / μmol $h^{-1}g^{-1}$ [b]**
P1-58 ([$PdCl_2$(dppf)])	2.53	371
P1-58 ($Pd_2(dba)_3$ / (*o*-tol)$_3$P)	2.16	0

[a] Optical gap calculated from the absorption on-set; [b] Reaction conditions: 5 mg polymer was suspended in 5 mL water/methanol/triethylamine solution, irradiated by solar simulator (AM1.5G, Class AAA, IEC/JIS/ASTM, 1440 W Xenon, 12 × 12 in., MODEL: 94123A) 1 hour.

Table S-3. Photophysical properties and hydrogen evolution rates (HERs) for the sulfone co-polymer photocatalysts.

Polymers	Yield / %	Optical gap / eV[a]	PL Lifetime / ns[b]	Pd content / wt. %	T / %[c]	Degree of Crystallinity[d]	HER (TEA/ MeOH/ H_2O) / μmol h^{-1} g^{-1} [e]	HER (TEA/ MeOH/ H_2O/Pt) / μmol h^{-1} g^{-1} [f]	HER (Na_2S) / μmol h^{-1} g^{-1} [g]
P1-2	84	2.7	2.59	0.350	9.11	M	2253.5	3165.7	116.2
P1-3	Quant	2.45	1.55	0.422	3.51	L	1947.9	3815.3	219.1
P1-5	Quant	2.71	2.53	0.389	10.05	L	3363.4	3350.0	156.0
P1-6	76	2.63	2.4	0.414	28.67	L	2657.8	6463.0	61.0
P1-7	36	2.69	2.43	0.214	52.04	L	651.5	7670.9	9.7
P1-8	64	2.77	3.15	ND	9.01	M	1243.8	972.8	46.9
P1-11	80	2.55	1.82	ND	41.65	A	593.1	1383.6	0.0
P1-13	92	2.43	0.85	0.405	42.30	L	613.1	763.7	0.0
P1-14	Quant	2.56	1.88	0.672	3.63	M	8742.2	8227.8	922.7
P1-15	68	2.53	1.39	0.207	85.95	L	620.3	631.1	8.4
P1-16	Quant	2.59	2.2	0.317	4.74	L	2294.8	3763.7	35.5
P1-17	38	ND	2.24	0.104	77.72	L	1011.7	277.9	0.0
P1-18	31	2.65	3.73	ND[h]	ND[h]	A	3571.4	ND	199.3
P1-19	Quant	2.62	2.69	0.182	5.63	M	4155.4	3702.7	11.1
P1-20	55	2.25	2.14	0.450	59.26	L	527.3	1492.0	6.8
P1-21	67	2.52	1.3	0.664	7.86	L	4953.8	4019.9	79.2
P1-22	96	2.51	2.5	0.274	9.45	M	4413.0	3702.7	182.6
P1-23	Quant	2.52	3.05	0.138	5.12	L	5630.5	10155.2	240.5
P1-24	75	2.38	1.6	0.194	7.50	M	1985.6	2483.7	147.2
P1-26	57	2.29	0.82	0.709		H	1231.8	1745.8	0.0
P1-27	99	2.56	2.3	0.171	3.46	A	1053.4	10720.6	187.5
P1-28	76	2.01	0.75	0.588	78.29	L	20.5	135.2	9.7
P1-29	98	2.3	0.84	0.326	7.73	M	806.3	979.3	62.3
P1-30	42	2.96	0.37	0.150	63.01	ND	0.0	18.8	55.5
P1-32	85	2.31	1.08	0.258	2.68	L	9772.2	9422.2	16.4
P1-33	92	2.67	0.68	0.307	1.13	M	1771.8	2578.5	90.4
P1-34	68	2.61	2	0.572	10.08	L	1581.8	1534.2	109.0
P1-35	Quant	2.38	0.76	0.257	73.89	L	0.0	39.3	19.2
P1-36	100	1.79	0.7	0.204	25.85	M	0.0	0	10.5
P1-37	56	2.41	3.82	0.769	15.92	M	2709.8	2160.6	270.4
P1-38	Quant	2.74	1.65	0.215	85.97	M	139.2	64.5	94.6
P1-39	57	2.56	2.81	0.236	10.97	H	2191.0	4244.8	309.5
P1-41	Quant	2.32	1.24	0.186	85.44	L	786.1	1346.3	91.6
P1-42	96	2.85	0.78	0.379	50.53	L	0.0	21.5	5.6
P1-43	84	2.34	0.7	0.244	21.03	H	0.0	0.0	0.0
P1-44	94	1.85	0.69	0.331	3.21	H	0.0	0.0	0.0
P1-45	Quant	ND	0.6	0.494	85.81	L	29.7	16.6	0.0
P1-46	Quant	2.79	0.76	0.190	79.92	L	0.0	0.0	8.8
P1-47	Quant	2.75	2.13	0.376	13.52	L	4461.9	7076.3	419.2

Polymers	Yield / %	Optical gap / eV[a]	PL Lifetime / ns[b]	Pd content / wt. %	T / %[c]	Degree of Crystallinity[d]	HER (TEA/ MeOH/ H_2O) / μmol h^{-1} g^{-1} [e]	HER (TEA/ MeOH/ H_2O/Pt) / μmol h^{-1} g^{-1} [f]	HER (Na_2S) / μmol h^{-1} g^{-1} [g]
P1-48	91	2.49	0.68	0.288	24.79	L	1051.2	1968.5	228.9
P1-49	60	2.44	2.24	0.230	76.89	L	987.4	1151.3	10.6
P1-51	66	2.5	1.89	0.150	24.02	M	1474.2	2416.8	53.9
P1-53	87	2.24	0.32	0.217	4.43	L	994.5	1317.9	72.1
P1-54	Quant	2.32	0.56	0.227	21.59	L	60.3	246.8	29.3
P1-55	67	2.36	11.7	0.236	27.17	H	100.4	765.6	16.1
P1-56	51	2.14	0.67	0.615	2.95	L	0.0	0.0	0.0
P1-57	97	2	0.25	0.359	1.03	L	45.9	123.0	0.0
P1-58	40	2.53	5.18	0.139	14.62	ND	371.3	227.9	17.6
P1-59	75	2.71	1.46	0.379	7.1	L	1929.9	2561.1	32.5
P1-60	91	2.65	4.03	0.177	9.85	L	7648.8	11319.6	142.5
P1-61	69	2.69	3.66	0.207	5.94	L	5248.0	8194.8	137.4
P1-62	92	2.7	0.74	0.722	12.08	M	3500.5	2861.9	398.8
P1-64	73	2.81	3.39	0.684	9.6	M	3533.8	3273.7	294.4
P1-65	72	2.77	3.33	0.402	5.67	M	3157.2	2613.7	25.4
P1-66	Quant	2.72	2.52	0.493	63.72	L	3581.2	5161.6	35.8
P1-67	63	2.77	0.7	0.195	48.5	A	1327.1	1405.2	0.0
P1-68	Quant	2.65	1.89	0.131	9.34	A	3968.9	6857.8	138.5
P1-70	Quant	2.7	1.67	0.072	17.66	L	2245.8	1917.9	112.6
P1-71	69	2.33	0.75	0.118	1.67	M	1535.7	5572.4	48.2
P1-72	44	2.4	1.44	0.569	35.62	M	6232.0	3347.5	133.5
P1-73	56	2.63	2.28	0.343	86.63	L	346.9	1595.5	66.1
P1-74	77	2.45	1.6	0.522	8.33	L	6038.3	8341.3	92.9
P1-75	72	2.49	1.78	0.713	8.7	M	265.5	3494.1	28.8
P1-77	56	2.47	0.64	0.534	7.57	L	813.2	3003.8	131.9
P1-78	48	1.86	0.71	0.869	87.05	A	314.5	2597.2	12.9
P1-79	47	2.28	0.6	0.315	0.42	L	242.9	2931.4	20.2
P1-83	69	2.43	1.01	0.363	8.95	M	23.5	112.2	5.7
P1-84	36	2.52	0.7	0.307	88.54	A	0.0	477.2	5.7
P1-85	58	2.65	1.73	0.109	36.18	H	380.7	2355.0	14.0
P1-86	78	2.53	2.1	0.485	16.26	L	578.4	796.1	8.2
P1-87	32	2.7	0.96	0.349	2.89	ND	82.5	2170.6	97.0
P1-88	63	1.95	0.69	0.265	19.83	L	0.0	81.4	0.0
P1-89	Quant	2.46	2.1	0.142	3.88	A	8390.1	12869.1	46.1
P1-90	96	2.45	2.36	0.247	2.8	M	5288.4	5089.0	227.7
P1-91	75	2.17	1.41	0.169	57.35	L	83.6	1129.7	66.8
P1-92	Quant	2.55	2.23	0.147	5.1	M	8461.6	9422.2	62.3
P1-93	86	2.51	3	0.311	0.79	M	3443.2	16718.8	254.3
P1-94	95	2.71	2.58	0.295	0.49	M	1835.6	3931.5	103.9
P1-95	95	2.13	1	0.383	76.76	A	349.5	127.1	14.1
P1-96	90	2.14	0.74	0.289	15.55	M	1854.1	1869.1	254.3
P1-97	48	2.41	0.88	0.151	23.7	L	672.1	3024.3	23.1

Polymers	Yield / %	Optical gap / eV[a]	PL Lifetime / ns[b]	Pd content / wt. %	T / %[c]	Degree of Crystallinity[d]	HER (TEA/ MeOH/ H_2O) / µmol h^{-1} g^{-1} [e]	HER (TEA/ MeOH/ H_2O/Pt) / µmol h^{-1} g^{-1} [f]	HER (Na_2S) / µmol h^{-1} g^{-1} [g]
P1-99	65	2.14	0.72	0.744	8.58	M	2090.6	4267.1	620.0
P1-102	49	2.15	0.64	0.538	66.95	M	2691.0	3332.9	640.2
P1-104	30	3.06	0.22	1.112	53.78	L	152.7	225.3	23.7
P1-108	89	1.99	0.65	0.196	5.54	M	669.2	525.3	653.2
P1-109	Quant	1.94	0.7	0.294	4.24	L	164.0	318.1	143.5
P1-110	91	2.18	0.72	0.275	3.64	H	2390.4	5933.9	136.3
P1-111	94	2.58	0.71	0.228	1.44	L	0.0	0.0	35.9
P1-113	73	2.51	1.1	0.291	68.84	L	153.1	403.6	118.7
P1-114	86	2.33	0.74	0.424	7.94	M	1459.4	1994.0	580.4
P1-116	94	ND	1.2	0.674	80.65	A	52.6	298.3	39.4
P1-118	Quant	2.32	0.66	0.586	2.42	A	2327.7	2387.5	474.3
P1-119	75	2.65	0.75	1.088	86.26	A	277.7	470.9	28.2
P1-120	53	2.75	0.7	0.168	75.92	A	215.7	109.8	58.2
P1-122	39	2.6	0.74	0.468	82.23	A	0.0	0.0	8.3
P1-123	46	2.52	0.77	0.448	83.83	A	217.6	483.5	27.1
P1-125	Quant	1.61	0.62	0.374	86.57	A	88.4	324.0	0.0
P1-126	42	ND	0.52	0.171	83.12	L	0.0	48.3	6.2
P1-127	42	2.91	0.61	ND[h]	74.82	H	19.1	16.6	9.9

[a] Optical gap calculated from the absorption on-set; [b] Estimated weighted average life-time of the excited state determined by time-correlated single-photon counting. Calculated by fitting the following equation: $A + B_1 \times \exp(-i/\tau_1) + B_2 \times \exp(-i/\tau_2) + B_3 \times \exp(-i/\tau_3) + B_4 \times \exp(-i/\tau_4)$. Initial amplitudes (A, B_1, B_2, B_3, B_4) are estimated and iterated along with the life-times (τ_1, τ_2, τ_3, τ_4) until a fit is found. The prompt is measured separately and used for deconvolution of the instrument response; [c] A suspension containing water/methanol/trimethylamine (5 mL) and polymer (5 mg) was diluted with DI water (25 mL) into a cylindrical cell. For the transmittance measurement the average of the measurements between 0.5 mm to 30 mm height were averaged; [d] Degree of crystallinity was determined to be amorphous (A), low (L), medium (M), or high (H); [e] Reaction conditions: 5 mg polymer was suspended in 5 mL water/methanol/triethylamine solution, irradiated by solar simulator (AM1.5G, Class AAA, IEC/JIS/ASTM, 1440 W Xenon, 12 × 12 in., MODEL: 94123A) 1 hour; [f] Reaction conditions: 5 mg polymer was suspended in 5 mL water/methanol/triethylamine solution loaded with 1 wt. % Pt from H_2PtCl_6 , irradiated by Solar simulator (AM1.5G, Class AAA, IEC/JIS/ASTM, 1440 W Xenon, 12 × 12 in., MODEL: 94123A) 1 hour; [g] Reaction conditions: 5 mg polymer was suspended in 5 mL 0.026M Na_2S aqueous solution, irradiated by solar simulator (AM1.5G, Class AAA, IEC/JIS/ASTM, 1440 W Xenon, 12 × 12 in., MODEL: 94123A) 3 hours; [h] Not determined as the yield of the polymerization was too low giving insufficient amounts material for all measurements.

Table S-4. Batch-to-batch variation of photophysical properties and hydrogen evolution rates (HERs) for the sulfone co-polymer photocatalysts

Polymers	**Yield / %**	**Optical gap / eV[a]**	**PL Lifetime / ns[b]**	**T%[c]**	**HER (TEA/ MeOH/ H_2O) / μmol h^{-1} g^{-1} [d]**	**HER (Na_2S) / μmol h^{-1} g^{-1} [e]**
P1-19-1	Quant	2.62	2.69	5.6	4377.8	11.1
P1-19-2	96	2.63	3.27	1	3204.6	13.4
P1-56-1	51	2.14	0.67	2.9	0	0
P1-56-2	57	2.04	0.58	0.6	0	0
P1-57-1	97	2.00	0.25	1.0	45.9	5.5
P1-57-2	95	2.03	0.72	0.8	222.4	6.4
P1-62-1	92	2.70	0.74	12.1	3500.5	398.8
P1-62-2	94	2.70	3.09	16.3	2144.6	81.8
P1-83-1	48	2.45	0.85	9.9	33.5	0.0
P1-83-2	69	2.43	1.01	9.0	23.5	5.7
P1-93-1	86	2.51	3.00	0.7	3443.2	254.3
P1-93-2	82	2.49	1.96	0.6	4436.8	304.2
P1-96-1	90	2.14	0.74	15.5	1854.2	254.3
P1-96-2	84	2.16	0.68	3.1	1773.4	240.5

[a] Optical gap calculated from the absorption on-set; [b] Estimated weighted average life-time of the excited state determined by time-correlated single-photon counting. Calculated by fitting the following equation: $A + B_1 \times \exp(-i/\tau_1) + B_2 \times \exp(-i/\tau_2) + B_3 \times \exp(-i/\tau_3) + B_4 \times \exp(-i/\tau_4)$. Initial amplitudes (A, B_1, B_2, B_3, B_4) are estimated and iterated along with the life-times (τ_1, τ_2, τ_3, τ_4) until a fit is found. The prompt is measured separately and used for deconvolution of the instrument response; [c] A suspension containing water/methanol/trimethylamine (5 mL) and polymer (5 mg) was diluted with DI water (25 mL) into a cylindrical cell. For the transmittance measurement the average of the measurements between 0.5 mm to 30 mm height were averaged; [d] Reaction conditions: 5 mg polymer was suspended in 5 mL water/methanol/triethylamine solution, irradiated by solar simulator (AM1.5G, Class AAA, IEC/JIS/ASTM, 1440 W Xenon, 12 × 12 in., MODEL: 94123A) 1 hour; [e] Reaction conditions: 5 mg polymer was suspended in 5 mL 0.026M Na_2S aqueous solution, irradiated by solar simulator (AM1.5G, Class AAA, IEC/JIS/ASTM, 1440 W Xenon, 12 × 12 in., MODEL: 94123A) 3 hours.

4. Other co-polymers made via microwave heating

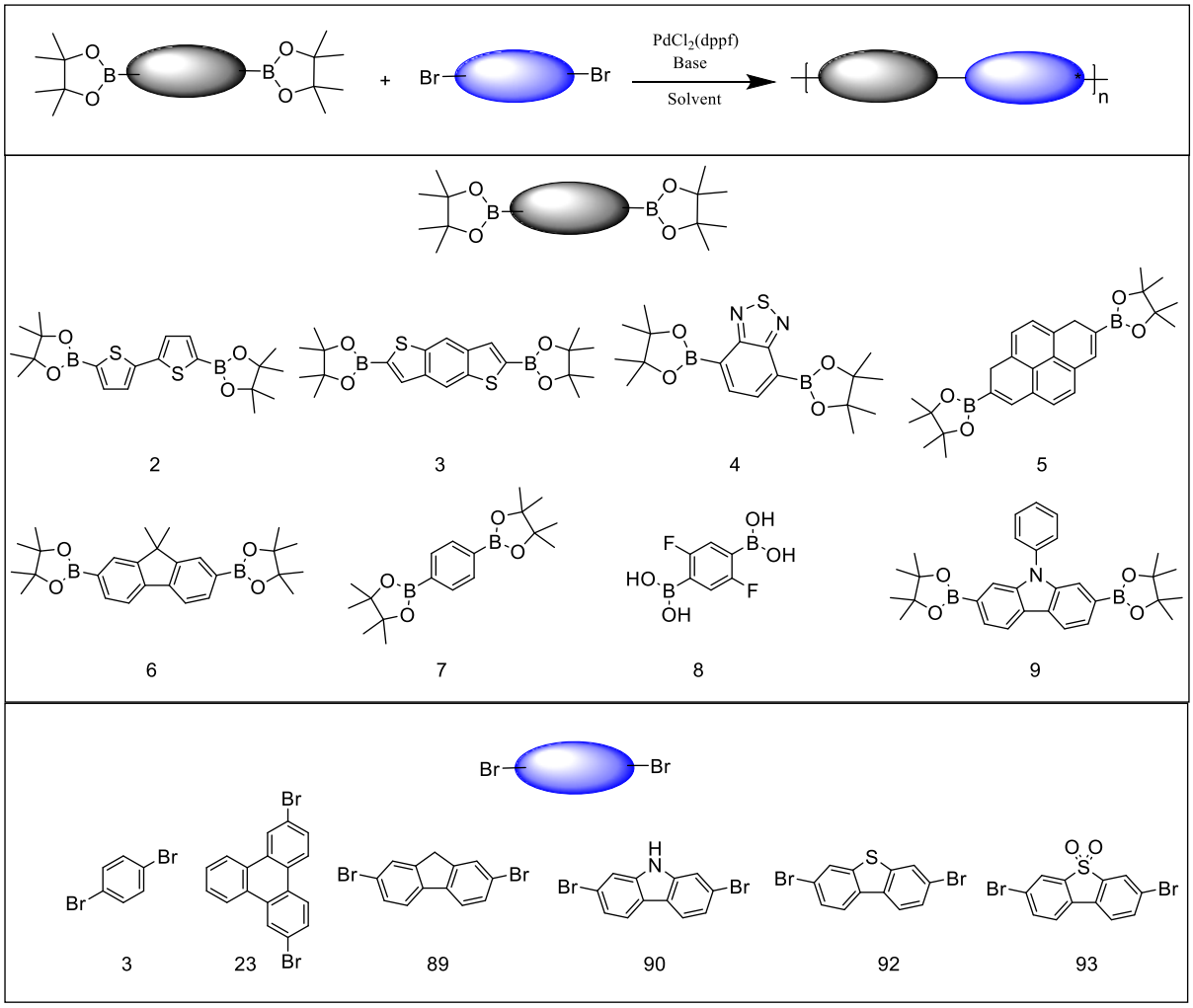

Figure S-93. a) Synthesis route for the second, focused conjugated polymer library; b) Diboronic acids / acid ester arenes and c) dibromo arenes used for co-polymers library synthesis.

4.1 UV-visible Spectra

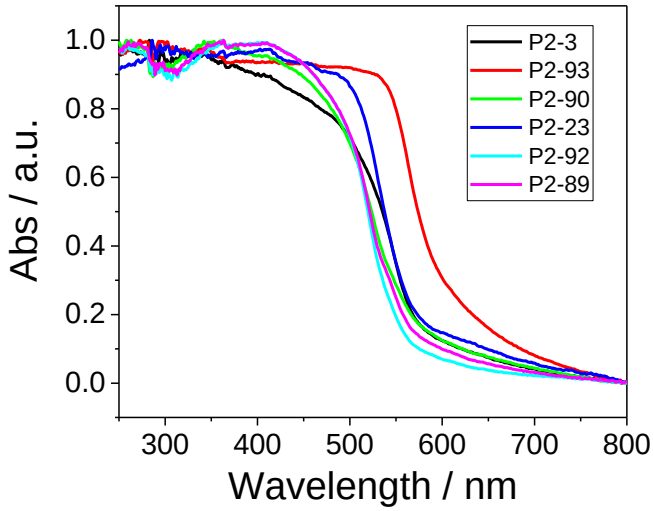

Figure S-94. Solid-state UV-vis spectrum of **P2-X** co-polymers.

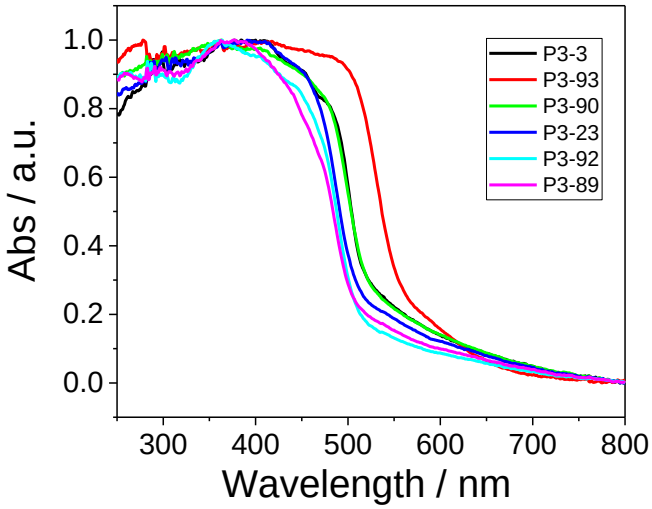

Figure S-95. Solid-state UV-vis spectrum P3-X co-polymers

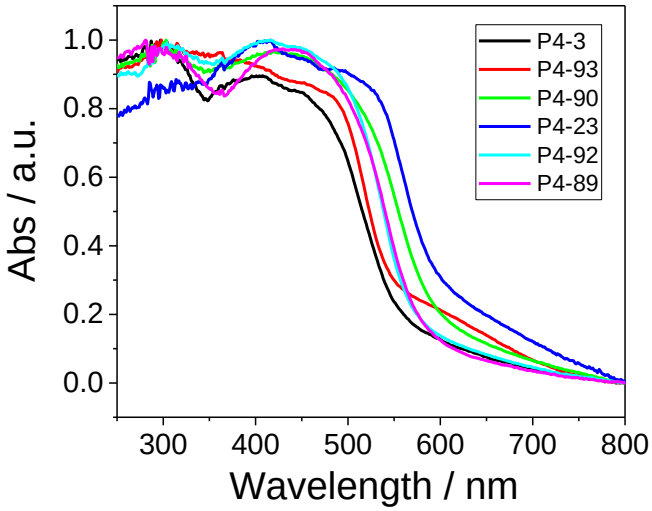

Figure S-96. Solid-state UV-vis spectrum of **P4-X** co-polymers.

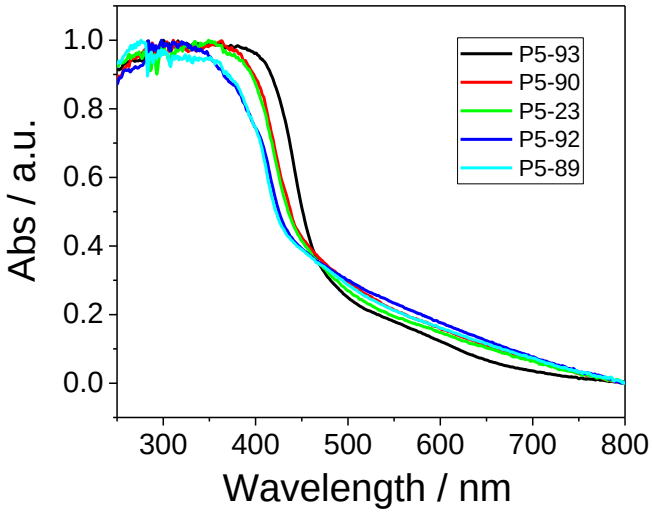

Figure S-97. Solid-state UV-vis spectrum of **P5-X** co-polymers.

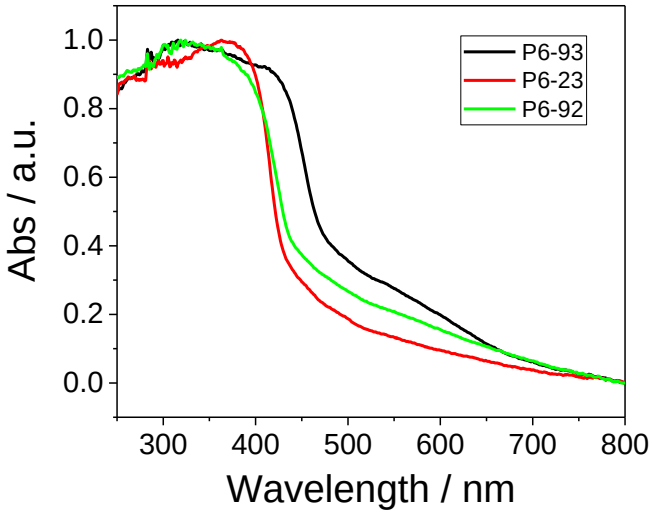

Figure S-98. Solid-state UV-vis spectrum of **P6-X** co-polymers.

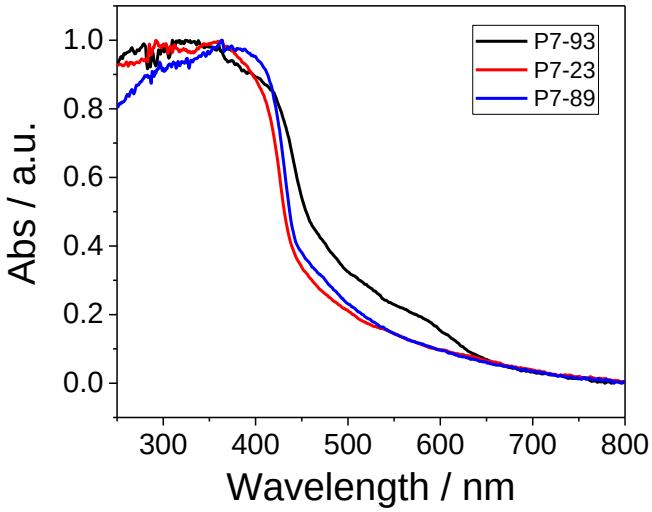

Figure S-99. Solid-state UV-vis spectrum of **P7-X** co-polymers.

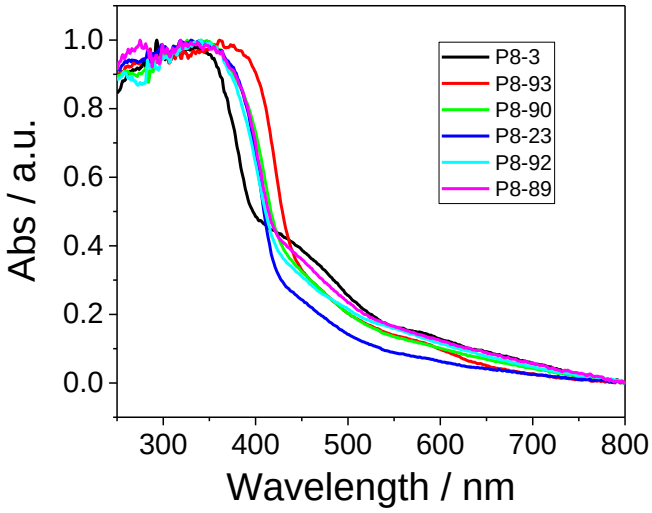

Figure S-100. Solid-state UV-vis spectrum of **P8-X** co-polymers.

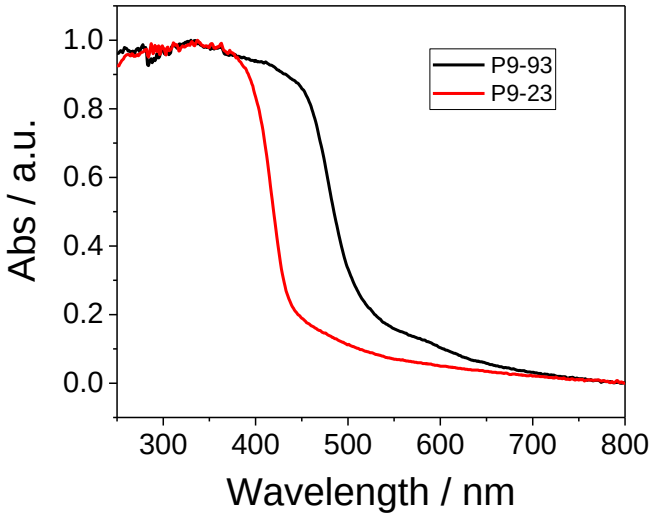

Figure S-101. Solid-state UV-vis spectrum of **P9-X** co-polymers.

4.2 Fourier-Transform Infrared Spectra

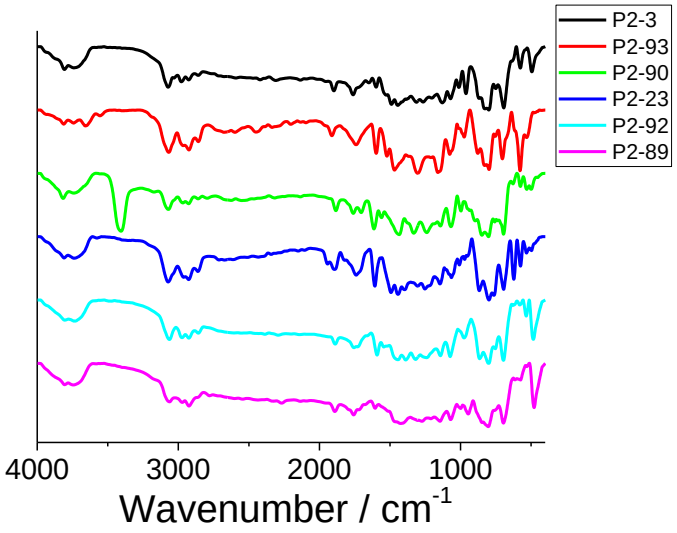

Figure S-102. Transmission FT-IR spectra of **P2-X** co-polymers.

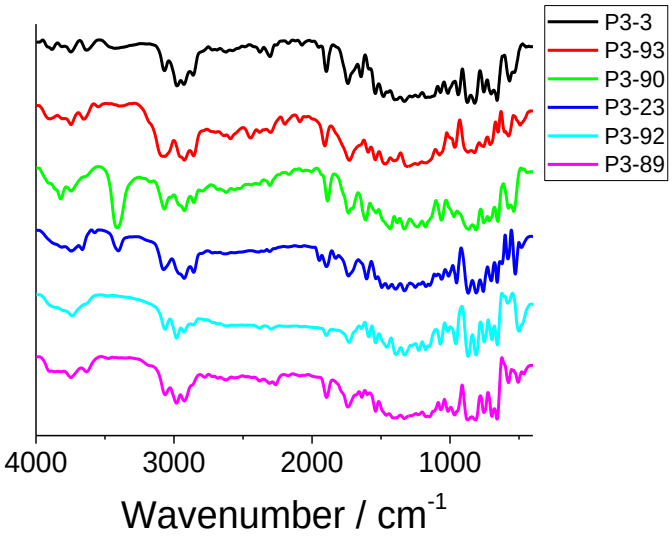

Figure S-103. Transmission FT-IR spectra of **P3-X** co-polymers.

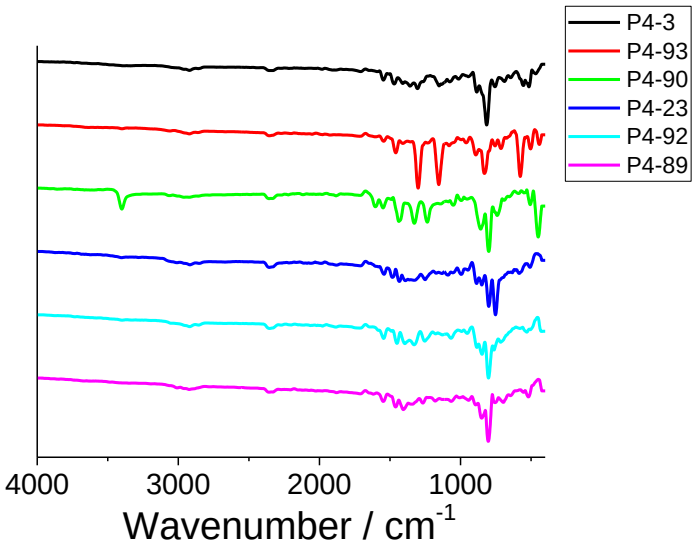

Figure S-104. Transmission FT-IR spectra of **P4-X** co-polymers.

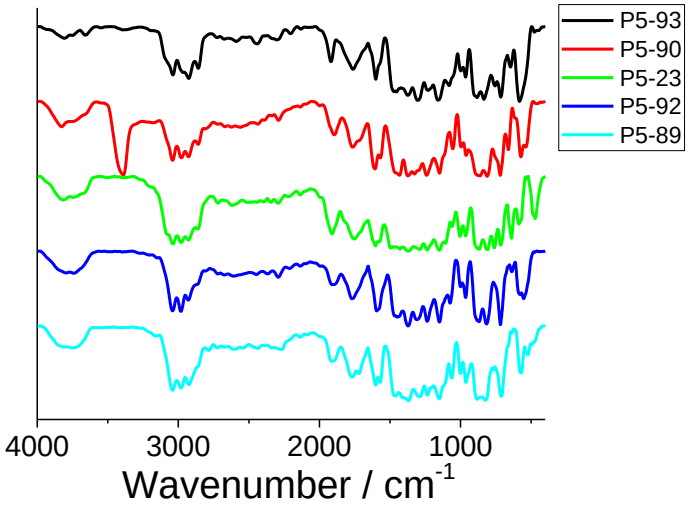

Figure S-105. Transmission FT-IR spectra of **P5-X** co-polymers.

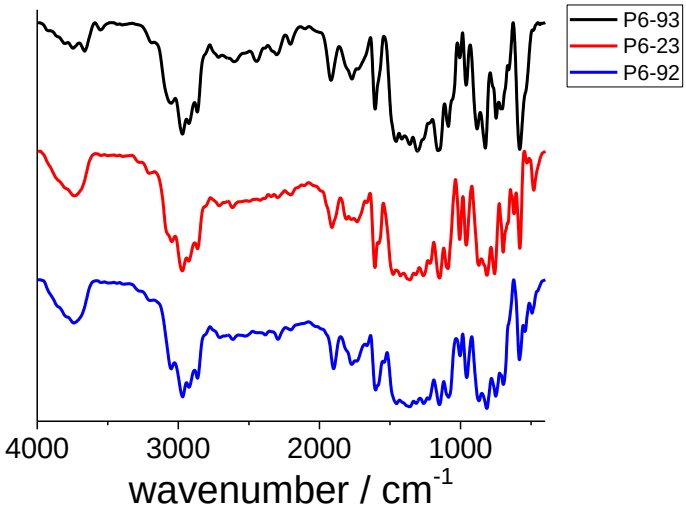

Figure S-106. Transmission FT-IR spectra of **P6-X** co-polymers.

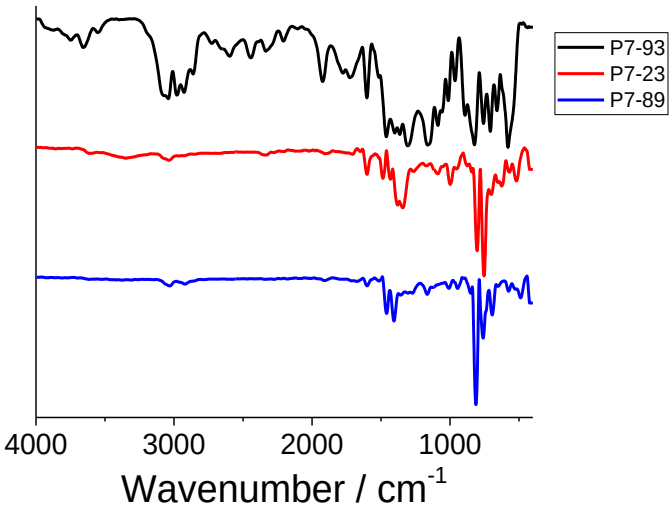

Figure S-107. Transmission FT-IR spectra of **P7-X** co-polymers.

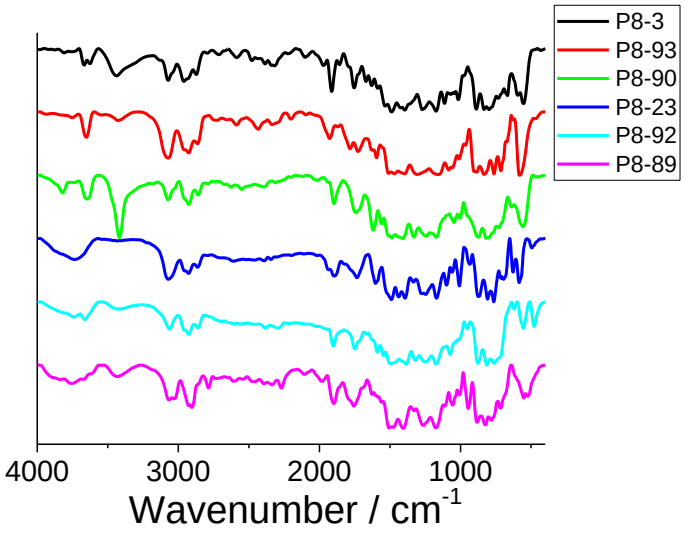

Figure S-108. Transmission FT-IR spectra of **P8-X** co-polymers.

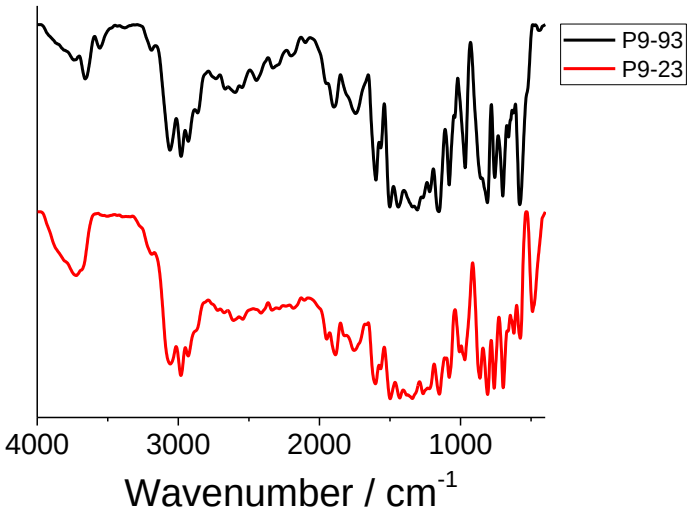

Figure S-109. Transmission FT-IR spectra of **P9-X** co-polymers.

4.3 Powder X-Ray Diffraction Patterns

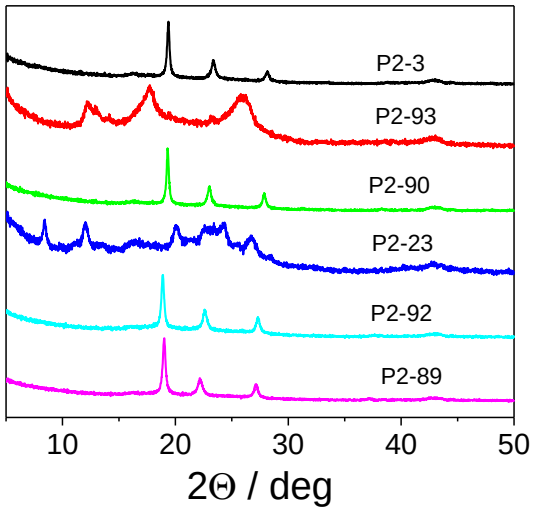

Figure S-110. PXRD patterns for P2-X co-polymers.

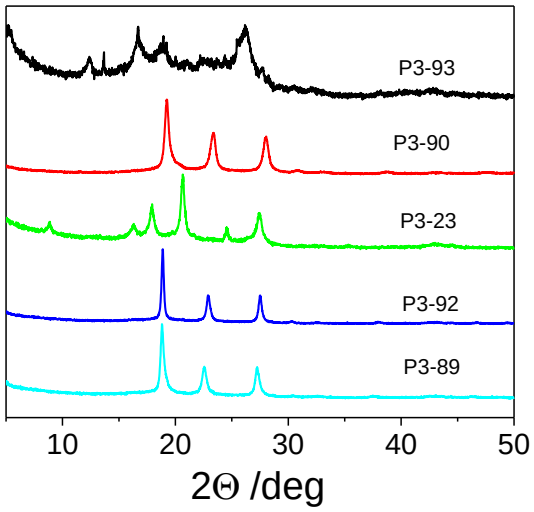

Figure S-111. PXRD patterns for P3-X co-polymers

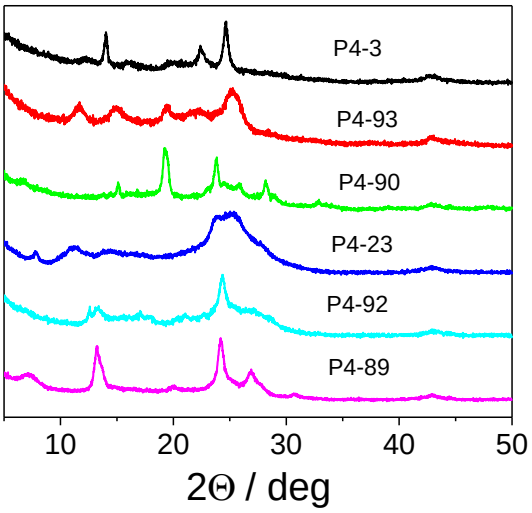

Figure S-112. PXRD patterns for P4-X co-polymers.

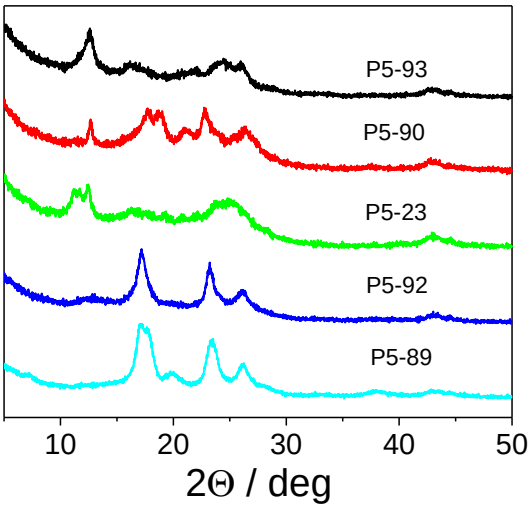

Figure S-113. PXRD patterns for P5-X co-polymers

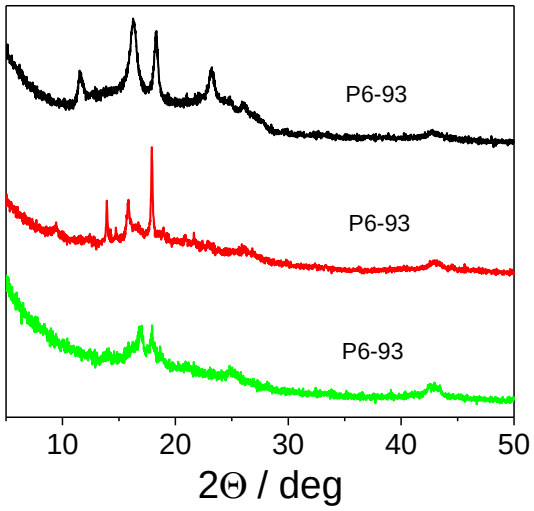

Figure S-114. PXRD patterns for P6-X co-polymers.

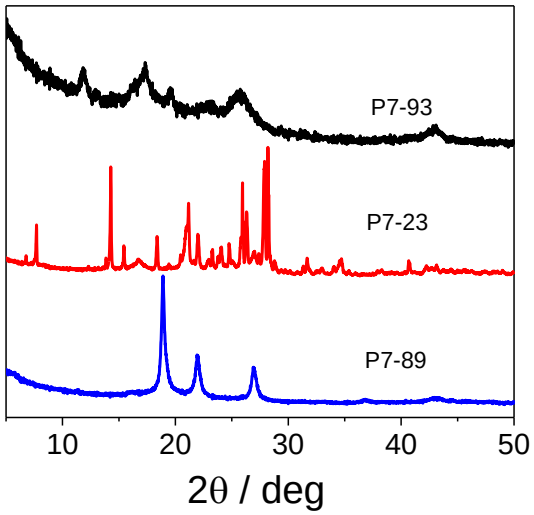

Figure S-115. PXRD patterns for P7-X co-polymers.

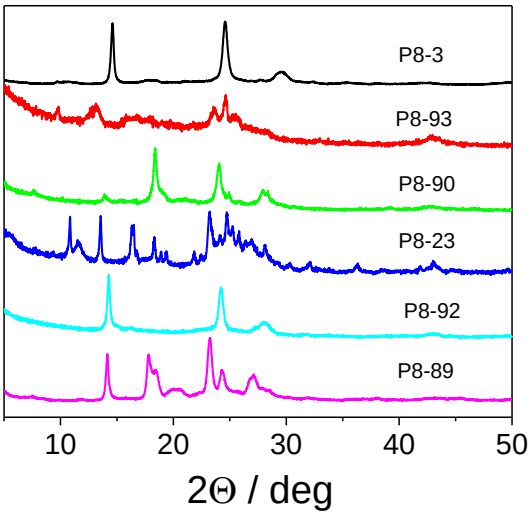

Figure S-116. PXRD patterns for P8-X co-polymers.

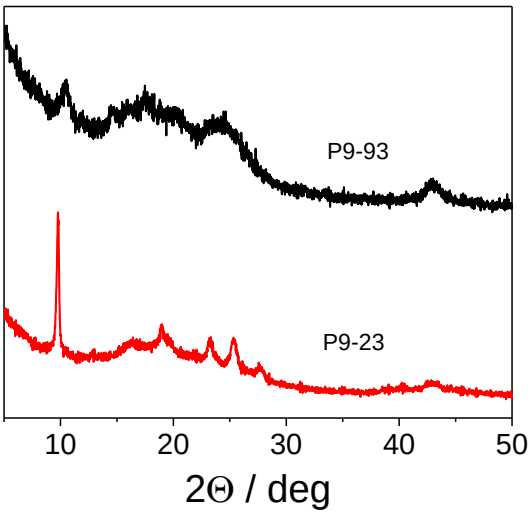

Figure S-117. PXRD patterns for P9-X co-polymers.

4.4 HER *vs.* HT Polymers Characterization

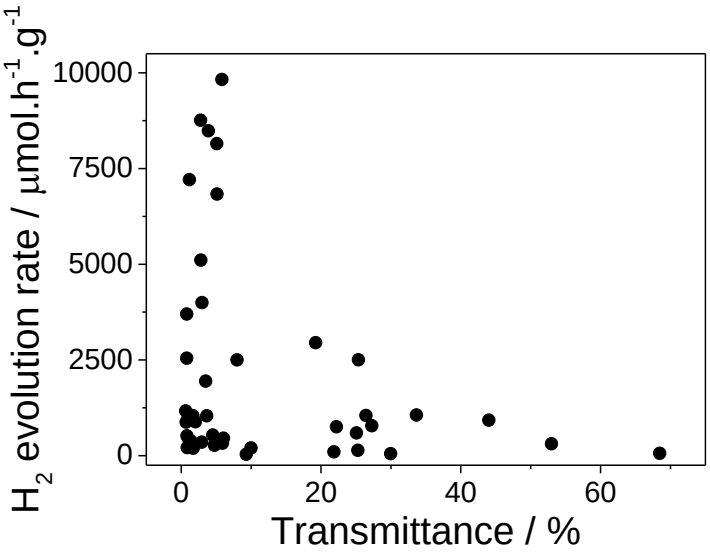

Figure S-118. Photocatalytic hydrogen evolution rate (HER) of photocatalysts from TEA/MeOH/H_2O mixtures plotted against the sample's transmittance in the suspension. Polymer (5 mg) was suspended in 5 mL water/methanol/triethylamine solution, irradiated by a solar simulator (AM1.5G, Class AAA, IEC/JIS/ASTM, 1440 W xenon, 12 × 12 in., MODEL: 94123A, illumination time: 1 hour).

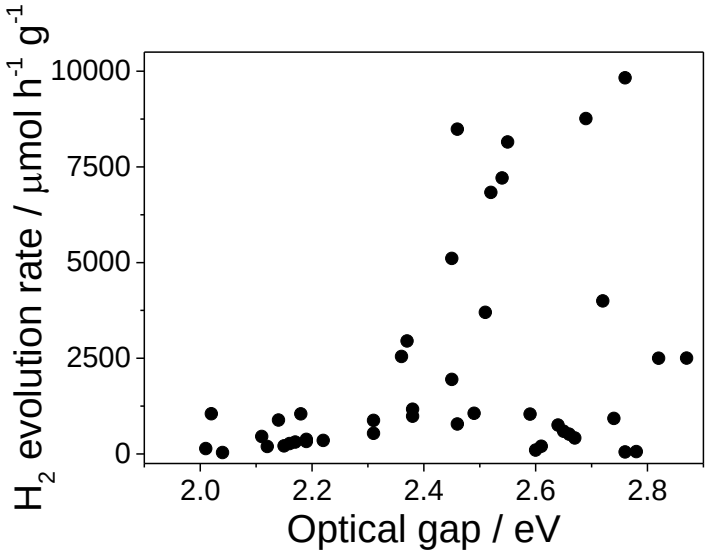

Figure S-119. Photocatalytic hydrogen evolution rate (HER) of photocatalysts from TEA/MeOH/H_2O mixtures plotted against the optical gap of the polymers. Polymer (5 mg) was suspended in 5 mL water/methanol/triethylamine solution, irradiated by a solar simulator (AM1.5G, Class AAA, IEC/JIS/ASTM, 1440 W xenon, 12 × 12 in., MODEL: 94123A, illumination time: 1 hour).

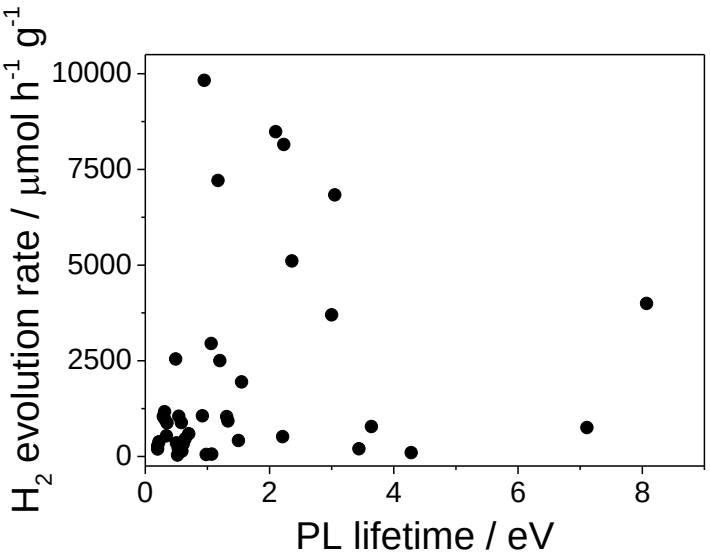

Figure S-120. Photocatalytic hydrogen evolution rate (HER) of photocatalysts from TEA/MeOH/H_2O mixtures plotted against the PL lifetime of the polymers. Polymer (5 mg) was suspended in 5 mL water/methanol/triethylamine solution, irradiated by a solar simulator (AM1.5G, Class AAA, IEC/JIS/ASTM, 1440 W xenon, 12 × 12 in., MODEL: 94123A, illumination time: 1 hour).

4.5 Calculation result *vs.* HER

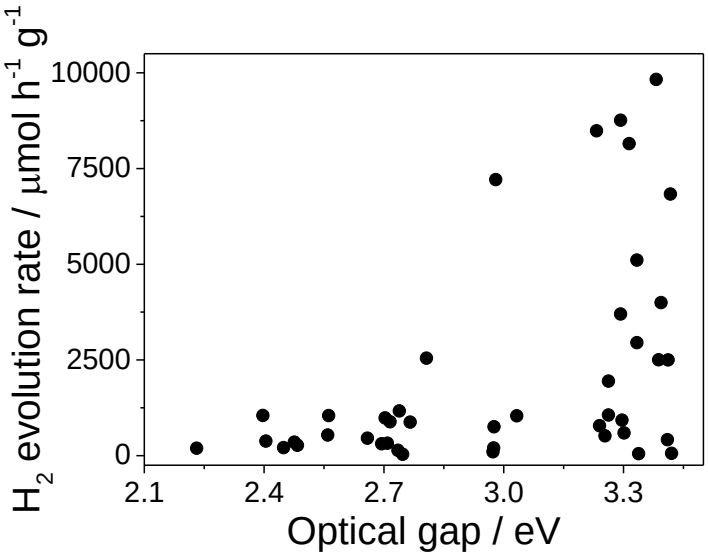

Figure S-121. Photocatalytic hydrogen evolution rate (HER) of photocatalysts plotted against the polymers optical gap. Polymer (5 mg) was suspended in 5 mL water/methanol/triethylamine solution, irradiated by a solar simulator (AM1.5G, Class AAA, IEC/JIS/ASTM, 1440 W xenon, 12 × 12 in., MODEL: 94123A, illumination time: 1 hour).

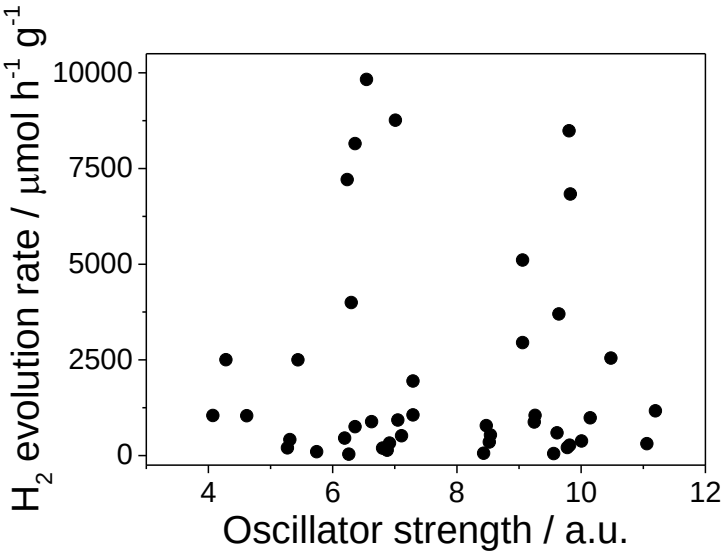

Figure S-122. Photocatalytic hydrogen evolution rate (HER) of photocatalysts plotted against the polymers oscillator strength. Polymer (5 mg) was suspended in 5 mL water/methanol/triethylamine solution, irradiated by a solar simulator (AM1.5G, Class AAA, IEC/JIS/ASTM, 1440 W xenon, 12 × 12 in., MODEL: 94123A, illumination time: 1 hour).

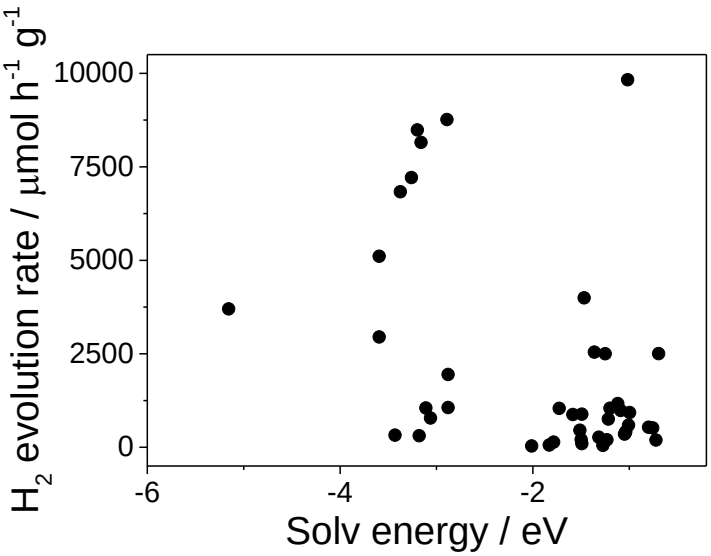

Figure S-123. Photocatalytic hydrogen evolution rate (HER) of photocatalysts plotted against the polymers solvent free energy. Polymer (5 mg) was suspended in 5 mL water/methanol/triethylamine solution, irradiated by a solar simulator (AM1.5G, Class AAA, IEC/JIS/ASTM, 1440 W xenon, 12 × 12 in., MODEL: 94123A, illumination time: 1 hour).

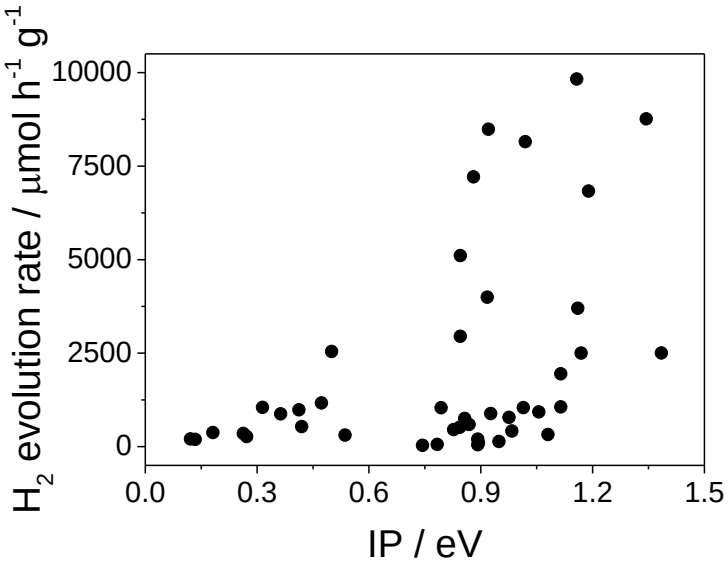

Figure S-124. Photocatalytic hydrogen evolution rate (HER) of photocatalysts plotted against the polymers ionisation potential (IP). Polymer (5 mg) was suspended in 5 mL water/methanol/triethylamine solution, irradiated by a solar simulator (AM1.5G, Class AAA, IEC/JIS/ASTM, 1440 W xenon, 12 × 12 in., MODEL: 94123A, illumination time: 1 hour).

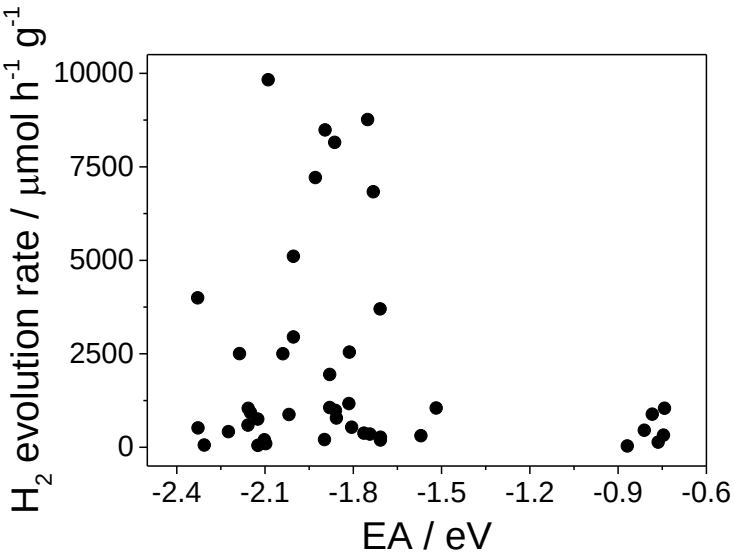

Figure S-125. Photocatalytic hydrogen evolution rate (HER) of photocatalysts plotted against the polymers electron affinity (EA). Polymer (5 mg) was suspended in 5 mL water/methanol/triethylamine solution, irradiated by a solar simulator (AM1.5G, Class AAA, IEC/JIS/ASTM, 1440 W xenon, 12 × 12 in., MODEL: 94123A, illumination time: 1 hour).

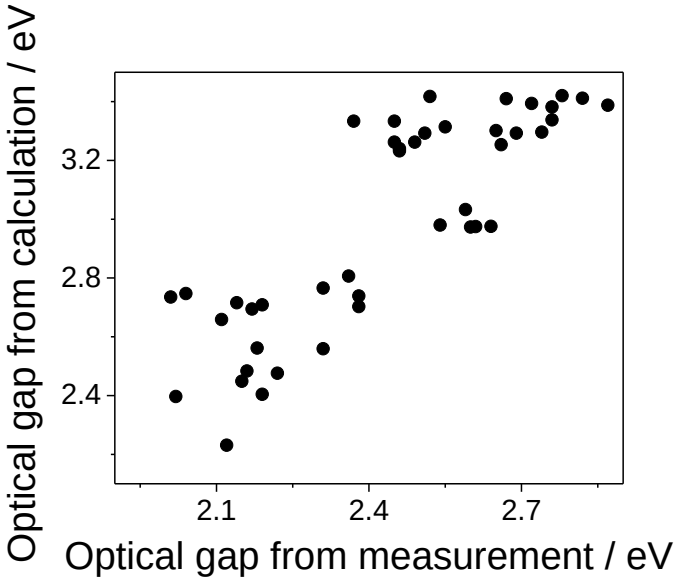

Figure S-126. Optical gap of photocatalysts from calculation plotted against the optical gap of the catalyst from experimental measurement.

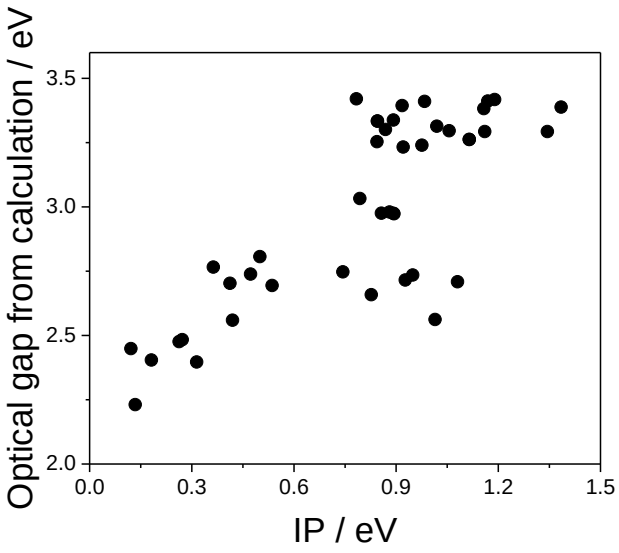

Figure S-127. Optical gap of catalyst from calculation plotted against the polymers' ionization potentials (IP).

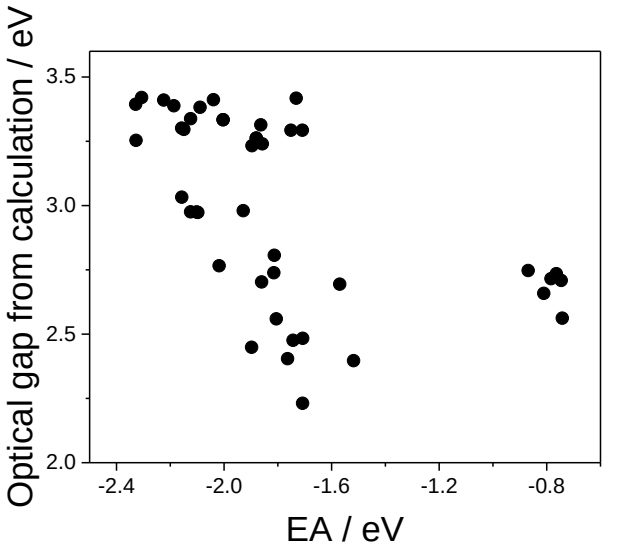

Figure S-128. Optical gap of catalyst from calculation plotted against the polymers' electron affinity (EA).

4.6 Energy potential *vs.* transmittance *vs.* HER

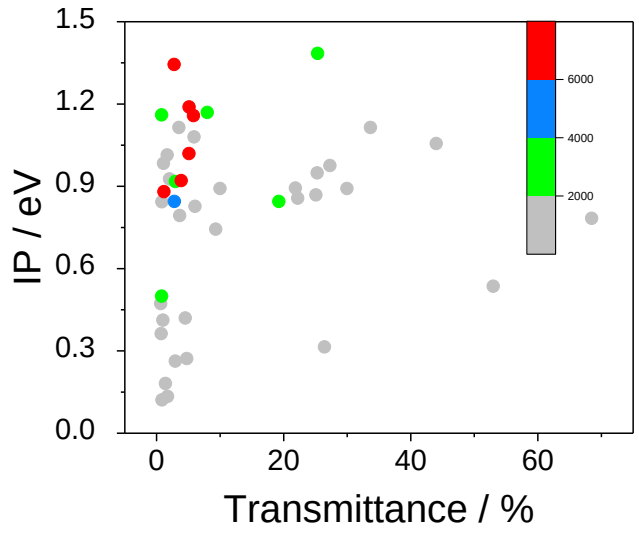

Figure S-129. Photocatalytic hydrogen evolution rate (HER) of photocatalysts from TEA/MeOH/H_2O mixtures plotted against the polymers ionization potential (IP) and the sample's transmittance in this suspension. Polymer (5 mg) was suspended in 5 mL water/methanol/triethylamine solution, irradiated by a solar simulator (AM1.5G, Class AAA, IEC/JIS/ASTM, 1440 W xenon, 12 × 12 in., MODEL: 94123A, illumination time: 1 hour).

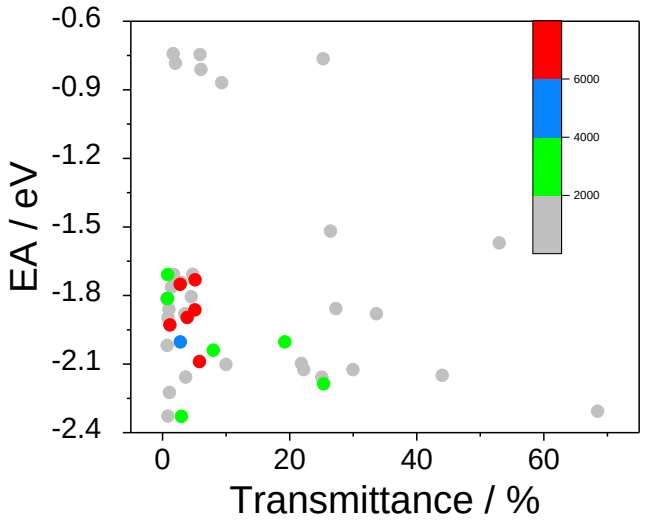

Figure S-130. Photocatalytic hydrogen evolution rate (HER) of photocatalysts from TEA/MeOH/H_2O mixtures plotted against the polymers electron affinity (EA) and the sample's transmittance in this suspension. Polymer (5 mg) was suspended in 5 mL water/methanol/triethylamine solution, irradiated by a solar simulator (AM1.5G, Class AAA, IEC/JIS/ASTM, 1440 W xenon, 12 × 12 in., MODEL: 94123A, illumination time: 1 hour).

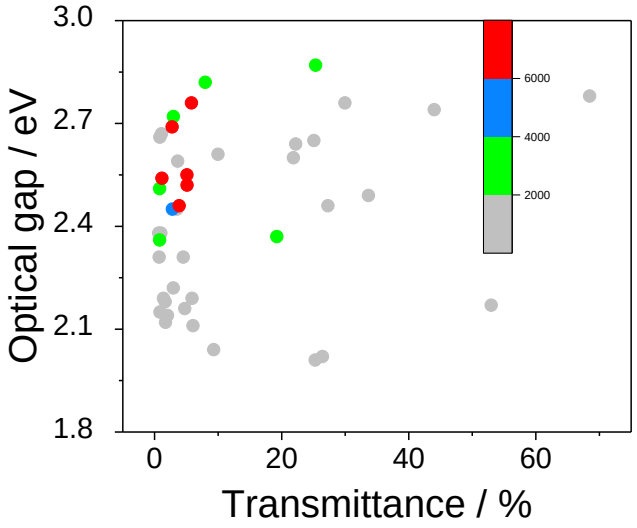

Figure S-131. Photocatalytic hydrogen evolution rate (HER) of photocatalysts from TEA/MeOH/H_2O mixtures plotted against the polymers optical gaps (experimental) and the sample's transmittance in this suspension. Polymer (5 mg) was suspended in 5 mL water/methanol/triethylamine solution, irradiated by a solar simulator (AM1.5G, Class AAA, IEC/JIS/ASTM, 1440 W xenon, 12 × 12 in., MODEL: 94123A, illumination time: 1 hour).

Table S-5. Photophysical properties and hydrogen evolution rates (HERs) for the small scale co-polymer photocatalysts.

Polymers	Yield / %	Optical gap / eV [a]	PL Lifetime / ns[b]	T /% [c]	HER (TEA/ MeOH/ H_2O) / μmol h^{-1} g^{-1} [d]
P2-23	87.9	2.16	0.2	4.8	269.7
P2-3	64.9	2.12	0.2	1.7	194.6
P2-89	85.9	2.19	0.22	1.4	379.3
P2-90	73.6	2.15	0.53	0.9	208.3
P2-92	82.8	2.22	0.5	2.9	352.4
P2-93	83.3	2.02	0.54	26.4	1049.9
P3-23	Quant	2.36	0.49	0.8	2546.0
P3-3	84	2.31	0.34	4.5	536.9
P3-89	Quant	2.38	0.31	1.0	985.4
P3-90	61.1	2.31	0.35	0.7	876.6
P3-92	Quant	2.38	0.31	0.6	1168.3
P3-93	35.1	2.17	0.59	53.0	308.4
P4-23	33.8	2.01	0.59	25.3	138.5
P4-3	63.1	2.18	0.29	1.7	1045.0
P4-89	87.8	2.11	0.64	6.0	457.2
P4-90	73.0	2.04	0.52	9.3	36.8
P4-92	81.1	2.14	0.58	2.0	885.5
P4-93	83.3	2.19	0.61	5.9	326.3
P5-23	37.8	2.6	4.28	21.8	99.3
P5-89	46.1	2.64	7.11	22.2	755.4
P5-90	32	2.59	1.31	3.6	1041.3
P5-92	60.5	2.61	3.44	10.0	201.4
P5-93	91.6	2.54	1.17	1.2	7211.1
P6-23	16	2.76	0.98	30.0	52.6
P6-92	20.9	2.65	0.7	25.1	592.5
P6-93	88.1	2.46	3.64	27.3	782.9
P7-23	86	2.67	1.5	1.1	417.1
P7-89	93	2.66	2.21	0.8	518.2
P7-93	62.2	2.49	0.92	33.7	1061.9
P8-23	61.9	2.82	13.96	8.0	2502.0
P8-3	39.9	2.87	1.2	25.3	2504.9
P8-89	54.2	2.74	1.33	44.0	928.8
P8-90	54.8	2.72	8.07	3.0	3996.3
P8-92	64.1	2.76	0.95	5.8	9828.6
P8-93	81	2.69	0.87	2.8	8763.1
P9-23	37.1	2.78	1.07	68.5	59.6
P9-93	44.5	2.37	1.06	19.2	2951.3

[a] Optical gap calculated from the absorption on-set; [b] Estimated weighted average life-time of the excited state determined by time-correlated single-photon counting. Calculated by fitting the following equation: $A + B_1 \times \exp(-i/\tau_1) + B_2 \times \exp(-i/\tau_2) + B_3 \times \exp(-i/\tau_3) + B_4 \times \exp(-i/\tau_4)$. Initial amplitudes ($A$, B_1, B_2, B_3, B_4) are estimated and iterated along with the life-times (τ_1, τ_2, τ_3, τ_4) until a fit is found. The prompt is measured separately and used for deconvolution of the instrument response; [c] A suspension containing water/methanol/trimethylamine (5 mL) and polymer (5 mg) was diluted with DI water (25 mL) into a cylindrical cell. For the transmittance measurement the average of the measurements between 0.5 mm to 30 mm height were averaged; [d] Reaction conditions: 5 mg polymer was suspended in 5 mL water/methanol/triethylamine solution, irradiated by solar simulator (AM1.5G, Class AAA, IEC/JIS/ASTM, 1440 W Xenon, 12 × 12 in., MODEL: 94123A) 1 hour irradiation.

5. Non-dibenzo[*b,d*]thiophene sulfone co-polymers

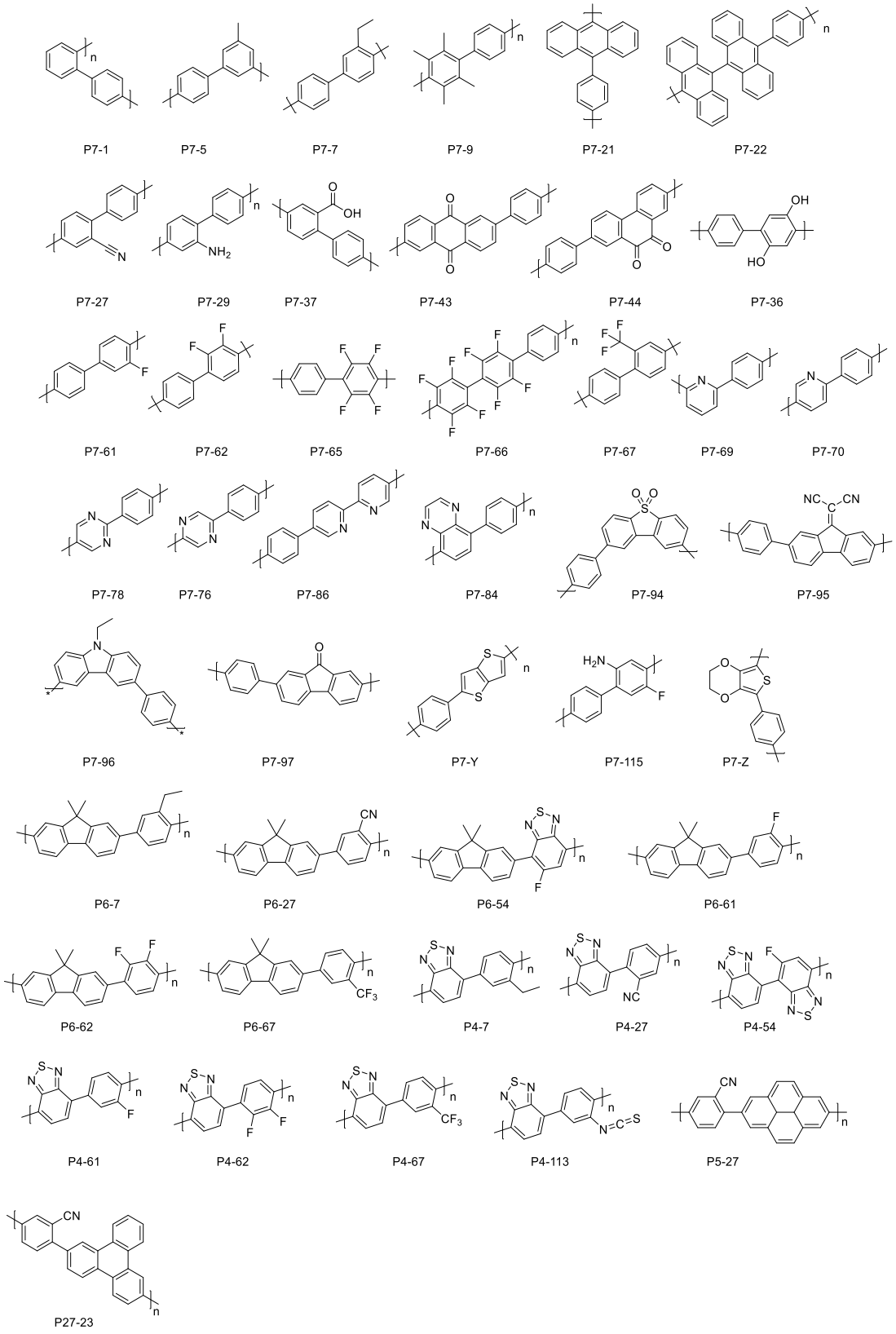

Figure S-132. Structures of 1,4-benzene, 4,7-benzo[1,2,5]thiadiazole, 2,7-dimethyl-9*H*-flouorene co-polymers made via high-throughput microwave synthesis route.

5.1 UV-visible Spectra

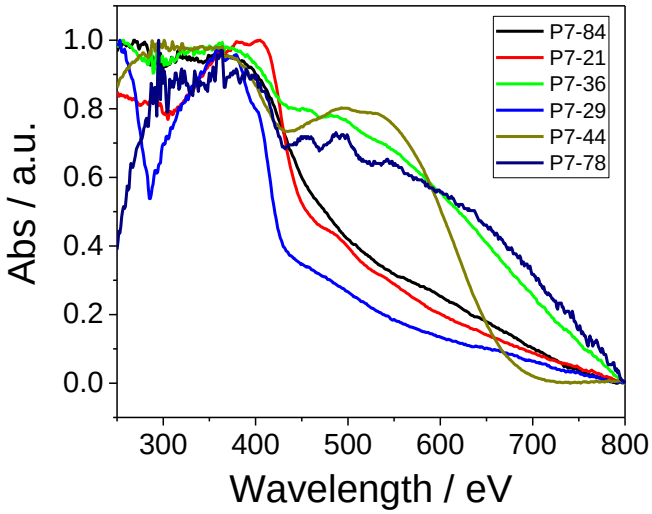

Figure S-133. Solid-state UV-vis spectrum of benzene co-polymers

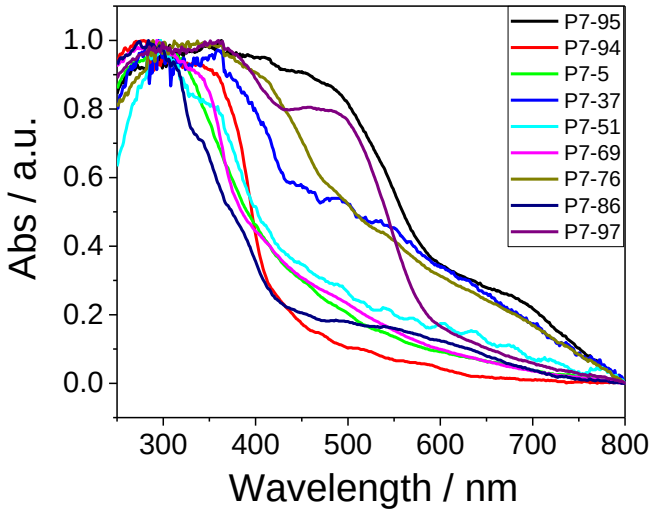

Figure S-134. Solid-state UV-vis spectrum of benzene co-polymers

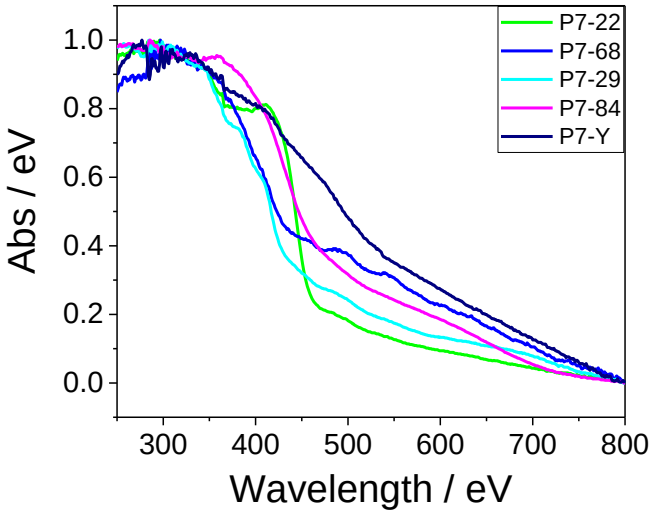

Figure S-135. Solid-state UV-vis spectrum of benzene co-polymers

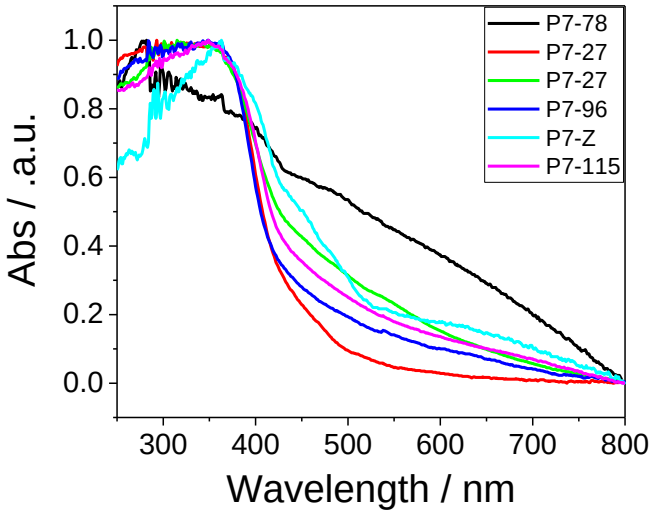

Figure S-136. Solid-state UV-vis spectrum of benzene co-polymers

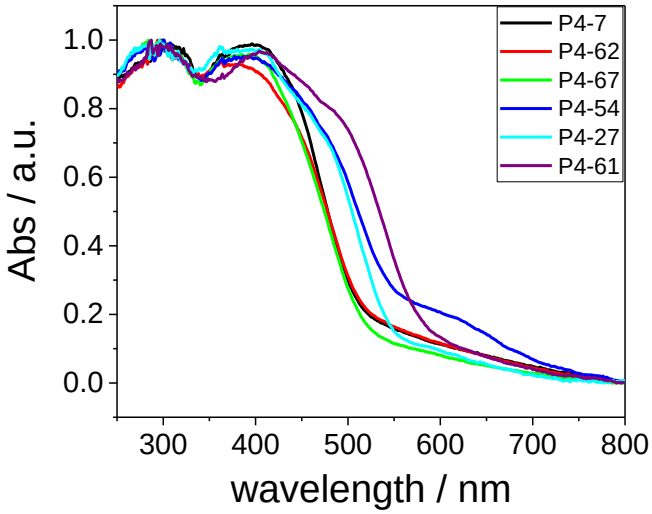

Figure S-137. Solid-state UV-vis spectrum of 4,7-benzo[1,2,5]thiadiazole co-polymers

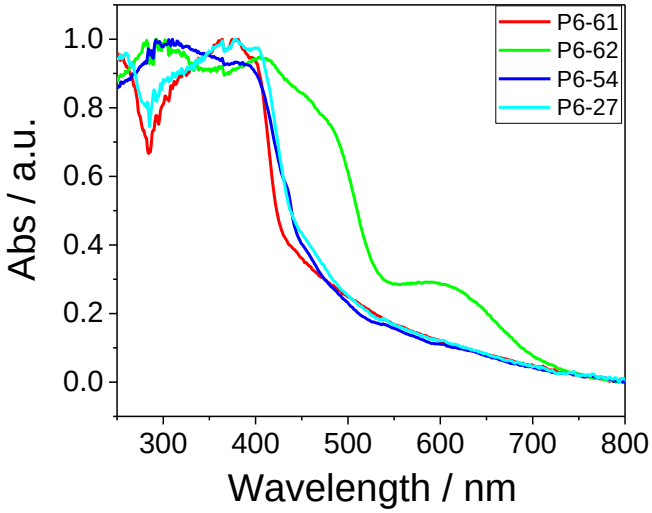

Figure S-138. Solid-state UV-vis spectrum of dimethylfluorene co-polymers

5.2 Fourier-Transform Infrared Spectra

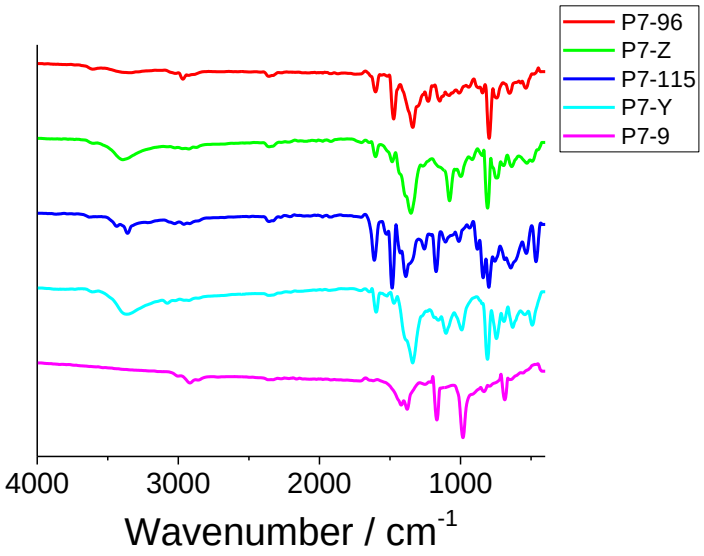

Figure S-139. Transmission FT-IR spectra of benzene co-polymers

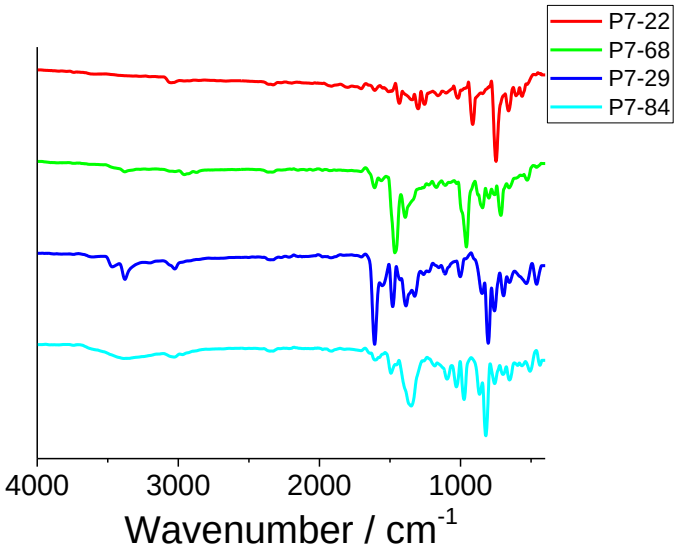

Figure S-140. Transmission FT-IR spectra of benzene co-polymers

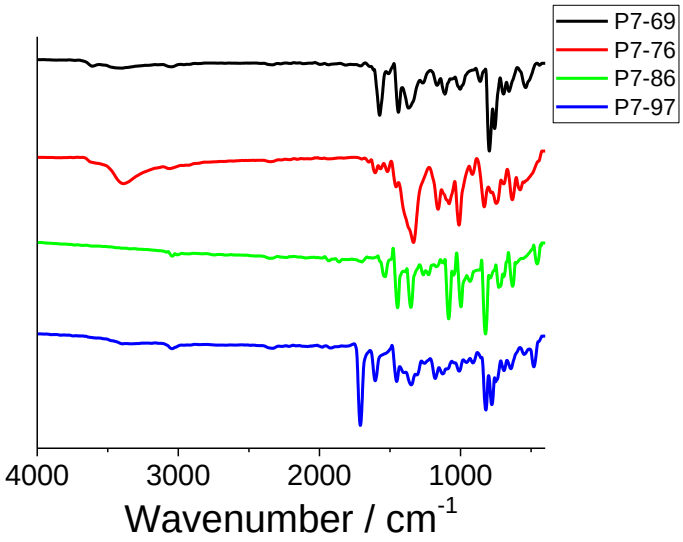

Figure S-141. Transmission FT-IR spectra of benzene co-polymers

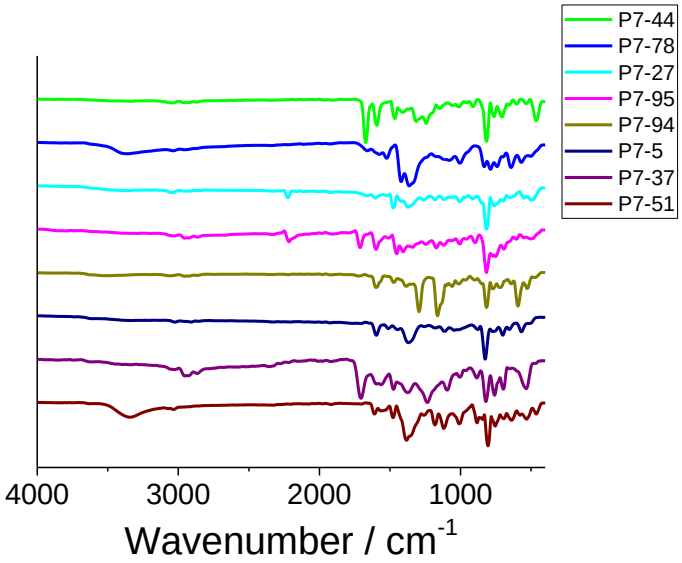

Figure S-142. Transmission FT-IR spectra of benzene co-polymers

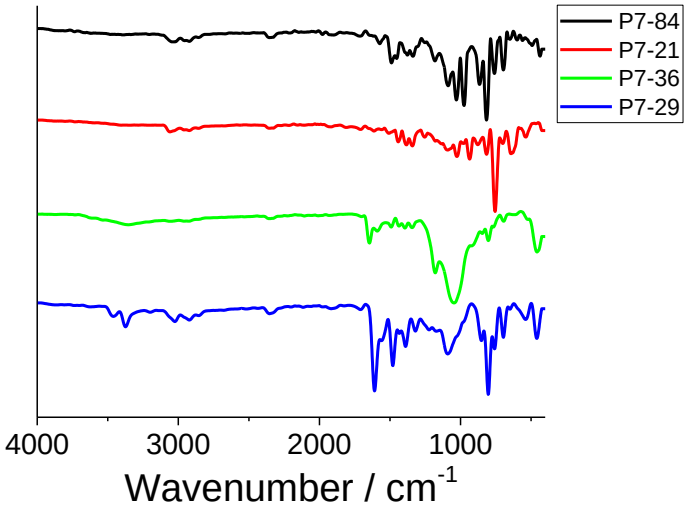

Figure S-143. Transmission FT-IR spectra of benzene co-polymers

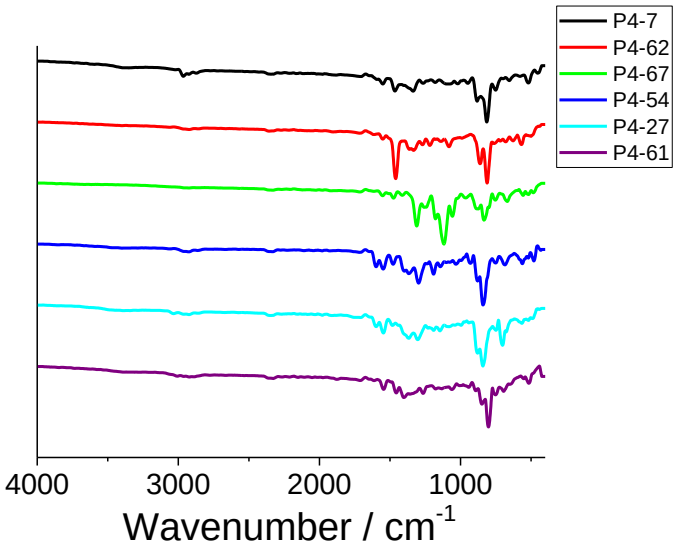

Figure S-144. Transmission FT-IR spectra of 2,1,3-benzothiadiazole co-polymers.

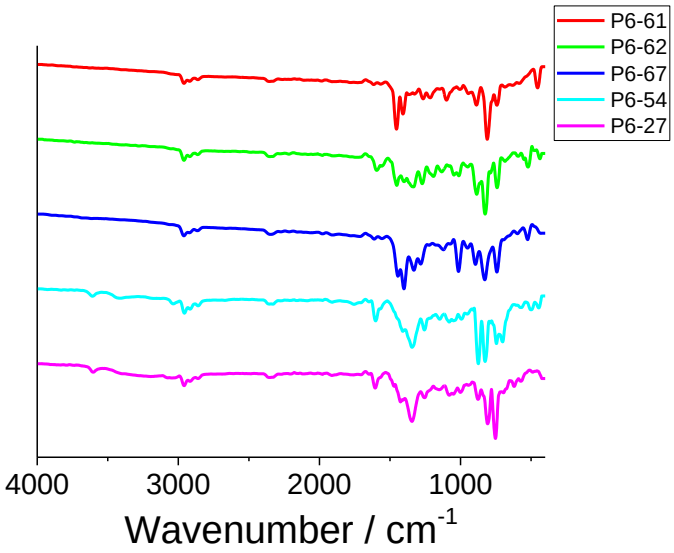

Figure S-145. Transmission FT-IR spectra of dimethylfluorene co-polymers.

5.3 Powder X-Ray Diffraction Patterns

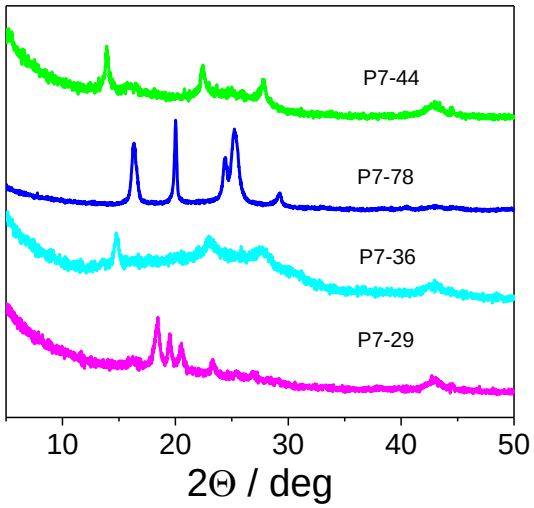

Figure S-146. PXRD patterns for benzene co-polymers.

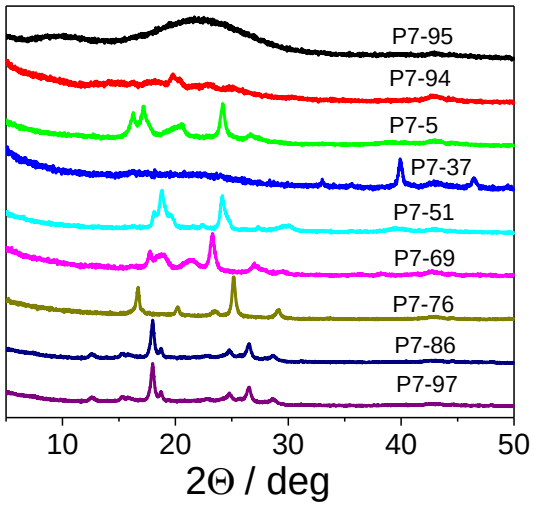

Figure S-147. PXRD patterns for benzene co-polymers.

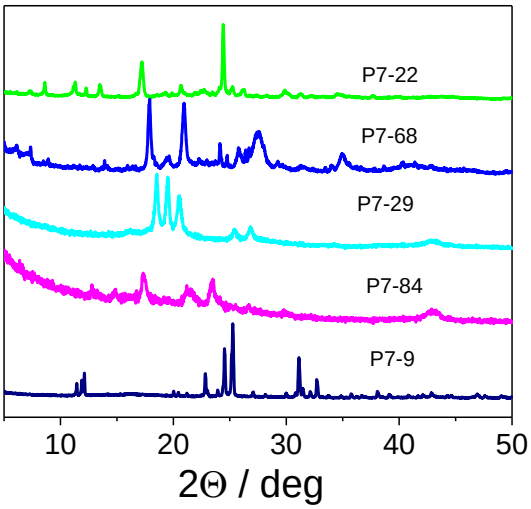

Figure S-148. PXRD patterns for benzene co-polymers.

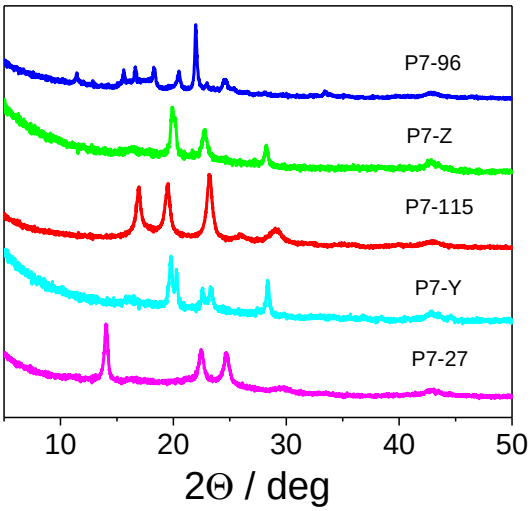

Figure S-149. PXRD patterns for benzene co-polymers.

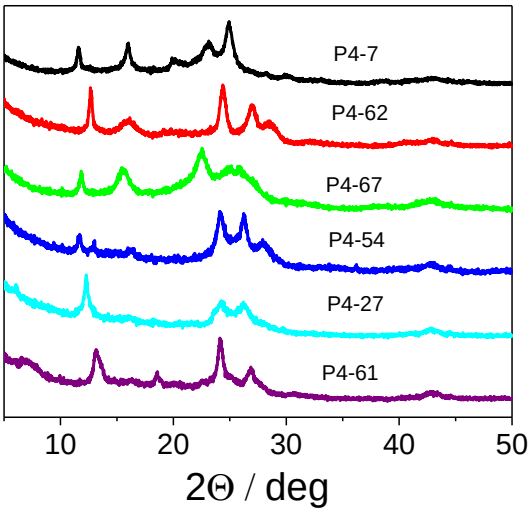

Figure S-150. PXRD patterns for 4,7-benzo[1,2,5]thiadiazole co-polymers.

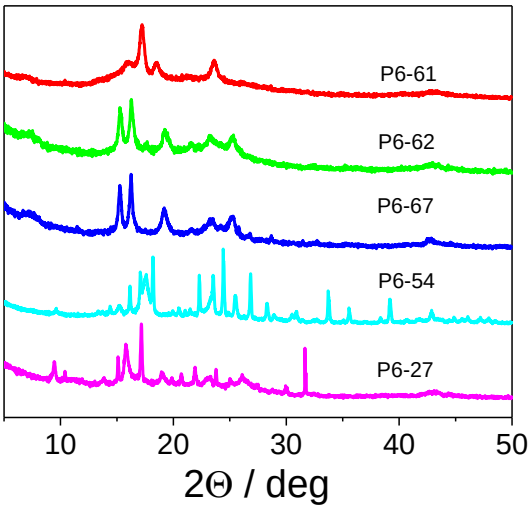

Figure S-151. PXRD patterns for dimethylfluorene co-polymers.

5.4 HER *vs.* HT Polymers Characterization

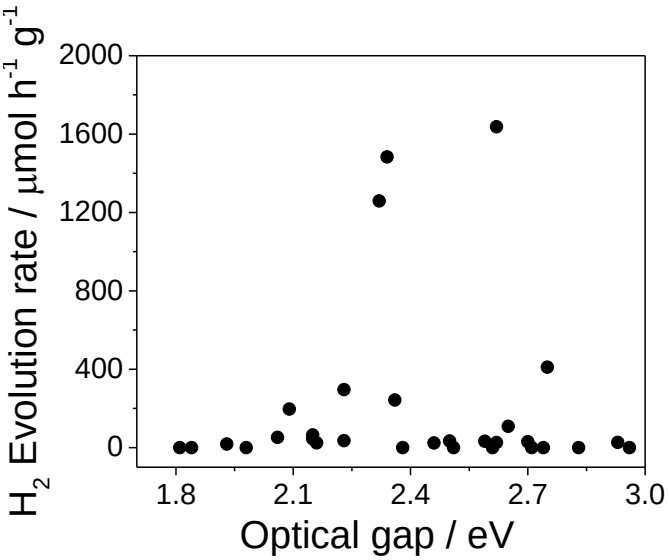

Figure S-152. Photocatalytic hydrogen evolution rate (HER) of photocatalysts from TEA/MeOH/H_2O mixtures plotted against the polymers optical gap. Polymer (5 mg) was suspended in 5 mL water/methanol/triethylamine solution, irradiated by a solar simulator (AM1.5G, Class AAA, IEC/JIS/ASTM, 1440 W xenon, 12 × 12 in., MODEL: 94123A, illumination time: 1 hour).

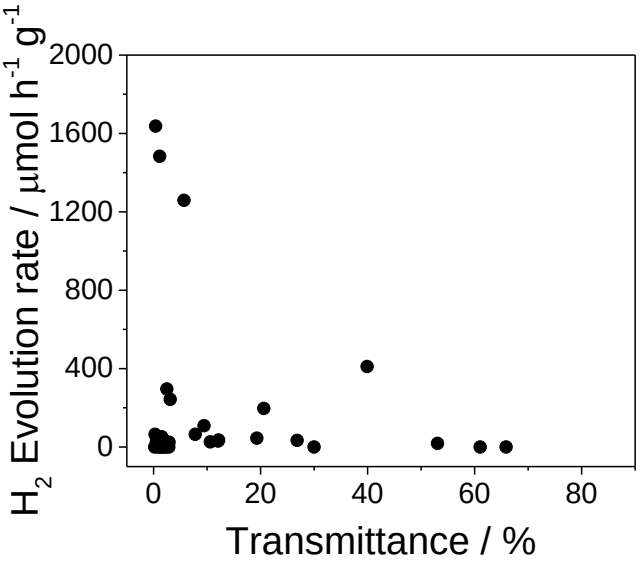

Figure S-153. Photocatalytic hydrogen evolution rate (HER) of photocatalysts from TEA/MeOH/H_2O mixtures plotted against the sample's transmittance in this suspension. Polymer (5 mg) was suspended in 5 mL water/methanol/triethylamine solution, irradiated by a solar simulator (AM1.5G, Class AAA, IEC/JIS/ASTM, 1440 W xenon, 12 × 12 in., MODEL: 94123A, illumination time: 1 hour).

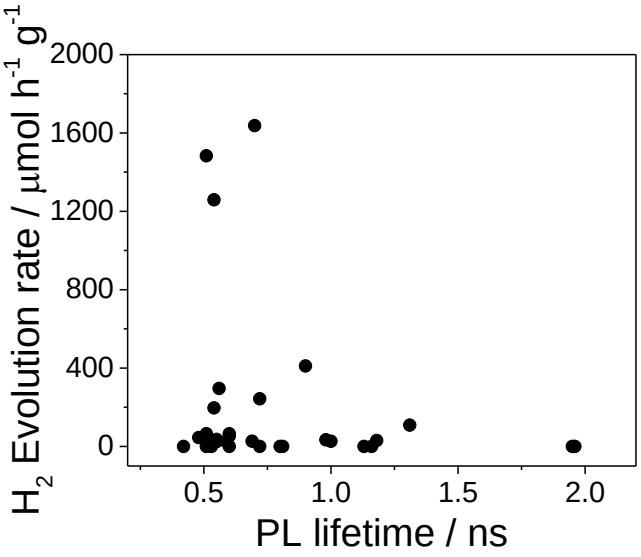

Figure S-154. Photocatalytic hydrogen evolution rate (HER) of photocatalysts from TEA/MeOH/H_2O mixtures plotted against PL lifetime of polymers. Polymer (5 mg) was suspended in 5 mL water/methanol/triethylamine solution, irradiated by a solar simulator (AM1.5G, Class AAA, IEC/JIS/ASTM, 1440 W xenon, 12 × 12 in., MODEL: 94123A, illumination time: 1 hour).

5.5 Computational result *vs.* HER

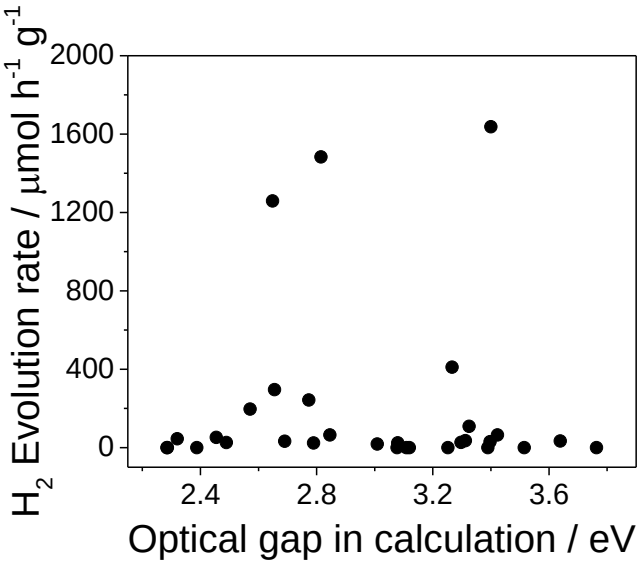

Figure S-155. Photocatalytic hydrogen evolution rate (HER) of photocatalysts plotted against the polymers optical gap. Polymer (5 mg) was suspended in 5 mL water/methanol/triethylamine solution, irradiated by a solar simulator (AM1.5G, Class AAA, IEC/JIS/ASTM, 1440 W xenon, 12 × 12 in., MODEL: 94123A, illumination time: 1 hour).

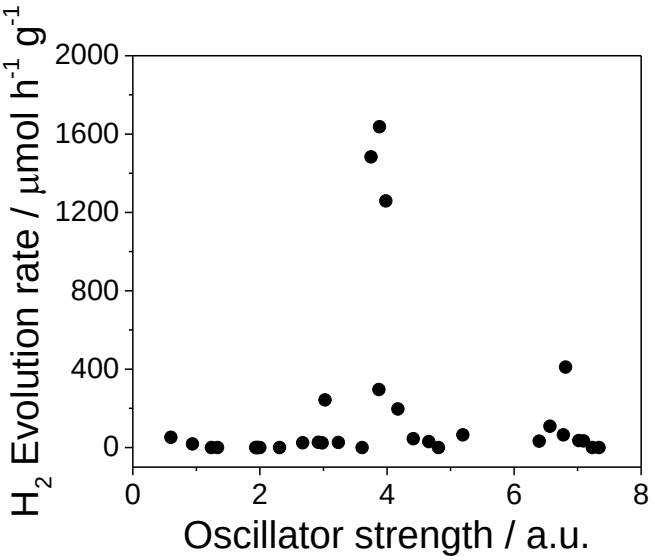

Figure S-156. Photocatalytic hydrogen evolution rate (HER) of photocatalysts plotted against the polymers oscillator strength. Polymer (5 mg) was suspended in 5 mL water/methanol/triethylamine solution, irradiated by a solar simulator (AM1.5G, Class AAA, IEC/JIS/ASTM, 1440 W xenon, 12 × 12 in., MODEL: 94123A, illumination time: 1 hour).

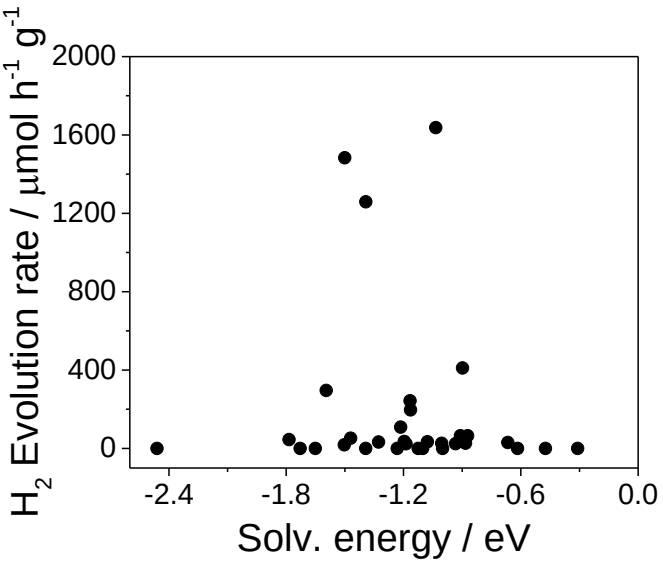

Figure S-157. Photocatalytic hydrogen evolution rate (HER) of photocatalysts plotted against the polymers solvent free energy. Polymer (5 mg) was suspended in 5 mL water/methanol/triethylamine solution, irradiated by a solar simulator (AM1.5G, Class AAA, IEC/JIS/ASTM, 1440 W xenon, 12 × 12 in., MODEL: 94123A, illumination time: 1 hour).

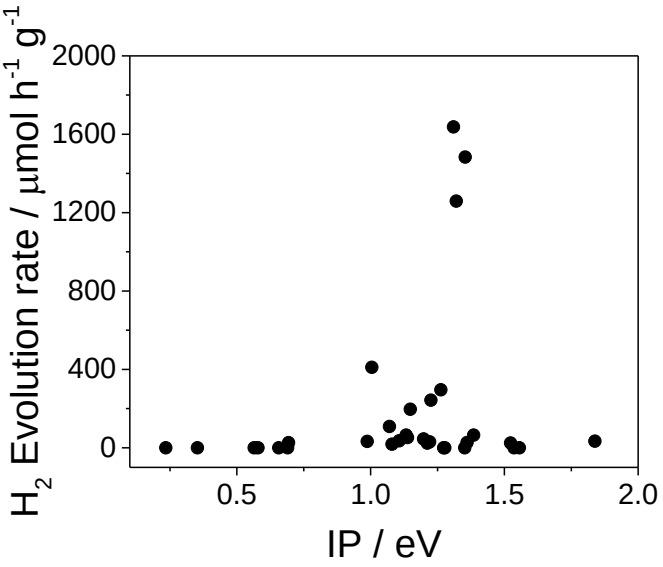

Figure S-158. Photocatalytic hydrogen evolution rate (HER) of photocatalysts plotted against the polymers ionisation potential (IP). Polymer (5 mg) was suspended in 5 mL water/methanol/triethylamine solution, irradiated by a solar simulator (AM1.5G, Class AAA, IEC/JIS/ASTM, 1440 W xenon, 12 × 12 in., MODEL: 94123A, illumination time: 1 hour).

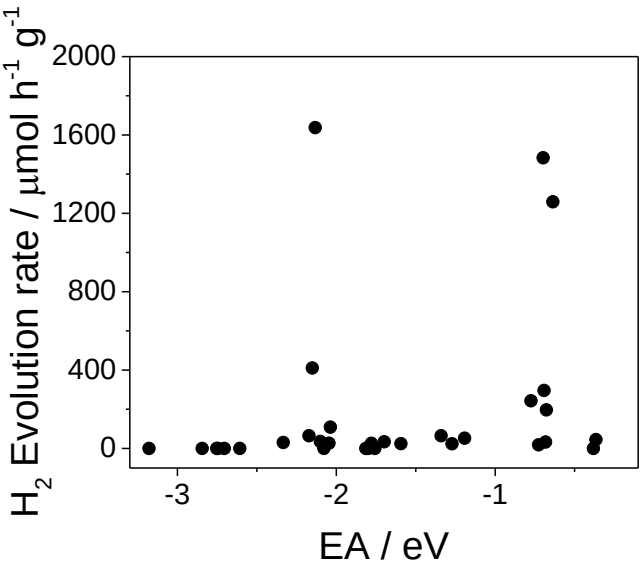

Figure S-159. Photocatalytic hydrogen evolution rate (HER) of photocatalysts plotted against the polymers electron affinity (EA). Polymer (5 mg) was suspended in 5 mL water/methanol/triethylamine solution, irradiated by a solar simulator (AM1.5G, Class AAA, IEC/JIS/ASTM, 1440 W xenon, 12 × 12 in., MODEL: 94123A, illumination time: 1 hour).

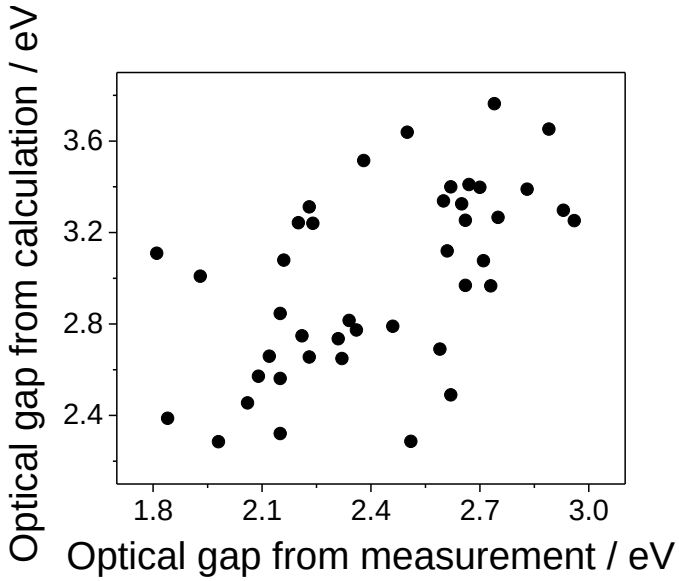

Figure S-160. Optical gap of photocatalysts from calculation plotted against optical gap of catalyst from measurement. Polymer (5 mg) was suspended in 5 mL water/methanol/triethylamine solution, irradiated by a solar simulator (AM1.5G, Class AAA, IEC/JIS/ASTM, 1440 W xenon, 12 × 12 in., MODEL: 94123A, illumination time: 1 hour).

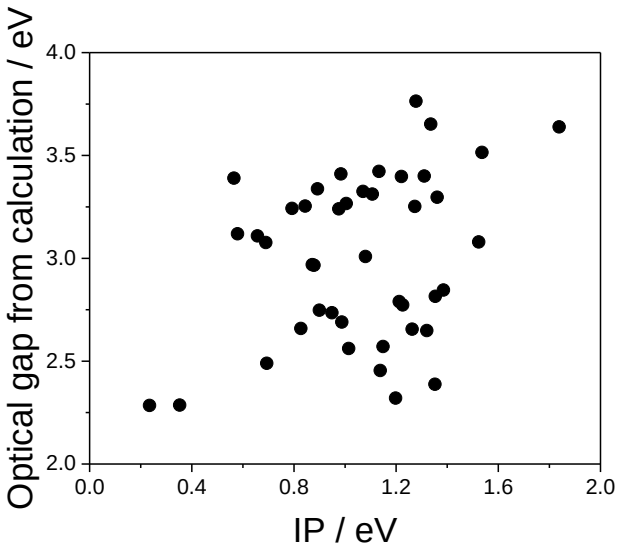

Figure S-161. Optical gap of catalyst from calculation plotted against the polymers ionisation potential (IP).

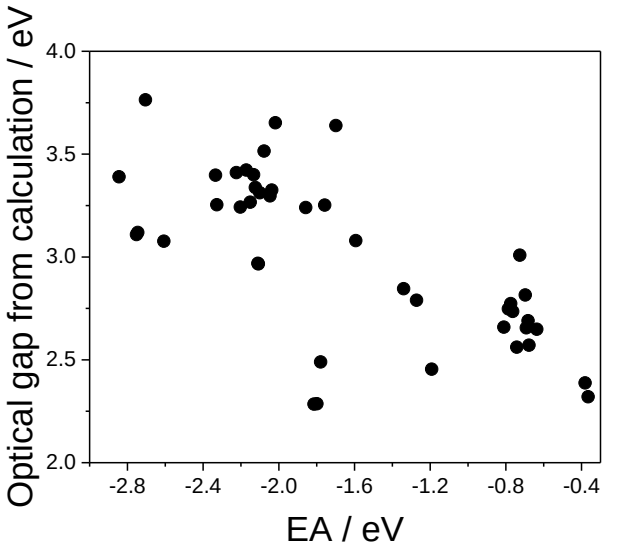

Figure S-162. Optical gap of catalyst from calculation plotted against the polymers electron affinity (EA).

5.6 Energy potential *vs.* Transmittance *vs.* HER

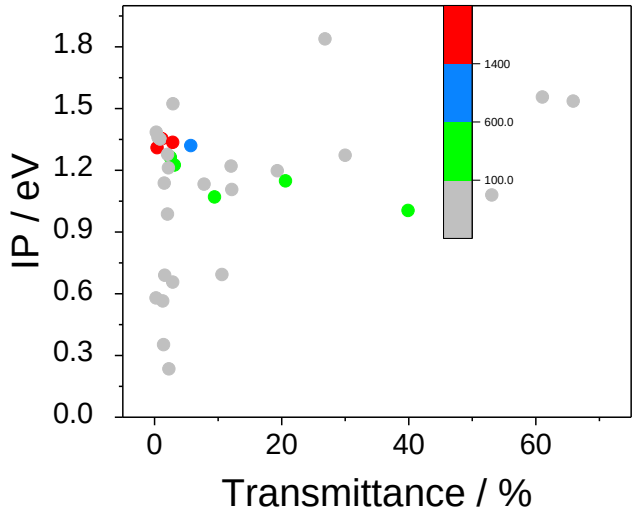

Figure S-163. Photocatalytic hydrogen evolution rate (HER) of photocatalysts from TEA/MeOH/H_2O mixtures correlated with the polymers ionisation potential (IP) and the sample's transmittance in this suspension. Polymer (5 mg) was suspended in 5 mL water/methanol/triethylamine solution, irradiated by a solar simulator (AM1.5G, Class AAA, IEC/JIS/ASTM, 1440 W xenon, 12 × 12 in., MODEL: 94123A, illumination time: 1 hour).

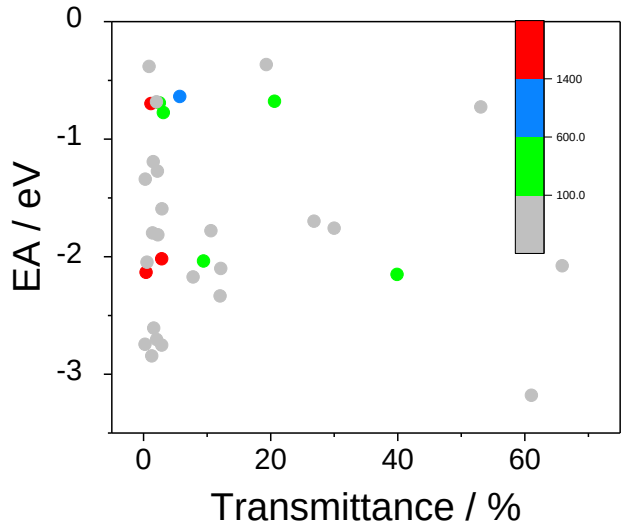

Figure S-164. Photocatalytic hydrogen evolution rate (HER) of photocatalysts from TEA/MeOH/H_2O mixtures correlated with the polymers electron affinity (EA) and the sample's transmittance in this suspension. Polymer (5 mg) was suspended in 5 mL water/methanol/triethylamine solution, irradiated by a solar simulator (AM1.5G, Class AAA, IEC/JIS/ASTM, 1440 W xenon, 12 × 12 in., MODEL: 94123A, illumination time: 1 hour).

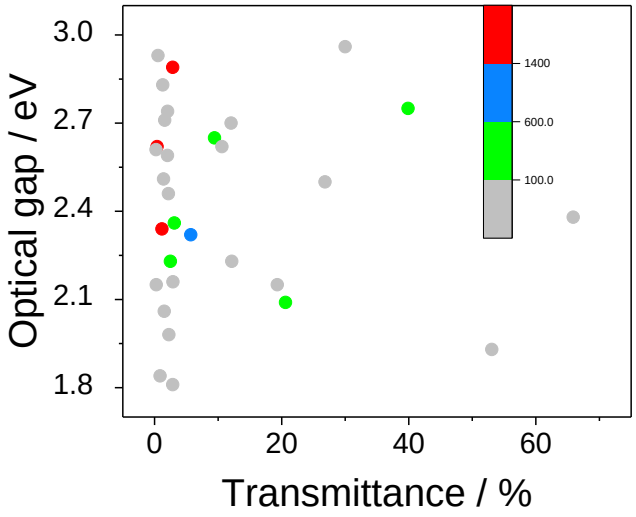

Figure S-165. Photocatalytic hydrogen evolution rate (HER) of photocatalysts from TEA/MeOH/H_2O mixtures correlated with the polymers optical gaps (experimental) and the sample's transmittance in this suspension. Polymer (5 mg) was suspended in 5 mL water/methanol/triethylamine solution, irradiated by a solar simulator (AM1.5G, Class AAA, IEC/JIS/ASTM, 1440 W xenon, 12 × 12 in., MODEL: 94123A, illumination time: 1 hour).

Table S-6. Photophysical properties and HERs for the random co-polymer photocatalysts.

Polymers	Yield / %	Optical gap / eV [a]	PL Lifetime / ns [b]	T(TEA) / % [c]	HER (TEA/MeOH/H_2O) / μmol h^{-1} g^{-1} [d]
P4-27	97	2.23	0.56	2.5	295.9
P4-54	Quant	2.15	0.48	19.3	45.3
P4-61	99	2.09	0.54	20.6	196.6
P4-62	ND	2.32	0.54	5.7	1258.8
P4-67	67	2.34	0.51	1.2	1483.3
P4-7	72	2.36	0.72	3.1	243.2
P6-27	Quant	2.65	1.31	9.4	108.9
P6-54	Quant	2.59	9.9	2.0	32.7
P6-61	Quant	2.75	0.9	39.9	410.8
P6-62	Quant	2.23	0.55	12.2	35.2
P6-67	Quant	ND	0.51	7.8	64.9
P7-115	74	2.71	1.16	1.6	0.0
P7-22	63	2.62	1	10.6	25.9
P7-27	Quant	2.62	0.7	0.4	1637.5
P7-29	48	2.61	0.8	0.2	0.0
P7-36	87	1.81	0.6	2.9	0.0
P7-37	5	2.38	0.53	65.9	0.0
P7-44	Quant	1.84	0.51	0.9	0.0
P7-5	68	2.74	1.95	2.0	0.0
P7-51	71	2.7	1.18	12.0	30.4
P7-68	64	2.5	0.98	26.8	33.6
P7-69	63	2.93	0.69	0.5	26.4
P7-76	41	2.15	0.6	0.3	64.5
P7-78	74	2.16	0.55	2.9	24.3
P7-84	Quant	2.46	0.59	2.2	23.9
P7-86	Qunt	2.96	1.13	30.0	0.0
P7-9	63	ND	0.42	61.0	0.0
P7-94	Quant	2.89	2.27	2.8	3604.8
P7-95	81	1.93	0.53	53.1	18.4
P7-96	65	2.83	1.96	1.3	0.0
P7-97	95	2.06	0.6	1.5	52.4
P7-Y	30	1.98	0.72	2.2	0.0
P7-Z	15	2.51	0.81	1.4	0.0

[a] Optical gap calculated from the absorption on-set; [b] Estimated weighted average life-time of the excited state determined by time-correlated single-photon counting. Calculated by fitting the following equation: $A + B_1 \times \exp(-i/\tau_1) + B_2 \times \exp(-i/\tau_2) + B_3 \times \exp(-i/\tau_3) + B_4 \times \exp(-i/\tau_4)$. Initial amplitudes ($A$, B_1, B_2, B_3, B_4) are estimated and iterated along with the life-times (τ_1, τ_2, τ_3, τ_4) until a fit is found. The prompt is measured separately and used for deconvolution of the instrument response; [c] A suspension containing water/methanol/trimethylamine (5 mL) and polymer (5 mg) was diluted with DI water (25 mL) into a cylindrical cell. For the transmittance measurement the average of the measurements between 0.5 mm to 30 mm height were averaged; [d] Reaction conditions: 5 mg polymer was suspended in 5 mL water/methanol/triethylamine solution, irradiated by solar simulator (AM1.5G, Class AAA, IEC/JIS/ASTM, 1440 W Xenon, 12 × 12 in., MODEL: 94123A) 1 hour.

6. Polymers synthesis using conventional heating

6.1 General procedure (Suzuki-Miyaura-type polycondensation):

Synthesis of P61

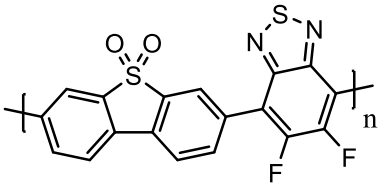

3,7-Bis(4,4,5,5-tetramethyl-1,3,2-dioxaborolan-2-yl)dibenzo[*b*,*d*]thiophene sulfone (0.234 g, 0.5 mmol), 4,7-dibromo-5,6-difluoro-2,1,3-benzothiadiazole (0.165 g, 0.5 mmol), *N*,*N*-dimethylformamide (30 mL), and an aqueous solution of K_2CO_3 (2 M, 5.4 mL) were combined and the mixture was degassed by bubbling with N_2 for 30 minutes. Then [$Pd(PPh_3)_4$] (20 mg, 3.5 mol%) was added, and heated to 150 °C for 2 days. The mixture was cooled to room temperature and poured into water. The precipitate was collected by filtration and washed with H_2O and methanol. After work-up and Soxhlet extraction with chloroform, the product was obtained as a brown powder (190.6 mg, 92 %). Anal. Calcd for $(C_{20}H_{12}F_2N_2O_2S_2)_n$: C, 57.96%; H, 2.92%; N, 6.76%; S, 15.47%;Found C, 42.02%; H, 2.26%; N, 5.86%, Pd, 0.26%.

Synthesis of P62

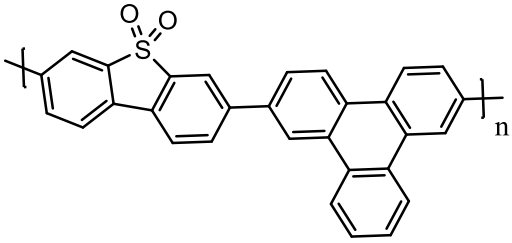

3,7-Bis(4,4,5,5-tetramethyl-1,3,2-dioxaborolan-2-yl)dibenzo[*b*,*d*]thiophene sulfone (0.234g, 0.5 mmol), 2,7-dibromotriphenylene (0.193 g, 0.5 mmol), *N*,*N*-dimethylformamide (30 mL), and an aqueous solution of K_2CO_3 (2 M, 5.4 mL) were combined and the mixture was degassed by bubbling with N_2 for 30 minutes. Then [$Pd(PPh_3)_4$] (20 mg, 3.5 mol%) was added, and heated to 150 °C for 2 days. The mixture was cooled to room temperature and poured into water. The precipitate was collected by filtration and washed with H_2O and methanol. After work-up and Soxhlet extraction with chloroform, the product was obtained as a dark-green powder (218.8 mg, 93%). Anal. Calcd for $(C_{32}H_{22}O_2S)_n$: C, 81.68%; H, 4.71%, S, 6.81%,; Found C, 76.53%; H, 3.61%, S, 6.25%, Pd, 0.54%.

Synthesis of P63

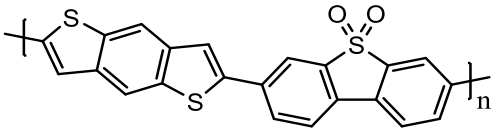

3,7-Bis(4,4,5,5-tetramethyl-1,3,2-dioxaborolan-2-yl)dibenzo[*b*,*d*]thiophene sulfone (0.234 g, 0.5 mmol), 2,6-dibromobenzo[1,2-*b*:4,5-*b*']dithiophene (0.174 g, 0.5 mmol), *N*,*N*-dimethylformamide (30 mL), and an aqueous solution of K_2CO_3 (2 M, 5.4 mL) were combined and the mixture was degassed by bubbling with N_2 for 30 minutes. Then [$Pd(PPh_3)_4$] (20 mg, 3.5 mol%) was added, and heated to 150 °C for 2 days. The mixture was cooled to room temperature and poured into water. The precipitate was collected by filtration and washed with H_2O and methanol. After work-up and Soxhlet extraction with chloroform, the product was obtained as a red-brown powder (217.4 mg, quant.). Anal. Calcd for $(C_{24}H_{16}O_2S_3)_n$: C, 66.64%; H, 3.73%, S, 22.23%; Found C, 51.68%; H, 2.48%, S, 18.32%, Pd, 0.40%.

Synthesis of P64

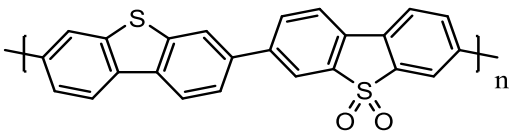

3,7-Bis(4,4,5,5-tetramethyl-1,3,2-dioxaborolan-2-yl)dibenzo[*b*,*d*]thiophene sulfone (0.234 g, 0.5 mmol), 3,7-dibromodibenzo[*b*,*d*]thiophene (0.171 g, 0.5 mmol), *N*,*N*-dimethylformamide (30 mL), and an aqueous solution of K_2CO_3 (2 M, 5.4 mL) were combined and the mixture was degassed by bubbling with N_2 for 30 minutes. Then [$Pd(PPh_3)_4$] (20 mg, 3.5 mol%) was added, and heated to 150 °C for 2 days. The mixture was cooled to room temperature and poured into water. The precipitate was collected by filtration and washed with H_2O and methanol. After work-up and Soxhlet extraction with chloroform, the product was obtained as a light-green powder (204.8 mg, 96%). Anal. Calcd for $(C_{26}H_{18}O_2S_2)_n$: C, 73.21%; H, 4.25%, S, 15.03%,; Found C, 66.94%; H, 3.02%, S, 14.72%,Pd, 0.60%.

Synthesis of P65

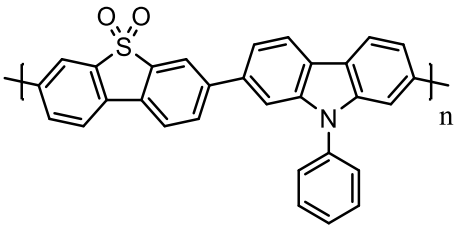

3,7-Bis(4,4,5,5-tetramethyl-1,3,2-dioxaborolan-2-yl)dibenzo[*b*,*d*]thiophene sulfone (0.234g, 0.5 mmol), 2,7-dibromo-9-phenyl-9*H*-carbazole (200.5 g, 0.5 mmol), *N*,*N*-dimethylformamide (30 mL), and an aqueous solution of K_2CO_3 (2 M, 5.4 mL) were combined and the mixture was degassed by bubbling with N_2 for 30 minutes. Then [$Pd(PPh_3)_4$] (20 mg, 3.5 mol%) was added, and heated to 150 °C for 2 days. The mixture was cooled to room temperature and poured into water. The precipitate

was collected by filtration and washed with H_2O and methanol. After work-up and Soxhlet extraction with chloroform, the product was obtained as a green powder (250.6 mg, quant.). Anal. Calcd for $(C_{32}H_{23}NO_2S)_n$: C, 79.15%; H, 4.77%, N, 2.88%, S, 6.60%,; Found C, 67.38%; H, 3.38%, N, 2.40%, S, 5.53%, Pd, 0.30%.

Synthesis of P66

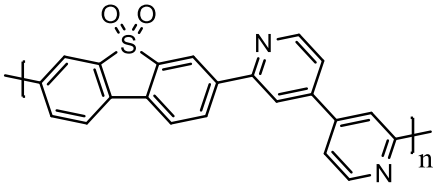

3,7-Bis(4,4,5,5-tetramethyl-1,3,2-dioxaborolan-2-yl)dibenzo[*b*,*d*]thiophene sulfone (0.234 g, 0.5 mmol), 2,2'-dibromo-4,4'-bipyridine (0.157 g, 0.5 mmol), *N*,*N*-dimethylformamide (30 mL), and an aqueous solution of K_2CO_3 (2 M, 5.4 mL) were combined and the mixture was degassed by bubbling with N_2 for 30 minutes. Then $[Pd(PPh_3)_4]$ (20 mg, 3.5 mol%) was added, and heated to 150 °C for 2 days. The mixture was cooled to room temperature and poured into water. The precipitate was collected by filtration and washed with H_2O and methanol. After work-up and Soxhlet extraction with chloroform, the product was obtained as a dark-grey powder (181.5 mg, 91%). Anal. Calcd for $(C_{24}H_{18}N_2O_2S)_n$: C, 72.34%; H, 4.55%, N, 7.03%, S, 8.05%; Found C, 64.98%; H, 3.14%, N, 6.65%, S, 7.68%, Pd, 0.68%.

Synthesis of P67

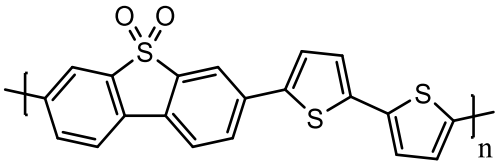

3,7-Bis(4,4,5,5-tetramethyl-1,3,2-dioxaborolan-2-yl)dibenzo[*b*,*d*]thiophene sulfone (0.234 g, 0.5 mmol), 5,5'-dibromo-2,2'-bithiophene (0.162 g, 0.5 mmol), *N*,*N*-dimethylformamide (30 mL), and an aqueous solution of K_2CO_3 (2 M, 5.4 mL) were combined and the mixture was degassed by bubbling with N_2 for 30 minutes. Then $[Pd(PPh_3)_4]$ (20 mg, 3.5 mol%) was added, and heated to 150 °C for 2 days. The mixture was cooled to room temperature and poured into water. The precipitate was collected by filtration and washed with H_2O and methanol. After work-up and Soxhlet extraction with chloroform, the product was obtained as a red powder (184.1 mg, 90%). Anal. Calcd for $(C_{22}H_{16}O_2S_3)_n$: C, 64.68%; H, 3.95%, S, 23.54%; Found C, 57.74%; H, 2.81%; S, 23%, Pd, 0.41%.

Synthesis of P68

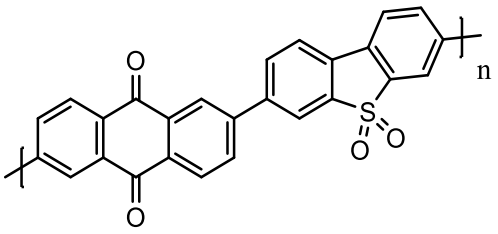

3,7-Bis(4,4,5,5-tetramethyl-1,3,2-dioxaborolan-2-yl)dibenzo[*b*,*d*]thiophene sulfone (0.234 g, 0.5 mmol), 2,6-dibromo-9,10-anthracenedione (0.183 g, 0.5 mmol), *N*,*N*-dimethylformamide (30 mL), and an aqueous solution of K_2CO_3 (2 M, 5.4 mL) were combined and the mixture was degassed by bubbling with N_2 for 30 minutes. Then [$Pd(PPh_3)_4$] (20 mg, 3.5 mol%) was added, and heated to 150 °C for 2 days. The mixture was cooled to room temperature and poured into water. The precipitate was collected by filtration and washed with H_2O and methanol. After work-up and Soxhlet extraction with chloroform, the product was obtained as a brown powder (102.0 mg, 45%). Anal. Calcd for $(C_{28}H_{18}O_4S)_n$: C, 74.65%; H, 4.03%; S, 7.12%; Found C, 51.95%; H, 3.05%; S, 5.73%, Pd, 0.91%.

Synthesis of P69

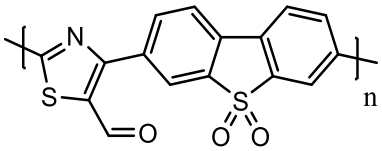

3,7-Bis(4,4,5,5-tetramethyl-1,3,2-dioxaborolan-2-yl)dibenzo[*b*,*d*]thiophene sulfone (0.234 g, 0.5 mmol), 2,4-dibromothiazole (0.121 g, 0.5 mmol), *N*,*N*-dimethylformamide (30 mL), and an aqueous solution of K_2CO_3 (2 M, 5.4 mL) were combined and the mixture was degassed by bubbling with N_2 for 30 minutes. Then [$Pd(PPh_3)_4$] (20 mg, 3.5 mol%) was added, and heated to 150 °C for 2 days. The mixture was cooled to room temperature and poured into water. The precipitate was collected by filtration and washed with H_2O and methanol. After work-up and Soxhlet extraction with chloroform, the product was obtained as a white powder (2.0 mg, 1%).

Synthesis of P70

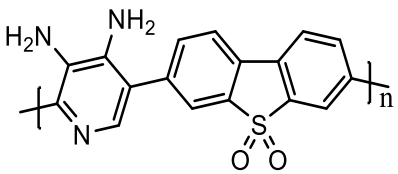

3,7-Bis(4,4,5,5-tetramethyl-1,3,2-dioxaborolan-2-yl)dibenzo[*b*,*d*]thiophene sulfone (0.234 g, 0.5 mmol), 2,5-dibromo-3,4-pyridinediamine (0.133 g, 0.5 mmol), *N*,*N*-dimethylformamide (30 mL), and an aqueous solution of K_2CO_3 (2 M, 5.4 mL) were combined and the mixture was degassed by

bubbling with N_2 for 30 minutes. Then [$Pd(PPh_3)_4$] (20 mg, 3.5 mol%) was added, and heated to 150 °C for 2 days. The mixture was cooled to room temperature and poured into water. The precipitate was collected by filtration and washed with H_2O and methanol. After work-up and Soxhlet extraction with chloroform, the product was obtained as a yellow-brown powder (37.2 mg, 21%). Anal. Calcd for $(C_{19}H_{17}N_3O_2S)_n$: C, 64.94%; H, 4.88%; N, 11.94%, S, 9.12%; Found C, 25.02%; H, 2.20%; S, 3.78; N, 4.81%.

Synthesis of P71

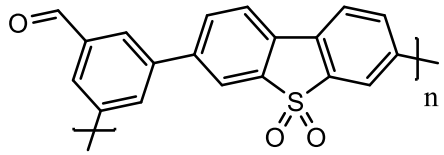

3,7-Bis(4,4,5,5-tetramethyl-1,3,2-dioxaborolan-2-yl)dibenzo[*b*,*d*]thiophene sulfone (0.234 g, 0.5 mmol), 3,5-dibromobenzaldehyde (0.132 g, 0.5 mmol), *N*,*N*-dimethylformamide (30 mL), and an aqueous solution of K_2CO_3 (2 M, 5.4 mL) T were combined and the mixture was degassed by bubbling with N_2 for 30 minutes. Then [$Pd(PPh_3)_4$] (20 mg, 3.5 mol%) was added, and heated to 150 °C for 2 days. The mixture was cooled to room temperature and poured into water. The precipitate was collected by filtration and washed with H_2O and methanol. After work-up and Soxhlet extraction with chloroform, the product was obtained as a light-grey powder (172 mg, 99%). Anal. Calcd for $(C_{21}H_{16}O_3S)_n$: C, 72.39%; H, 4.63%; S, 9.20%; Found C, 51.05%; H, 3.02%; S, 6.76%, Pd, 0.55%.

Synthesis of P72

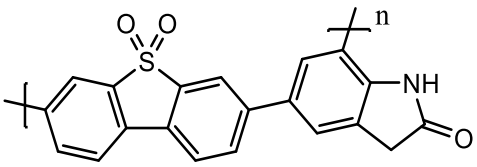

3,7-Bis(4,4,5,5-tetramethyl-1,3,2-dioxaborolan-2-yl)dibenzo[*b*,*d*]thiophene sulfone (0.234 g, 0.5 mmol), 4,6-dibromo-1,3-dihydro-2*H*-indol-2-one (0.146 g, 0.5 mmol), *N*,*N*-dimethylformamide (30 mL), and an aqueous solution of K_2CO_3 (2 M, 5.4 mL) were combined and the mixture was degassed by bubbling with N_2 for 30 minutes. Then [$Pd(PPh_3)_4$] (20 mg, 3.5 mol%) was added, and heated to 150 °C for 2 days. The mixture was cooled to room temperature and poured into water. The precipitate was collected by filtration and washed with H_2O and methanol. After work-up and Soxhlet extraction with chloroform, the product was obtained as a green-grey powder (160 mg, 85%). Anal. Calcd for $(C_{22}H_{17}NO_3S)_n$: C, 70.38%; H, 4.56%; N,3.73%, S,8.54%,; Found C, 54.33%; H,3.41%, N,3.09%, S,6.79%, Pd, 0.59%.

Synthesis of P73

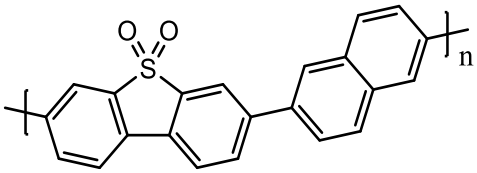

3,7-Bis(4,4,5,5-tetramethyl-1,3,2-dioxaborolan-2-yl)dibenzo[*b*,*d*]thiophene sulfone (0.234 g, 0.5 mmol), 2,6-dibromonaphthalene (0.143 g, 0.5 mmol), *N*,*N*-dimethylformamide (30 mL), and an aqueous solution of K_2CO_3 (2 M, 5.4 mL) were combined and the mixture was degassed by bubbling with N_2 for 30 minutes. Then [$Pd(PPh_3)_4$] (20 mg, 3.5 mol%) was added, and heated to 150 °C for 2 days. The mixture was cooled to room temperature and poured into water. The precipitate was collected by filtration and washed with H_2O and methanol. After work-up and Soxhlet extraction with chloroform, the product was obtained as a light-green powder (202 mg, quant.). Anal. Calcd for $(C_{24}H_{18}O_2S)_n$: C, 77.81%; H, 4.90%; S, 8.65%; Found C, 60.37%; H, 3.3%; S, 7.12%, Pd, 0.58%.

6.2 UV-Vis and PL Spectra

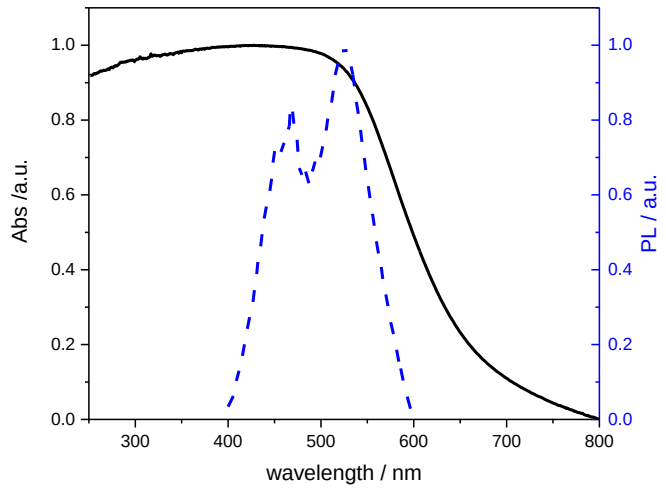

Figure S-166: UV-Vis reflectance spectrum of P61 (solid black line) and photoluminescence spectrum (λ_{exc} = 360 nm) in the solid-state (dashed blue line).

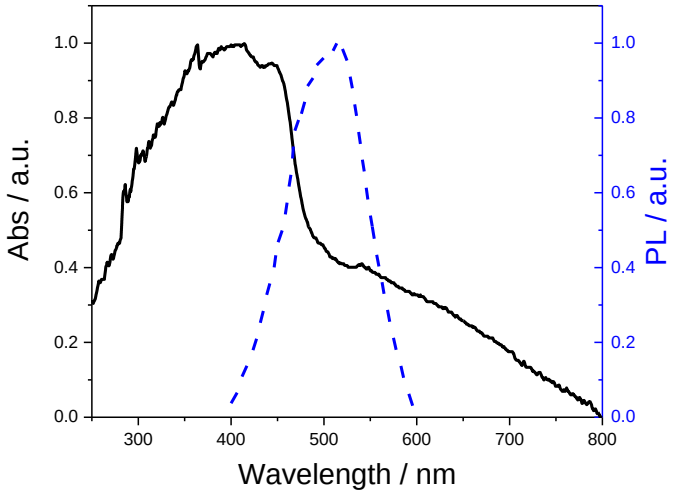

Figure S-167: UV-Vis reflectance spectrum of P62 (solid black line) and photoluminescence spectrum (λ_{exc} = 360 nm) in the solid-state (dashed blue line).

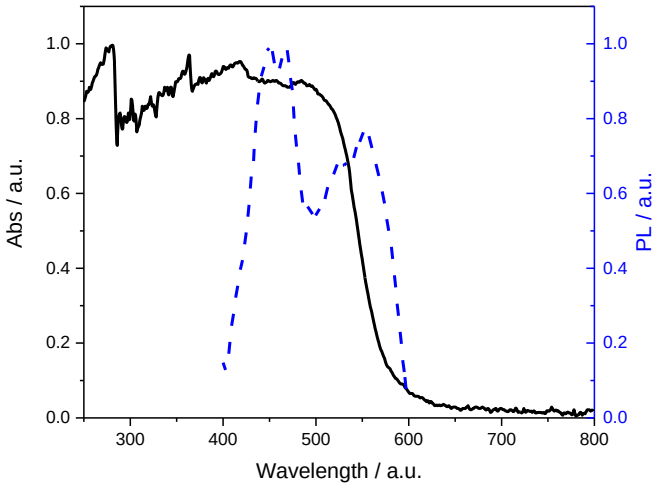

Figure S-168: UV-Vis reflectance spectrum of P63 (solid black line) and photoluminescence spectrum (λ_{exc} = 360 nm) in the solid-state (dashed blue line).

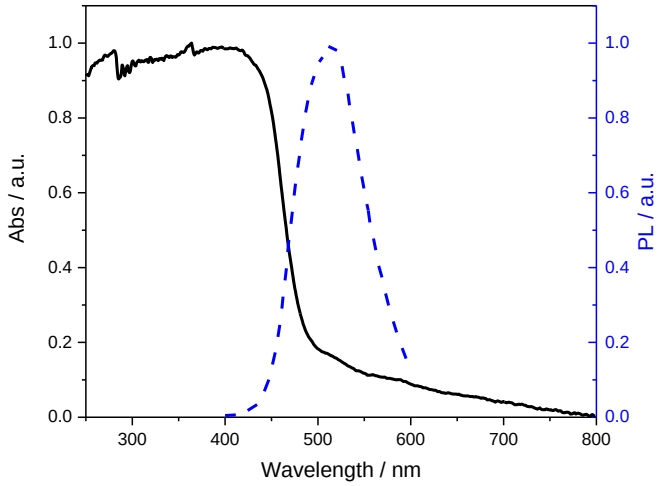

Figure S-169: UV-Vis reflectance spectrum of P64 (solid black line) and photoluminescence spectrum (λ_{exc} = 360 nm) in the solid-state (dashed blue line).

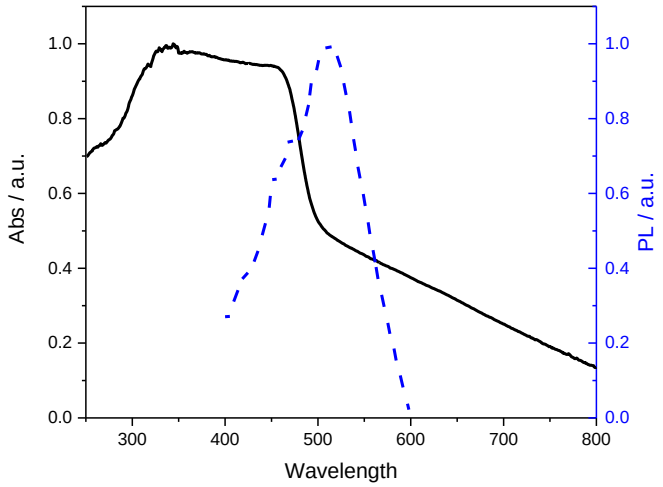

Figure S-170: UV-Vis reflectance spectrum of P65 (solid black line) and photoluminescence spectrum (λ_{exc} = 360 nm) in the solid-state (dashed blue line).

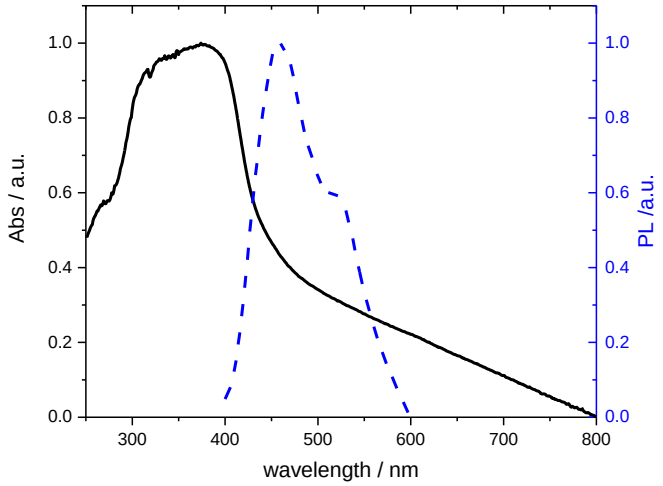

Figure S-171: UV-Vis reflectance spectrum of P66 (solid black line) and photoluminescence spectrum (λ_{exc} = 360 nm) in the solid-state (dashed blue line).

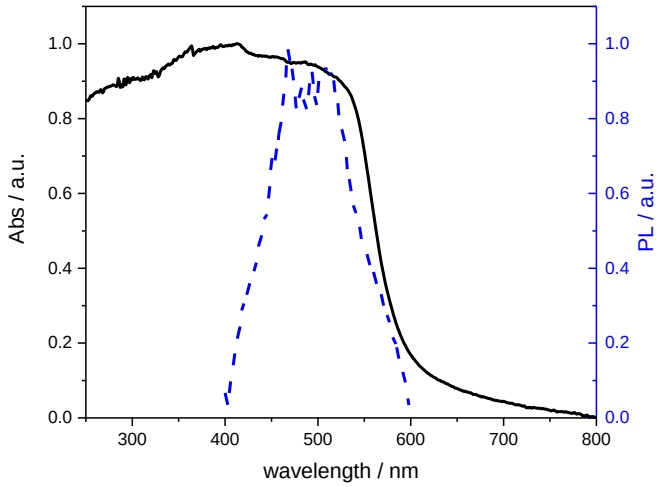

Figure S-172: UV-Vis reflectance spectrum of P67 (solid black line) and photoluminescence spectrum (λ_{exc} = 360 nm) in the solid-state (dashed blue line).

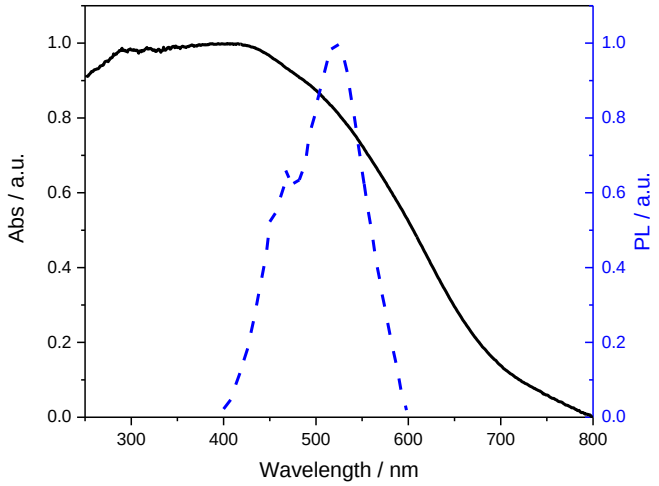

Figure S-173: UV-Vis reflectance spectrum of P68 (solid black line) and photoluminescence spectrum (λ_{exc} = 360 nm) in the solid-state (dashed blue line).

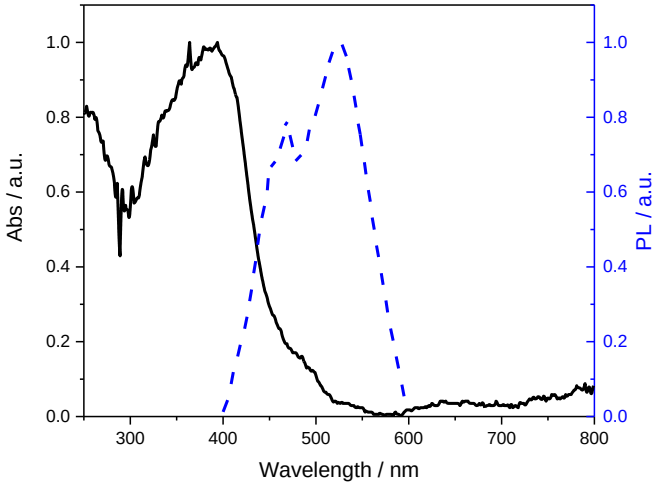

Figure S-174: UV-Vis reflectance spectrum of P69 (solid black line) and photoluminescence spectrum (λ_{exc} = 360 nm) in the solid-state (dashed blue line).

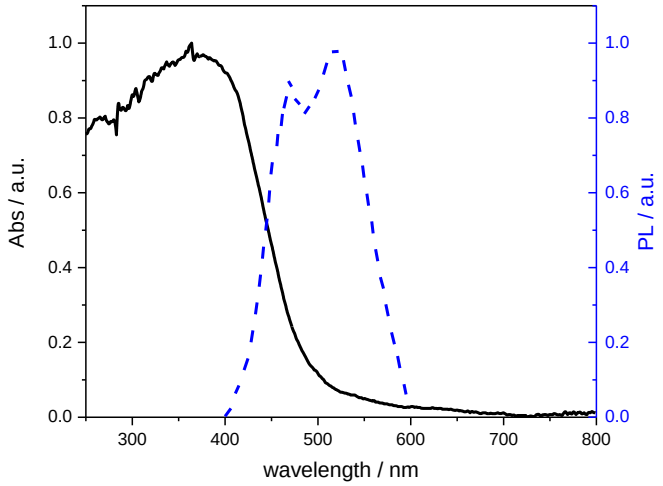

Figure S-175: UV-Vis reflectance spectrum of P70 (solid black line) and photoluminescence spectrum (λ_{exc} = 360 nm) in the solid-state (dashed blue line).

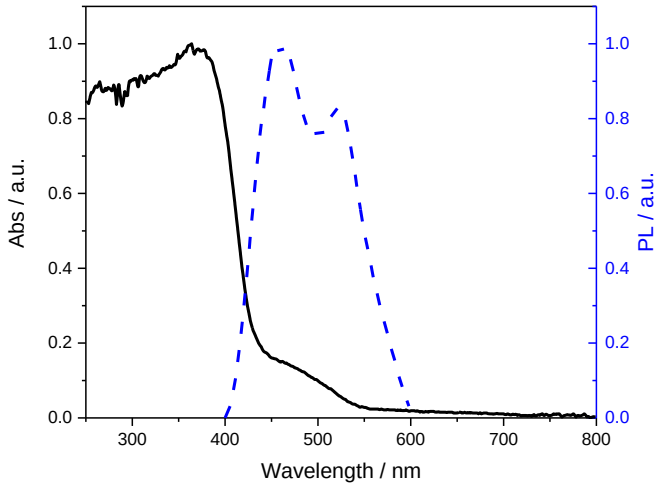

Figure S-176: UV-Vis reflectance spectrum of P71 (solid black line) and photoluminescence spectrum (λ_{exc} = 360 nm) in the solid-state (dashed blue line).

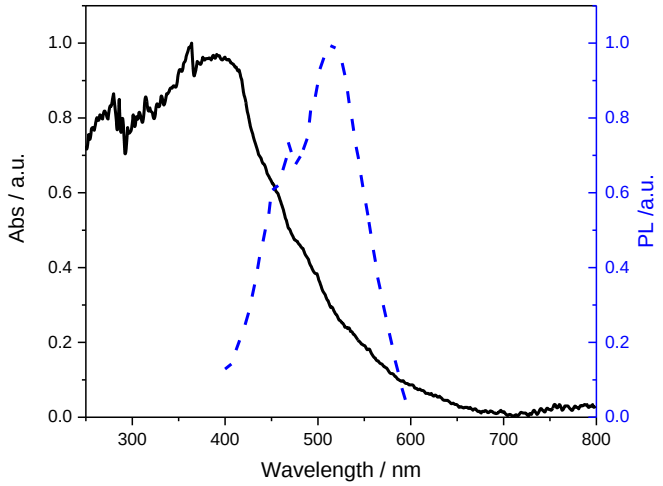

Figure S-177: UV-Vis reflectance spectrum of P72 (solid black line) and photoluminescence spectrum (λ_{exc} = 360 nm) in the solid-state (dashed blue line).

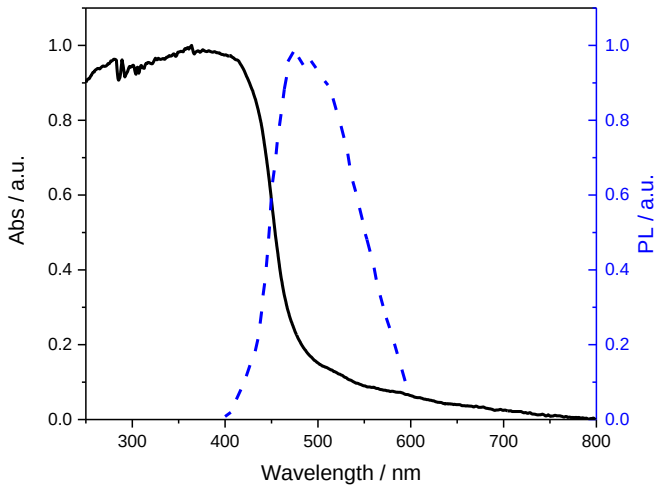

Figure S-178: UV-Vis reflectance spectrum of P73 (solid black line) and photoluminescence spectrum (λ_{exc} = 360 nm) in the solid-state (dashed blue line).

6.3 Fourier-Transform Infrared Spectra

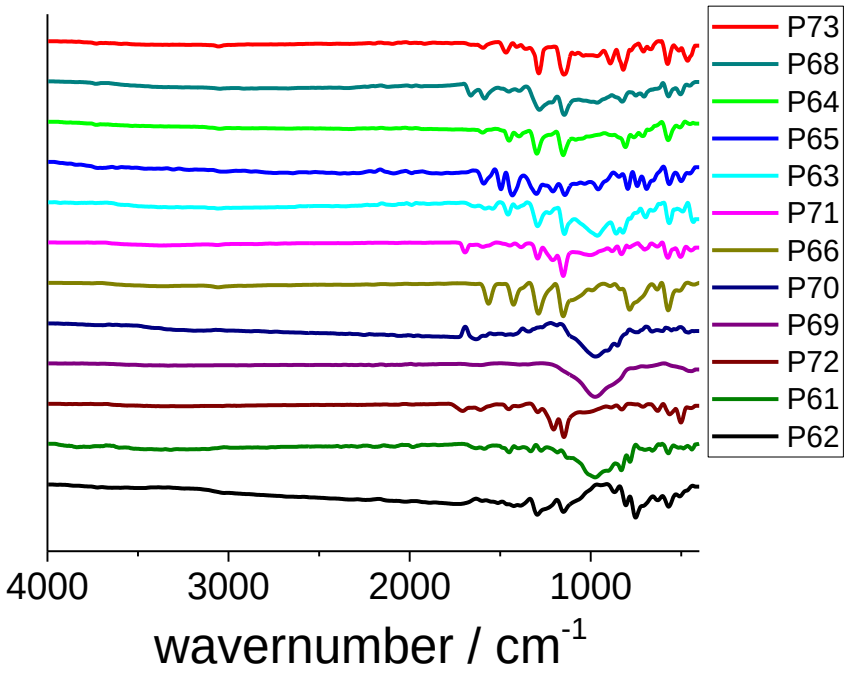

Figure S-179. Transmission FT-IR spectra of polymers made via conventional heating.

6.4 Powder X-Ray Diffraction Patterns

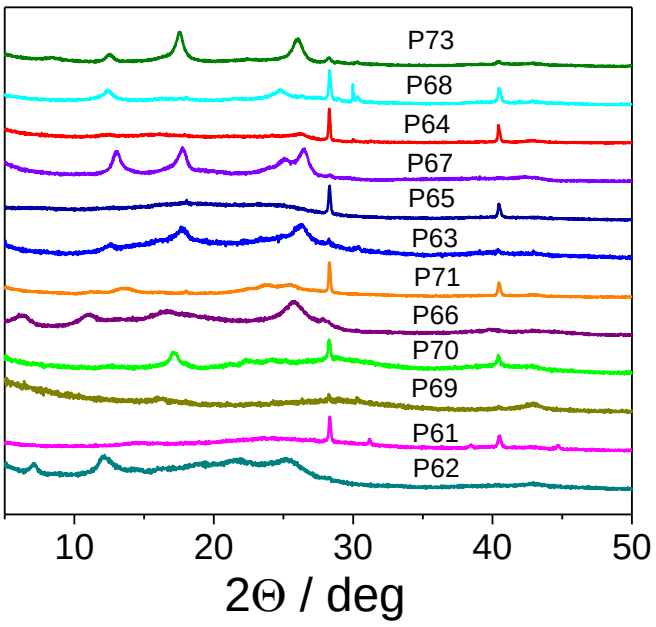

Figure S-180. PXRD patterns of polymers made via conventional heating .

6.5 Thermogravimetric Analysis

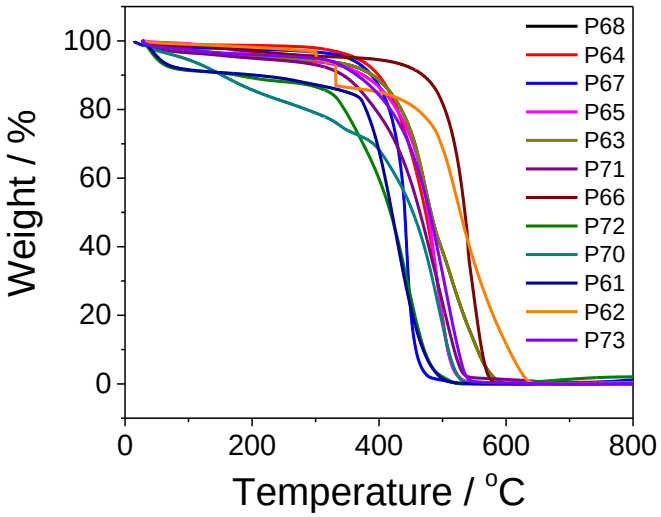

Figure S-181. Thermogravimetric analysis curves of polymers made via conventional heating in air with a heating rate of 10 °C min^{-1}.

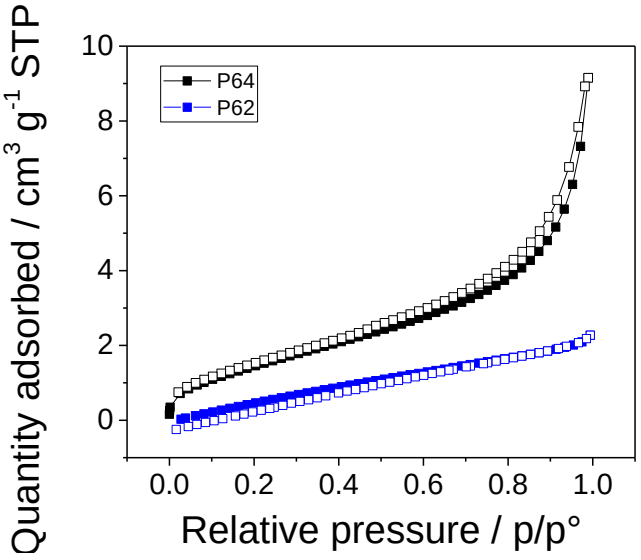

Figure S-182.bNitrogen sorption isotherm for P62 and P64 measured at 77.3 K and up to 1 bar (desorption curves shown as open symbols). SA_{BET} surface areas where determined to be 106 and 127 m^2 g^{-1} for P62 and P64.

6.6 Time-Correlated Single Photon Counting

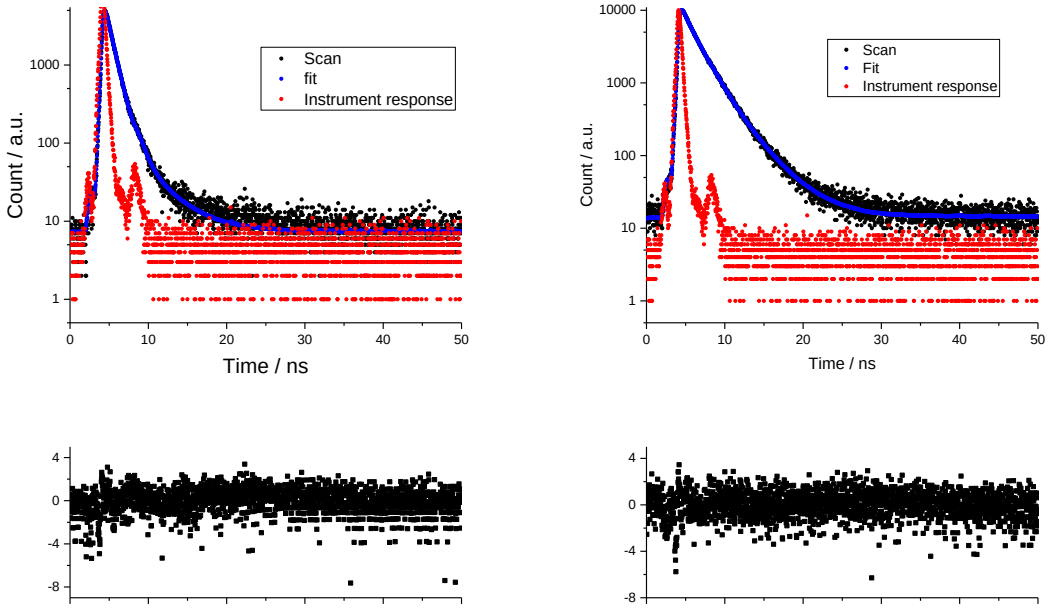

Figure S-183: Fluorescence life-time decays of P62, and P72 in THF suspension.

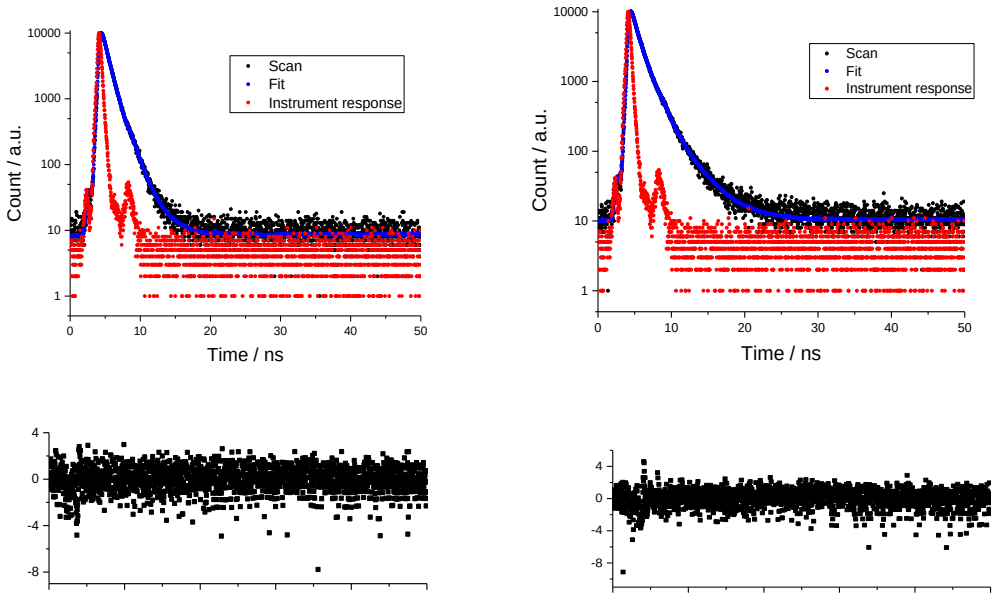

Figure S-184: Fluorescence life-time decays of P70, and P66 in THF suspension.

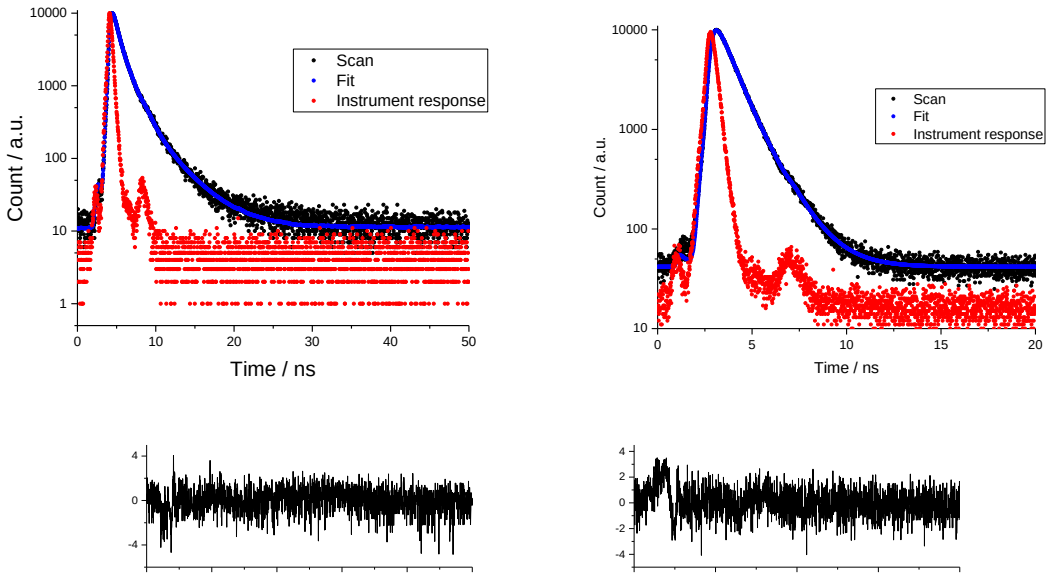

Figure S-185: Fluorescence life-time decays of P71, and P63 in THF suspension.

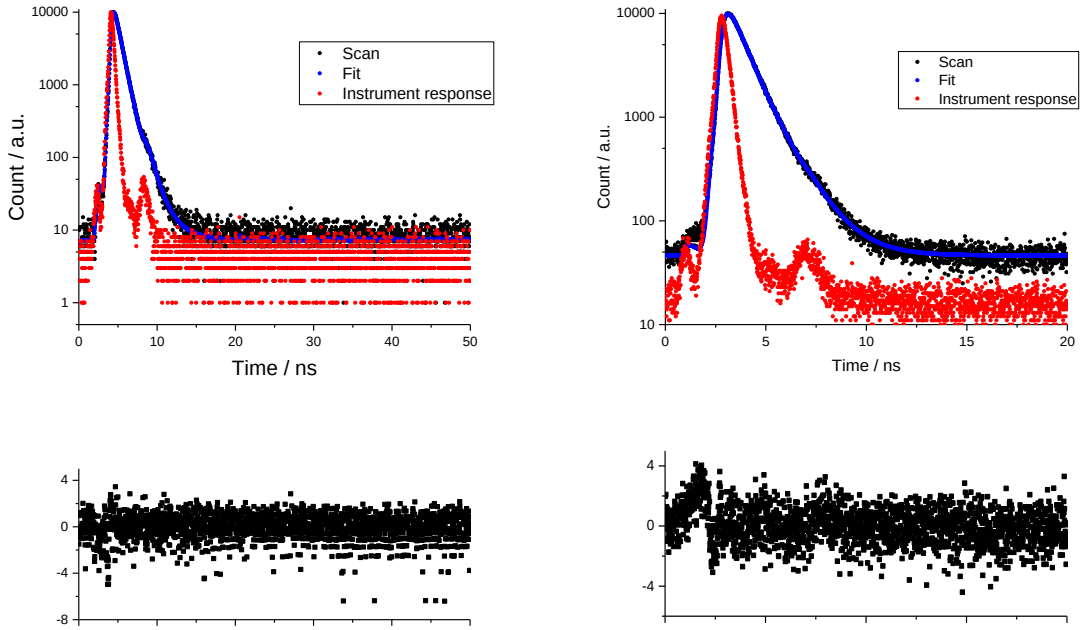

Figure S-186: Fluorescence life-time decays of P65, and P64 in THF suspension.

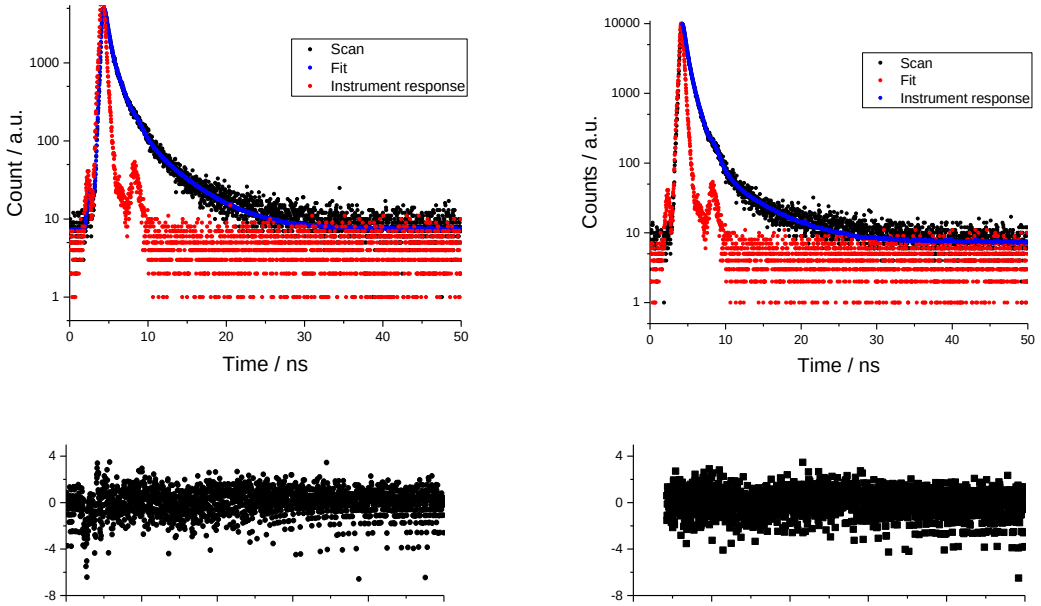

Figure S-187: Fluorescence life-time decays of P73, and P67 in THF suspension.

Table S-7. Estimated fluorescence life-times for all materials in THF suspension.

Polymer	λ_{em} / nm	τ_1 / ns	B_1 / %	τ_2 / ns	B_2 / %	τ_3 / ns	B_3 / %	χ^2	τ_{AVG} / ns
P64	433	5.866	0.071	51.900	0.715	42.234	1.307	1.464	0.93
P67	587	45.468	0.244	48.649	0.957	5.883	5.192	1.262	0.88
P63	454	9.088	0.051	49.837	0.713	41.075	1.295	1.266	0.89
P71	447	24.596	0.381	58.872	1.210	16.531	3.569	1.252	1.40
P62	450	15.290	0.069	77.265	0.900	7.446	3.682	1.417	0.98
P73	506	38.874	0.241	45.269	1.154	15.857	4.654	1.435	1.35
P66	425	14.561	0.286	68.871	1.194	16.568	3.059	1.312	1.37
P70	434	10.685	0.226	77.516	0.936	11.800	2.043	1.194	0.99
P72	452	6.568	0.186	65.658	1.761	27.774	3.563	1.276	2.15
P65	431	10.252	0.044	83.178	0.732	6.571	1.773	1.310	0.73

[a] Fluorescence life-times for all polymers in THF suspension obtained from fitting time-correlated single photon counting decays to a sum of three exponentials, which yield τ_1, τ_2, and τ_3 according to $\sum_{i=1}^{n}(A + B_i \exp(-t/\tau_i))$. τ_{AVG} is the weighted average lifetime calculated as $\sum_{i=1}^{n} B_i \tau_i$.

6.7 Static Light Scattering Data

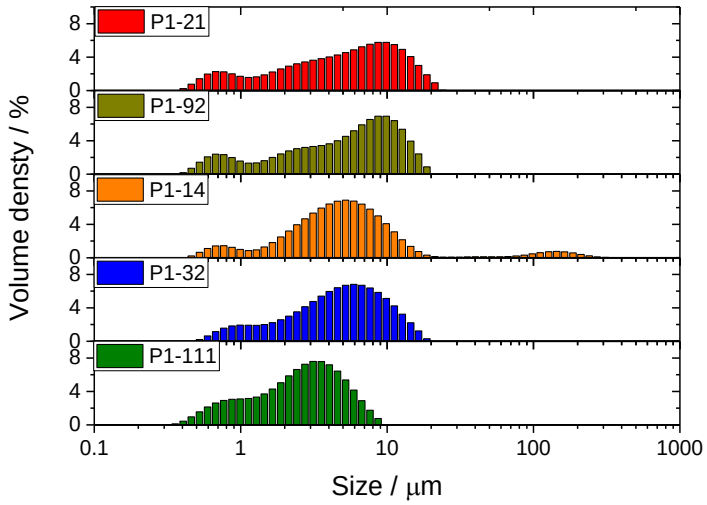

Figure S-188: Static light scattering experiments of high throughput microwave polymers in H_2O/MeOH/TEA.

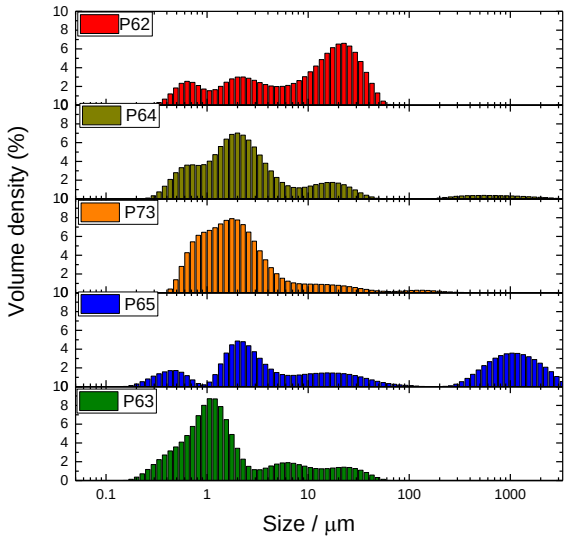

Figure S-189: Static light scattering experiments of polymers made via conventional heating in H_2O/MeOH/TEA.

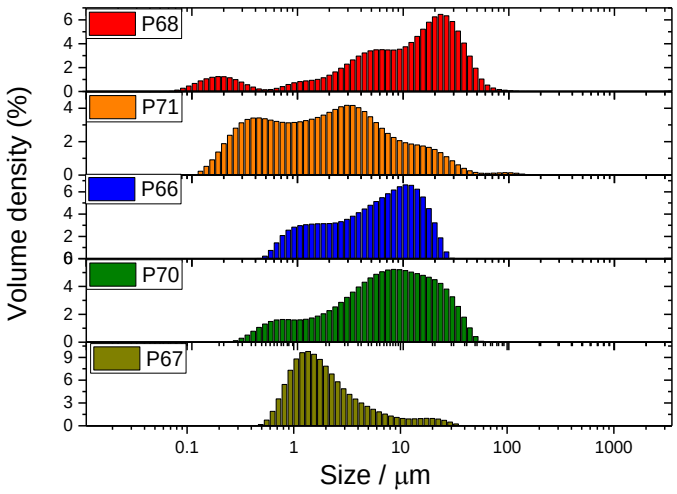

Figure S-190: Static light scattering experiments of polymers made via conventional heating in H_2O/MeOH/TEA.

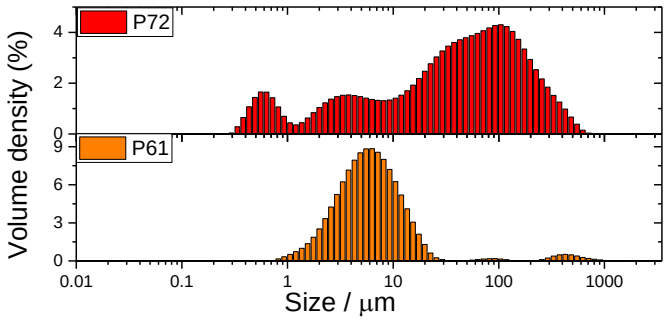

Figure S-191: Static light scattering experiments of polymers made via conventional heating in H_2O/MeOH/TEA.

Table S-8. Particle sizes by static light scattering.

Polymer	D_x50[a] (µm)	D[4,3][b] (µm)	D[3,2][c] (µm)	Relative external surface area[d] (m^2 kg^{-1})
P62	10.5	13.4	2.64	2272
P64	2.13	47.5	1.52	3953
P73	1.77	6.32	1.49	4027
P65	11.4	456	2.25	2671
P63	1.23	4.36	1.00	5986
P66	5.8	7.22	2.94	2044
P61	5.92	20.5	4.70	1278
P71	1.90	5.11	0.841	7135
P72	43.0	79.3	4.58	1309
P68	11.5	15.2	1.41	4262
P70	7.03	10.3	2.82	2129
P67	1.73	3.28	1.61	3725
P1-92	6.00	6.68	2.76	2172
P1-32	5.09	5.89	3.21	1871
P1-111	2.80	3.11	1.90	3157
P1-14	5.12	14.2	3.33	1802
P1-21	5.53	6.76	2.71	2218

[a] 50^{th} percentile of particle size volume distribution; [b] Volume mean diameter; [c] Surface area mean diameter (Sauter mean diameter);[5,6] [d] Relative extrinsic surface area calculated by dividing the total surface area of the particles by the total mass, assuming a density of 1 g cm^{-3}.

6.8 Contact Angle Measurements

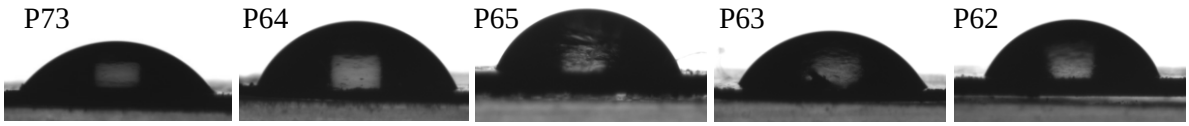

Figure S-192. Contact angle measurements for P73, P64, P65, P63 and P62.

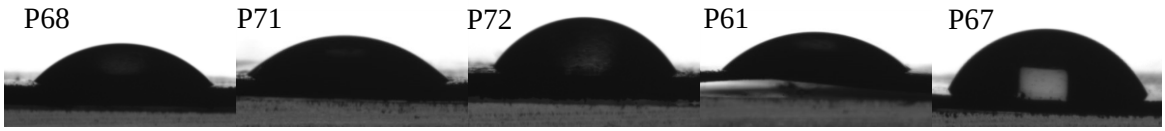

Figure S-193. Contact angle measurements for P68, P71, P72, P61 and P67.

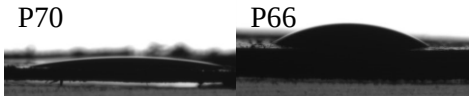

Figure S-194. Contact angle measurements for P61, P70, and P66. Samples take up the water droplet and seem to swell.

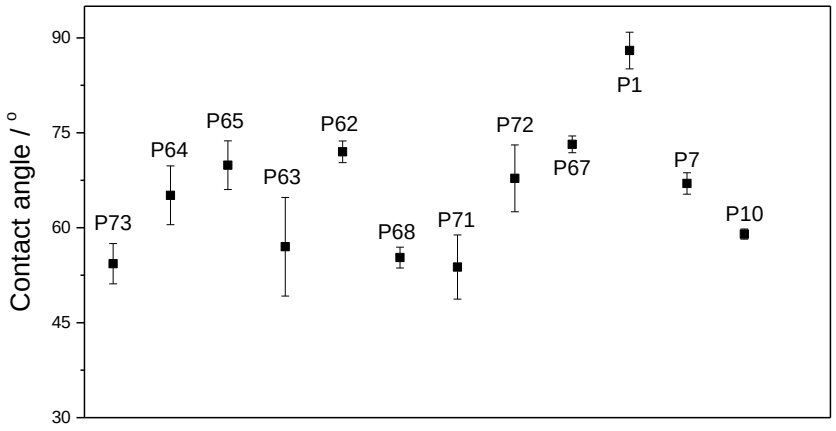

Figure S-195. Contact angles polymers against water.[7]

6.9 High throughput microwave polymerization *vs.* polymers made via conventional heating

Hydrogen evolution experiments: Here, we tested the HER for polymers synthesized by high-throughput microwave methods versus equivalent polymers prepared by thermal polymerization. A flask was charged with the polymer powder (25 mg), scavenger and water (trimethylamine/methanol/water, 1:1:1; Na_2S aq., 0.026 M; 25 mL), and sealed with a septum. The resulting suspension was ultrasonicated until the photocatalyst was dispersed before degassing by N_2 bubbling for 30 minutes. The reaction mixture was side illuminated with a solar simulator irradiation (AM1.5G, classification ABA, ASTME927-10) for the time specified. Gas samples were taken with a gas-tight syringe, and run on a Bruker 450-GC gas chromatograph equipped with a Molecular Sieve 13X 60-80 mesh 1.5 m × ⅛" × 2 mm ss column at 50 °C with an argon flow of 40.0 mL min^{-1}. Hydrogen was detected with a thermal conductivity detector referencing against standard gas with a known concentration of hydrogen. Hydrogen dissolved in the reaction mixture was not measured and the pressure increase generated by the evolved hydrogen was neglected in the calculations. The rates were determined from a linear regression fit and the error is given as the standard deviation of the amount of hydrogen evolved. No hydrogen evolution was observed for a mixture of TEA/MeOH/H_2O or Na_2S/water under solar illumination in absence of a photocatalyst.

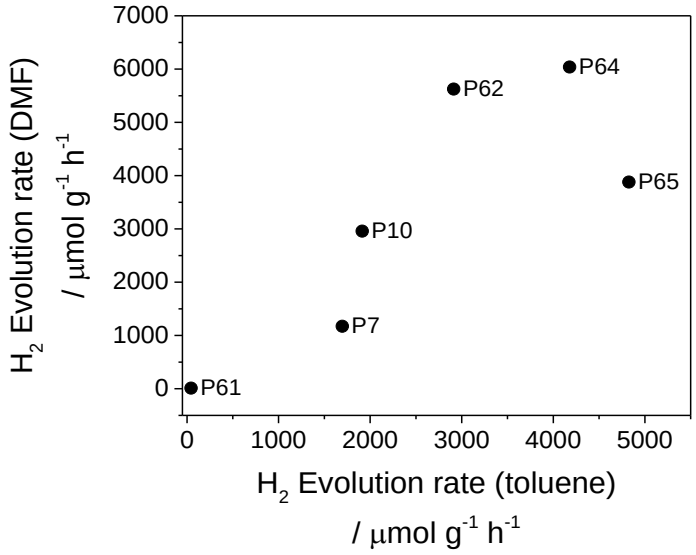

Figure S-196: Photocatalytic hydrogen evolution of polymers synthesis by conventional heating method correlated to microwave method. Polymer (25 mg) was suspended in 25 mL water/methanol/triethylamine solution (volume ratio, 1:1:1) under a solar simulator irradiation (AM1.5G, classification ABA, ASTME927-10), irradiation time: 3 hours.

6.10 Hydrogen evolution experiments

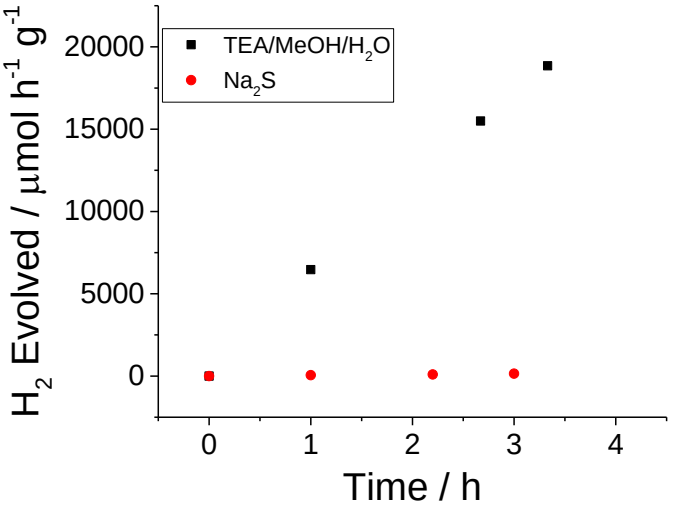

Figure S-197: Photocatalytic hydrogen evolution of P62 from water/methanol/triethylamine mixtures or Na_2S aqueous under solar simulator. Polymer (25 mg) was suspended in 25 mL water/methanol/triethylamine solution (volume ratio, 1:1:1) or 0.026 M Na_2S aqueous solution, irradiated by a solar simulator (AM1.5G, classification ABA, ASTME927-10).

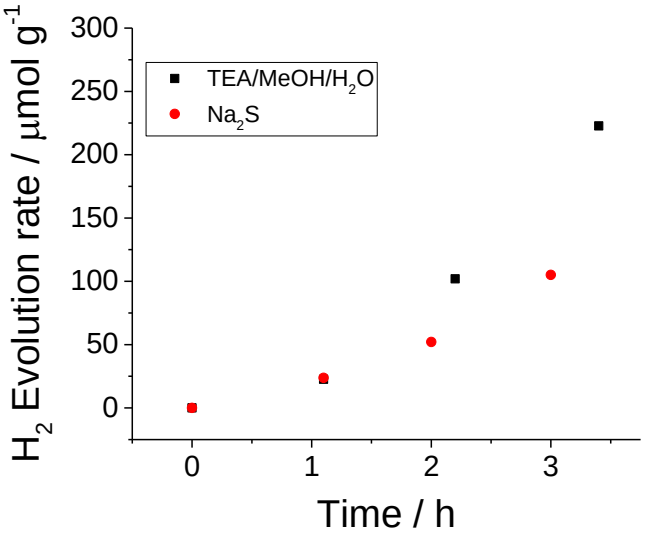

Figure S-198: Photocatalytic hydrogen evolution of P72 from water/methanol/triethylamine mixtures or Na_2S aqueous under solar simulator. Polymer (25 mg) was suspended in 25 mL water/methanol/triethylamine solution (volume ratio, 1:1:1) or 0.026 M Na_2S aqueous solution, irradiated by a solar simulator (AM1.5G, classification ABA, ASTME927-10).

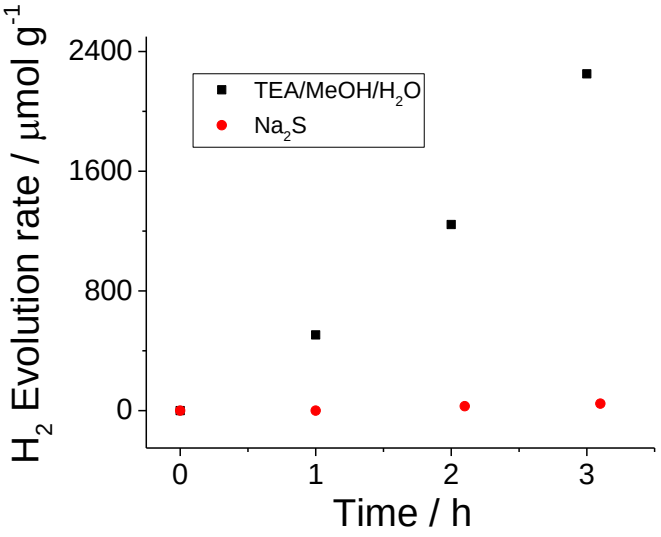

Figure S-199: Photocatalytic hydrogen evolution of P66 from water/methanol/triethylamine mixtures or Na_2S aqueous under solar simulator. Polymer (25 mg) was suspended in 25 mL water/methanol/triethylamine solution (volume ratio, 1:1:1) or 0.026 M Na_2S aqueous solution, irradiated by a solar simulator (AM1.5G, classification ABA, ASTME927-10).

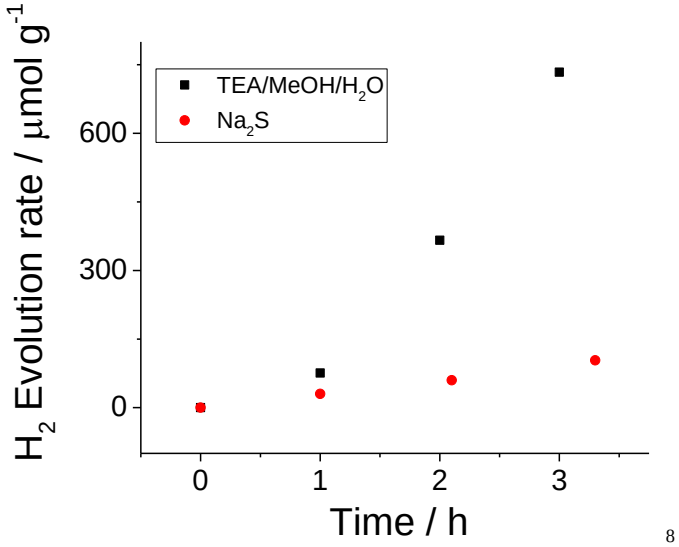

8

Figure S-200: Photocatalytic hydrogen evolution of P71 from water/methanol/triethylamine mixtures or Na_2S aqueous under solar simulator. Polymer (25 mg) was suspended in 25 mL water/methanol/triethylamine solution (volume ratio, 1:1:1) or 0.026 M Na_2S aqueous solution, irradiated by a solar simulator (AM1.5G, classification ABA, ASTME927-10).

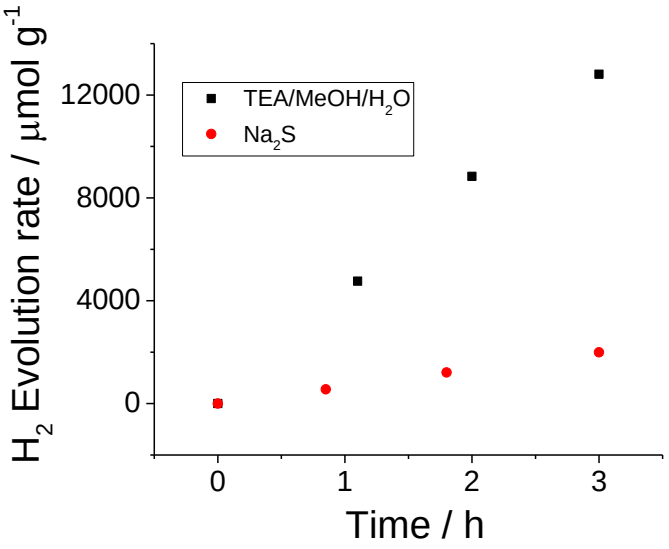

Figure S-201: Photocatalytic hydrogen evolution of P63 from water/methanol/triethylamine mixtures or Na_2S aqueous under solar simulator. Polymer (25 mg) was suspended in 25 mL water/methanol/triethylamine solution (volume ratio, 1:1:1) or 0.026 M Na_2S aqueous solution, irradiated by a solar simulator (AM1.5G, classification ABA, ASTME927-10).

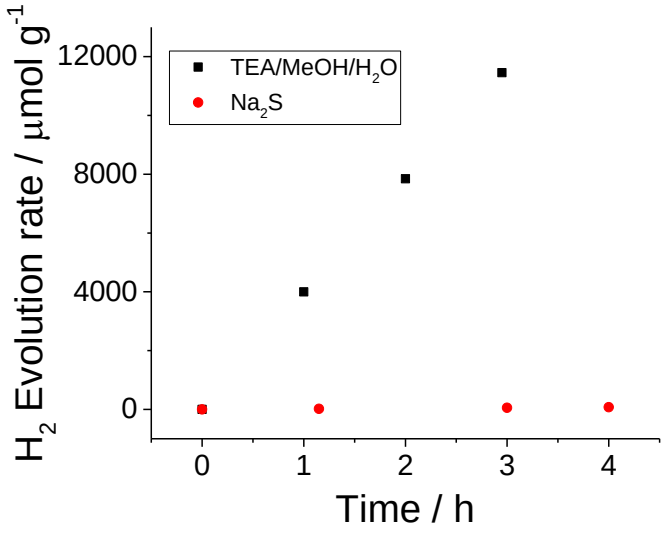

Figure S-202: Photocatalytic hydrogen evolution of P65 from water/methanol/triethylamine mixtures or Na_2S aqueous under solar simulator. Polymer (25 mg) was suspended in 25 mL water/methanol/triethylamine solution (volume ratio, 1:1:1) or 0.026 M Na_2S aqueous solution, irradiated by a solar simulator (AM1.5G, classification ABA, ASTME927-10).

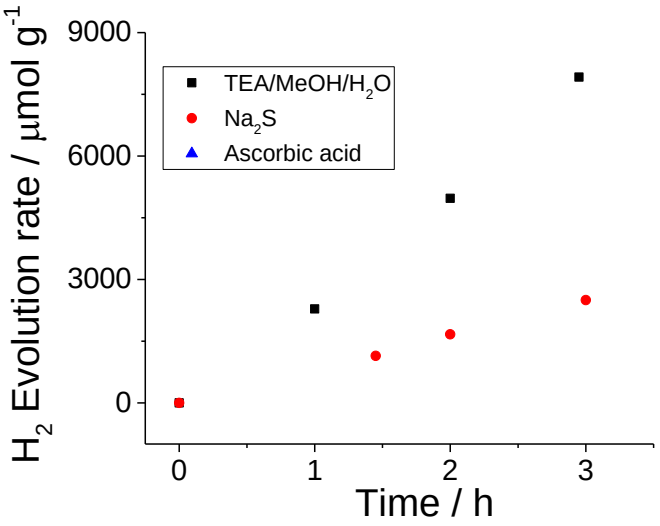

Figure S-203: Photocatalytic hydrogen evolution of P67 from water/methanol/triethylamine mixtures or Na_2S aqueous under solar simulator. Polymer (25 mg) was suspended in 25 mL water/methanol/triethylamine solution (volume ratio, 1:1:1) or 0.026 M Na_2S aqueous solution, irradiated by a solar simulator (AM1.5G, classification ABA, ASTME927-10).

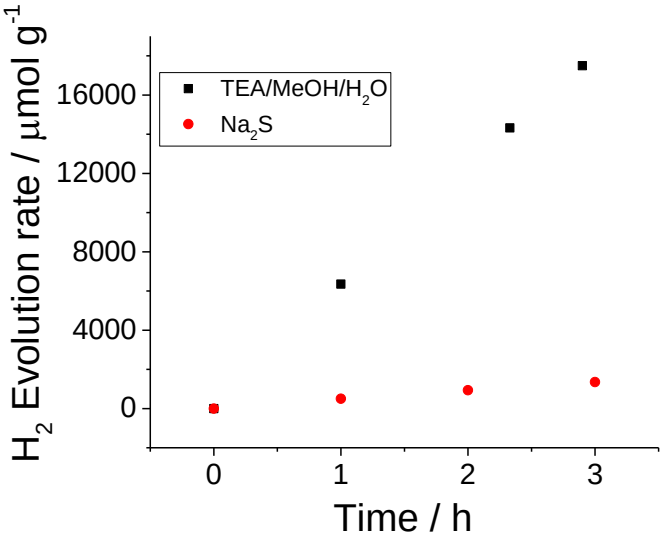

Figure S-204: Photocatalytic hydrogen evolution of P64 from water/methanol/triethylamine mixtures or Na_2S aqueous under solar simulator. Polymer (25 mg) was suspended in 25 mL water/methanol/triethylamine solution (volume ratio, 1:1:1) or 0.026 M Na_2S aqueous solution, irradiated by a solar simulator (AM1.5G, classification ABA, ASTME927-10).

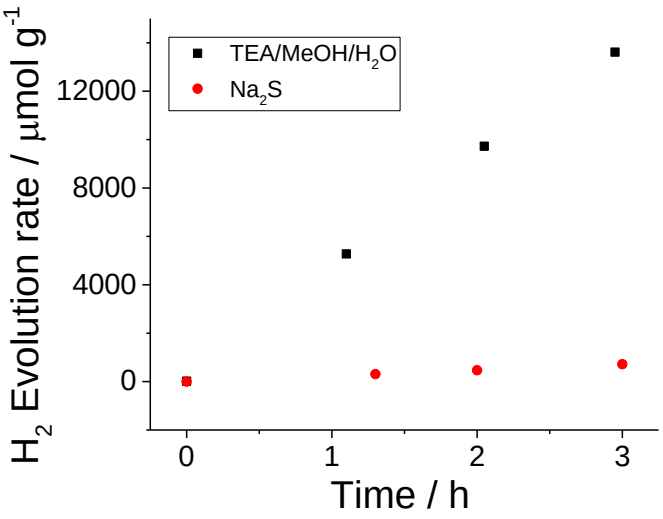

Figure S-205: Photocatalytic hydrogen evolution of P73 from water/methanol/triethylamine mixtures or Na_2S aqueous under solar simulator. Polymer (25 mg) was suspended in 25 mL water/methanol/triethylamine solution (volume ratio, 1:1:1) or 0.026 M Na_2S aqueous solution, irradiated by a solar simulator (AM1.5G, classification ABA, ASTME927-10).

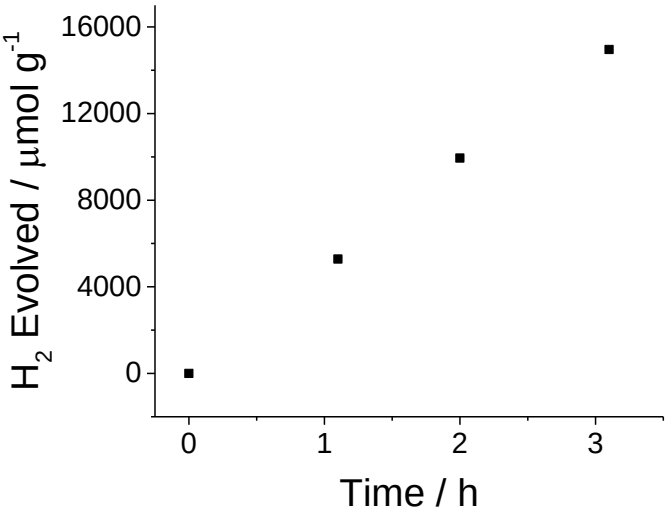

Figure S-206: Photocatalytic hydrogen evolution of P1-32 from water/methanol/triethylamine mixtures under solar simulator. Polymer (25 mg) was suspended in 25 mL water/methanol/triethylamine solution (volume ratio, 1:1:1), irradiated by a solar simulator (AM1.5G, classification ABA, ASTME927-10).

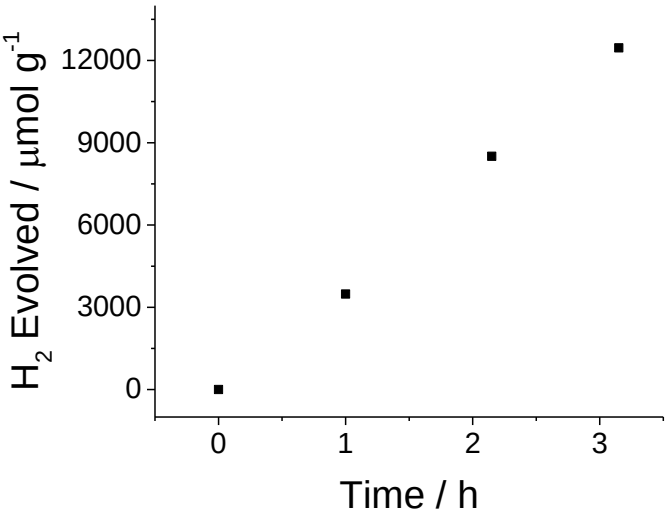

Figure S-207: Photocatalytic hydrogen evolution of P1-92 from water/methanol/triethylamine mixtures under solar simulator. Polymer (25 mg) was suspended in 25 mL water/methanol/triethylamine solution (volume ratio, 1:1:1), irradiated by a solar simulator (AM1.5G, classification ABA, ASTME927-10).

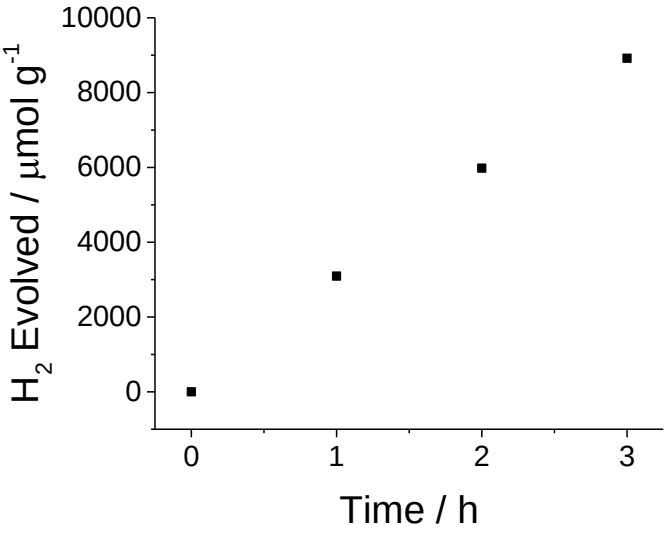

Figure S-208: Photocatalytic hydrogen evolution of P1-23 from water/methanol/triethylamine mixtures under solar simulator. Polymer (25 mg) was suspended 25 mL water/methanol/triethylamine solution (volume ratio, 1:1:1), irradiated by a solar simulator (AM1.5G, classification ABA, ASTME927-10).

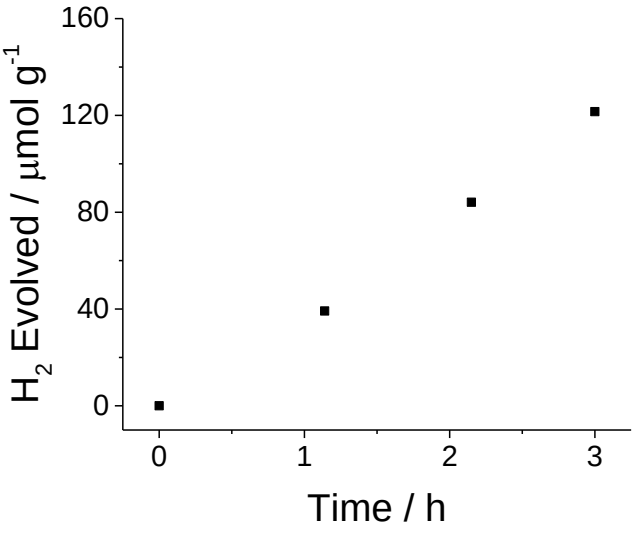

Figure S-209: Photocatalytic hydrogen evolution of P1-55 from water/methanol/triethylamine mixtures under solar simulator. Polymer (25 mg) was suspended in 25 mL water/methanol/triethylamine solution (volume ratio, 1:1:1), irradiated by a solar simulator (AM1.5G, classification ABA, ASTME927-10), illumination time: 3 hours.

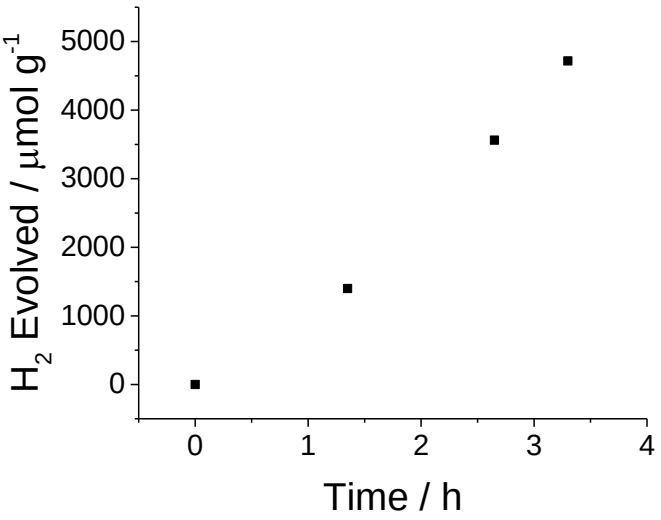

Figure S-210: Photocatalytic hydrogen evolution of P7 from water/methanol/triethylamine mixtures under solar simulator. Polymer (25 mg) was suspended in 25 mL water/methanol/triethylamine solution (volume ratio, 1:1:1), irradiated by a solar simulator (AM1.5G, classification ABA, ASTME927-10).

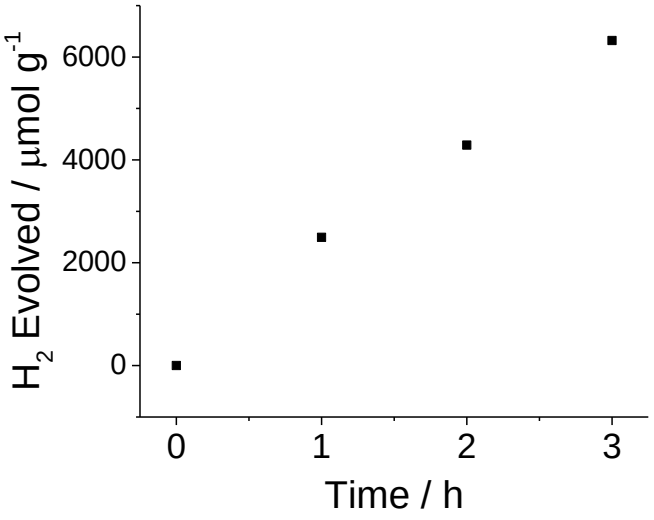

Figure S-211: Photocatalytic hydrogen evolution of P10 from water/methanol/triethylamine mixtures under solar simulator. Polymer (25 mg) was suspended in 25 mL water/methanol/triethylamine solution (volume ratio, 1:1:1), irradiated by a solar simulator (AM1.5G, classification ABA, ASTME927-10).

6.11 Pt doping experiment

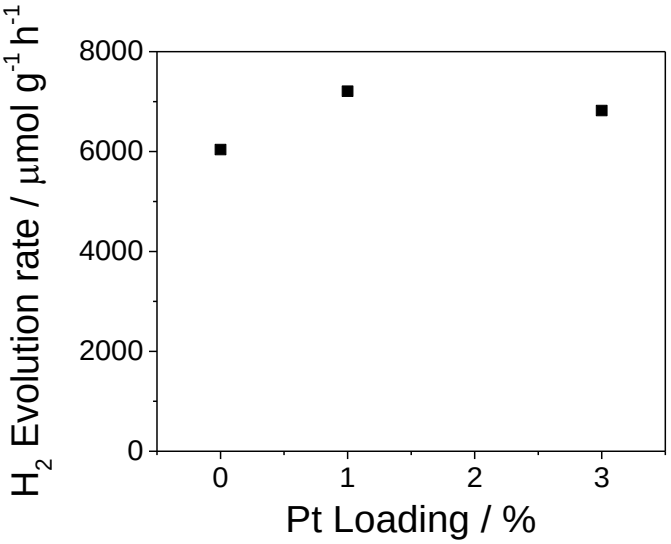

Figure S-212: Photocatalytic hydrogen evolution of P64 from water/methanol/triethylamine and H_2PtCl_6 mixtures under solar simulator. Polymer (25 mg) was suspended in 25 mL water/methanol/triethylamine solution (volume ratio, 1:1:1) with added Pt (from H_2PtCl_6, 8 wt. % solution), irradiated by a solar simulator (AM1.5G, classification ABA, ASTME927-10).

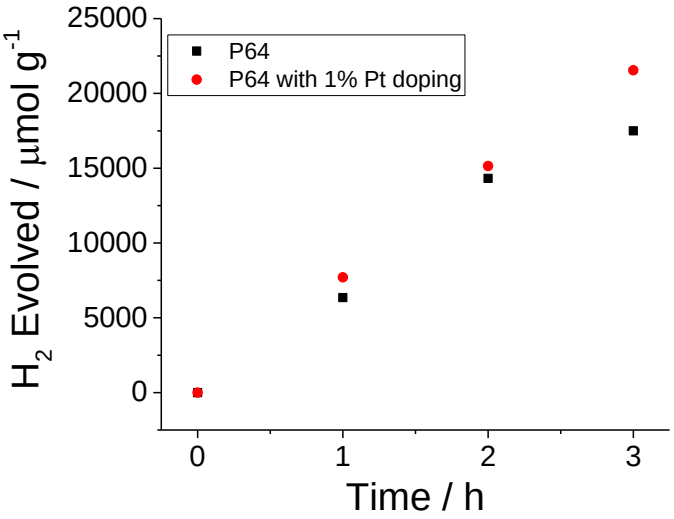

Figure S-213: Photocatalytic hydrogen evolution of P64 from water/methanol/triethylamine mixtures and 1 wt. % Pt doping under solar simulator. Polymer (25 mg) was suspended in 25 mL water/methanol/triethylamine solution (volume ratio, 1:1:1) with added Pt (from H_2PtCl_6, 8 wt. % solution), irradiated by a solar simulator (AM1.5G, classification ABA, ASTME927-10).

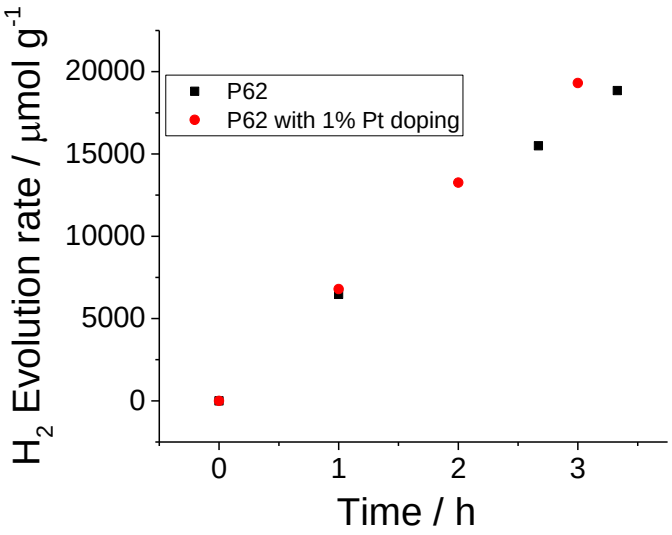

Figure S-214: Photocatalytic hydrogen evolution of P62 from water/methanol/triethylamine mixtures and 1 wt. % Pt doping under solar simulator. Polymer (25 mg) was suspended in 25 mL water/methanol/triethylamine solution (volume ratio, 1:1:1) with added Pt (from H_2PtCl_6, 8 wt. % solution), irradiated by a solar simulator (AM1.5G, classification ABA, ASTME927-10).

6.12 Before and after illumination

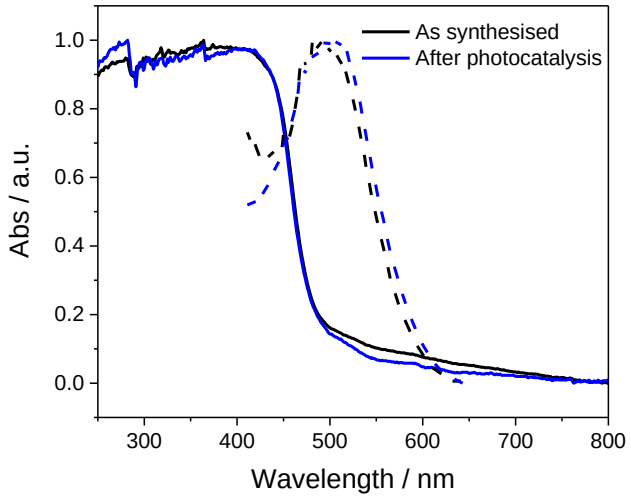

Figure S-215: Solid-state UV-vis and photoluminescence spectra of P64. After 36 hours under $\lambda > 420$ nm irradiation showing no significant changes.

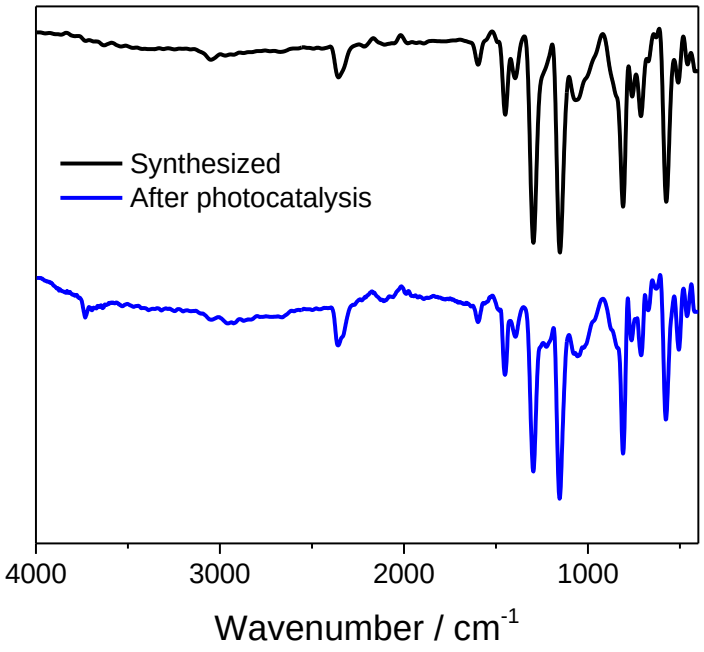

Figure S-216: Transmission FT-IR spectra of P64 as KBr pellets before and after photocatalysis

7. Theoretical Screening

7.1 Structure Generation and GFN/IPEA/sTDA-xTB Calculations

Polymer models are constructed using *stk*,[9,10] with which SMILES representations of monomers may be embedded in 3D and combined to form linear polymer structures. All polymer structures were restricted to 8 monomer units in length. Prior to property calculations, we perform a stochastic conformer search, conformational space of the polymer randomly using the Experimental-Torsion Distance Geometry with additional basic knowledge (ETKDG) method,[11] where we typically generate 500 conformers per polymer. The resulting conformers and undergo a subsequent optimisation and energy ranking procedure using the Merck Molecular Force Field (MMFF)[12] as implemented in RDKit.[13] This number of conformers is expected to be more than sufficient to converge each property calculated with respect to conformer energy, as we have shown previously that IP, EA and optical gap are largely insensitive to conformation for these materials.[14]

For IP/EA calculations, we use an extension of the parent GFN-xTB method, IPEA-xTB,[8] a differently parameterized variant of GFN-xTB for the calculation of ionisation potentials and electron affinities. For optical gaps, we use the tight binding simplified Tamm-Dancoff approach (sTDA)[15] applied to orbitals and orbital eigenvalues obtained through xTB (sTDA-xTB).[16] All GFN-xTB and IPEA-xTB calculations were performed using the *xtb* code, [17] while the sTDA results were obtained using the *stda* code. [18] All GFN-xTB calculations, but not sTDA calculations, used the generalized Born surface area solvation model for water, distributed with the *xtb* code.

7.2 Calibration of Semi-Empirical Data to DFT Data

Following our previously published methodology, we calibrate the IP/EA and optical gap data obtained through GFN/IPEA/sTDA-xTB to yield absolute property values that are comparable with density functional theory (DFT). This is done using a simple linear model, with parameters obtained previously (see Table S-9) using a set of ~40 polymers, their properties calculated using DFT.[19] This calibration procedure was shown to yield semi-empirically-derived results with a mean absolute error of 0.1 V for IP and EA and 0.15 eV for optical gap with respect to DFT, at a fraction of the computational cost.

Table *S-9*. Calibration parameters used to calibrate semi-empirical data to DFT-derived results, previously obtained using a subset of approximately 40 linear polymers.[19]

Semi-Empirical Method	(TD)-DFT Method	m	c
IPEA-xTB	B3LYP	1.02	-0.41
sTDA-xTB	B3LYP	0.85	0.35

Calibration performed using a linear model ($x_{DFT} = mx_{xtb} + c$).

7.3 Machine Learning

Machine learning was performed using the xgboost package [18] via scikit learn,[20] using a gradient boosted trees regressor. As descriptors, we provide calculated IP, EA, optical gap and experimentally measured transmittance data. The model is trained to minimize the error between predicted and measure hydrogen evolution rates observed using TEA as a sacrificial electron donor. The model hyper-parameters are given in Table S-10 and were obtained from a simple grid search. We evaluate the model using leave-one-out cross validation, where the model is trained using all but one point, and tested on the remaining

point. This process is repeated until all points have been left out once, forming a set of validation data that was not used to train the model.

Table *S-10*. Hyper-parameters used in training, obtained from a grid search. All other parameters were left at default values.

Parameter	Value
Number of estimators	40
Maximum depth	4
Learning rate	0.35

We further validated the model via a simple y-randomisation test (Fig. S-216), where the resulting model is not able to map the descriptors to HER, supporting the correlations observed by the model trained on non-randomized data.

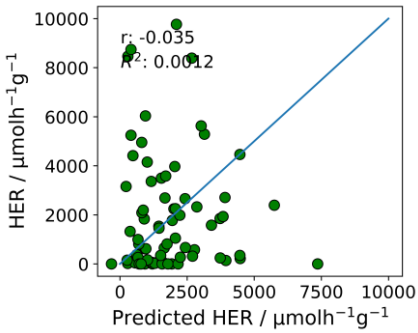

Figure S-217: Results obtained training a machine learning model using leave-one-out cross validation, with the HER values assigned to random descriptors (y-randomisation test).

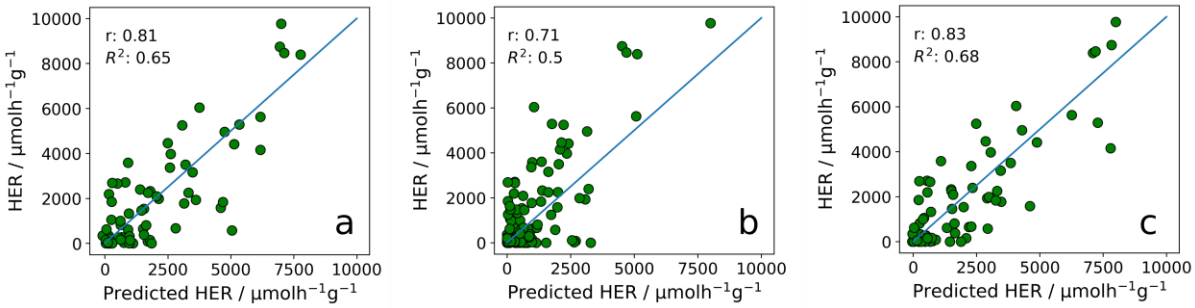

Figure S-218: Results obtained training a machine learning model using leave-one-out cross validation. In addition to the descriptors used previously, here the model is additionally given a) degree of crystallinity, b) palladium content and c) surface area. The degree of crystallinity was approximated by a categorical value by manually inspecting PXRD spectra, while the surface area was estimated using the high-throughput CO_2 sorption experiments.

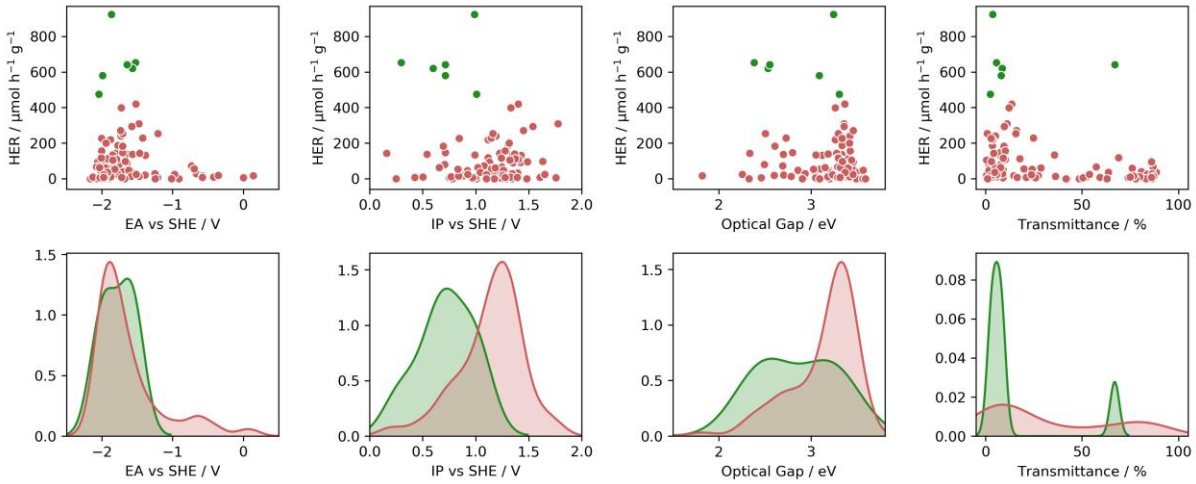

Figure S-219: Photocatalytic hydrogen evolution rates (HER) of the all synthesized co-polymers in this work in Na_2S/H_2O mixture under AM 1.5G illumination plotted *vs.* left: calculated EA, center: calculated IP, right: calculated optical gaps. Kernel density estimates of distributions of right) calculated IP, centre) calculated EA, right) calculated optical gap. In each figure, materials with a HER greater than 50% of that of the most active polymer in the library are denoted by green points; polymers with HER less than 50% of the most active polymer are denoted by red points.

8. Reference

(1) Kawano, S.; Baumgarten, M.; Chercka, D.; Enkelmann, V.; Mu, K. Electron Donors and Acceptors Based on 2,7-Functionalized Pyrene-4,5,9,10-tetraone. *Chem. Commun.* **2013**, 49, 5058–5060.

(2) Chakraborty, C.; Bera, M. K.; Rana, U.; Malik, S. *Vice versa* Donor Acceptor Fluorene–ferrocene Alternate Copolymer: a Twisted Ribbon for Electrical Switching. *Chem. Commun.* **2015**, *51*, 13123–13126.

(3) Murage, J.; Eddy, J. W.; Zimbalist, J. R.; McIntyre, T. B.; Wagner, Z. R.; Goodson, F. E. Effect of Reaction Parameters on the Molecular Weights of Polymers Formed in a Suzuki Polycondensation. *Macromolecules* **2008**, *41*, 7330–7338.

(4) Sakamoto, J.; Rehahn, M.; Wegner, G.; Schlüter, A. D. Suzuki Polycondensation: Polyarylenes à la Carte. *Macromol. Rapid Commun.* **2009**, *30*, 653–687.

(5) Sprick, R. S.; Bai, Y.; Guilbert, A. A. Y.; Zbiri, M.; Aitchison, C. M.; Wilbraham, L.; Yan, Y.; Woods, D. J.; Zwijnenburg, M. A.; Cooper, A. I. Photocatalytic Hydrogen Evolution from Water Using Fluorene and Dibenzothiophene Sulfone-Conjugated Microporous and Linear Polymers, *Chem. Mater*. **2019**, *31*, 305–313.

(6) *A Basic Guide to Particle Characterization*; Malvern Instruments Limited, **2015**.

(7) Sachs, M.; Sprick, R. S.; Pearce, D.; Hillman, S. A. J.; Monti, A.; Guilbert, A. A. Y.; Brownbill, N. J.; Dimitrov, S.; Shi, X.; Blanc, F.; Zwijnenburg, M. A.; Nelson, J.; Durrant, J. R.; Cooper, A. I. Understanding structure-activity Relationships in Linear Polymer Photocatalysts for Hydrogen Evolution. *Nat. Commun.* **2018**, *9*, 4968.

(8) Ásgeirsson, V.; Bauer, C. A.; Grimme, S. Quantum Chemical Calculation of Electron Ionization Mass Spectra for General Organic and Inorganic Molecules. *Chem. Sci.* **2017**, *8*, 4879–4895.

(9) Turcani, L.; Berardo, E.; Jelfs, K. E. Stk : A Python Toolkit for Supramolecular Assembly. **2018**, *44*, 1931–1942.

(10) https://github.com/JelfsMaterialsGroup/stk.

(11) Riniker, S.; Landrum, G. A. Better Informed Distance Geometry: Using What We Know To Improve Conformation Generation. *J. Chem. Inf. Model.*, **2015**, *55*, 2562-2574.

(12) Halgren, T. A. MMFF VI. MMFF94s Option for Energy Minimization Studies. *J. Comput. Chem.* **1999**, *20*, 720–729.

(13) https://www.rdkit.org/

(14) Heath-Apostolopoulos, I.; Wilbraham, L.; Zwijnenburg, M. A. Computational High-Throughput Screening of Polymeric Photocatalysts : Exploring the Effect of Composition, Sequence Isomerism and Conformational Degrees of Freedom. *Faraday Discuss.* **2019**, DOI: 10.1039/C8FD00171E.

(15) Bannwarth, C.; Grimme, S. A Simplified Time-Dependent Density Functional Theory Approach for Electronic Ultraviolet and Circular Dichroism Spectra of Very Large Molecules. *Comput. Theor. Chem.* **2014**, *1040–1041*, 45–53.

(16) Grimme, S.; Bannwarth, C. Ultra-Fast Computation of Electronic Spectra for Large Systems by Tight-Binding Based Simplified Tamm-Dancoff Approximation (sTDA-xTB). *J. Chem. Phys.* **2016**, *145*, 54103.

(17) https://www.chemie.uni-bonn.de/pctc/mulliken-center/software/xtb/xtb/

(18) https://www.chemie.uni-bonn.de/pctc/mulliken-center/software/stda/stda/

(19) Wilbraham, L.; Berardo, E.; Turcani, L.; Jelfs, K. E.; Zwijnenburg, M. A. High-Throughput Screening Approach for the Optoelectronic Properties of Conjugated Polymers. *J. Chem. Inf. Model.* **2018**, *58*, 2450–2459.

(20) Pedregosa, F.; Varoquaux, G.; Gramfort, A.; Michel, V.; Thirion, B.; Grisel, O.; Blondel, M.; Prettenhofer, P.; Weiss, R.; Dubourg, V. Scikit-Learn : Machine Learning in Python. *J. Mach. Learn. Res.* **2011**, *12*, 2825–2830.